Trying to Escape from Flatland: Generation and Biological Profiling of Bridged Bicyclic Compounds

Von der Fakultät für Lebenswissenschaften

der Technischen Universität Carolo-Wilhelmina zu Braunschweig

zur Erlangung des Grades eines

Doktors der Naturwissenschaften

(Dr. rer. nat.)

genehmigte

D i s s e r t a t i o n

von: Naga Venkata Suryanarayana Birudukota

aus: Palakollu/ Indien

1. Referent:	Prof. Dr. Stefan Schulz
2. Referentin:	Prof. Dr. Ursula Bilitewski
eingereicht am:	28.05.2014
mündliche Prüfung (Disputation) am:	15.08.2014

Druckjahr 2014

Vorveröffentlichungen der Dissertation

Teilergebnisse aus dieser Arbeit wurden mit Genehmigung der Fakultät für Lebenswissenschaften, vertreten durch den Mentor der Arbeit, in folgenden Beiträgen vorab veröffentlicht:

Tagungsbeiträge

Birudukota, N., V., S., Overwin, H., González, M., Méndez, V., Seeger, M. and Hofer, B.; Pursuing a Novel Chemo-Enzymatic Route to Drug-Like Compounds (Poster); 1st International HIPS symposium, Saarbruecken, Germany, 2011.

Birudukota, N., V., Overwin, H., González, M., Méndez, V., Seeger, M. and Hofer, B.; Evaluation of a Novel Route to Bioactive Compounds: Generation of Bridged Bicyclic Derivatives of an Aromatic Core Structure (Poster); EMBO Conference: Chemical Biology, Heidelberg, Germany, 2012.

Acknowledgements

I would like to express my sincere gratitude to my supervisor Dr. Bernd Hofer for his guidance with endless support. Thank you for giving me the complete freedom and allowing me to use my own ideas in the project. His constant encouragement along with the useful suggestions and constructive criticisms throughout the work made me to achieve this goal. It has been a great privilege to work under him.

I thank Dr. Ronald Frank for providing me the opportunity to work in this project.

I am grateful to my thesis committee members Prof. Dr. Stefan schulz and Dr. Florenz Sasse. Special thanks to Prof. Dr. Schulz for being my mentor during the Ph.D. studies and also for being for part of the examination committee. I extend my thanks to Dr.Florenz Sasse for giving me valuable suggestions in the biology part of this work and for reviewing it. I thank Prof. Dr. Ursula Bilitewski for her helpful advices and for agreeing to be part of the examination committee. I am thankful to Prof. Dr. Ulrich Engelhardt for being in the examination committee.

Many thanks to Dr. Raimo Franke for the evaluation of impedance measurement data and for reviewing it.

I acknowledge our fruitful collaboration with Prof. Dr. Michael Seeger (Valparaíso, Chile) and his group.

I thank Aruna Raja for her great support and help in the biology part of this work. I also appreciate BettinaHinkelman's help in the experiments with cells. I am very thankful to all of our current colleagues of chemical biology group for the friendly work environment, and former colleague Dr. Yazh Muthukumar for her help and advices.

I appreciate the help of Christel Kakosche for NMR spectrometry and Andera Abrahamik, Anje Meier for Mass spectrometry.

I am greatly indebted to my loving parents for their affection and unending support. Finally, I owe a big "Thank you" for my wife Swapna Ponnampalli for her encouragement, understanding and moral support.

Contents

Abstract

The synthesis of new chemical entities as potential drug candidates is a promising and challenging aspect in drug discovery. Investigations on success rates showed higher values for three-dimensional molecules than for planar ones and recommended an “escape from flatland” strategy for the chemical synthesis of compound collections. Following these suggestions, a synthetic route was devised for the generation of bridged bicyclic compounds as an example for molecules possessing a permanent three-dimensional structure. This route involved [4+2] cycloaddition reactions between a collection of cyclic dienes and a collection of dienophiles, thereby combining privileged core structures provided by the reaction partners. A considerable fraction of the novel molecules showed biological activity in a general assay based on interference with the proliferation of mammalian cells. Two profiling methods, cellular impedance measurement and high-content cellular image analysis, were used to obtain suggestions for the types of bioactivities exerted by the positive compounds. Although the results of these experiments showed considerable variation, it was in two instances possible to identify cellular processes with which the active compounds interfere. In one case, the inhibition of tubulin polymerization was observed, in the other case, interference with proteasome function could be confirmed. The bridged bicyclic compounds synthesized and examined in the course of this thesis are just one example for structures that possess a permanent three-dimensionality. The results obtained encourage further exploration of this region of the chemical space by generation of larger and more structurally diverse collections of bridged bicyclic compounds and related molecules. Furthermore, other synthetic pathways, leading to different types of three-dimensional compounds, may be developed and explored.

Zusammenfassung

Die Synthese „neuer chemischer Einheiten“ zur Gewinnung von Wirkstoff-Kandidaten ist ein vielversprechender und herausfordernder Aspekt der Wirkstoffforschung. Untersuchungen über Erfolgsraten ergaben höhere Werte für dreidimensionale Moleküle als für planare und legten eine “Ausstieg-aus-dem-Flachland“-Strategie für die Synthese von Molekülbibliotheken nahe. In Verfolgung dieses Vorschlags wurde eine Syntheseroute für die Erzeugung verbrückt bizyklischer Verbindungen als ein Beispiel für Moleküle mit permanent dreidimensionaler Struktur entwickelt. Diese Route beinhaltete [4+2]-Zykloadditionsreaktionen zwischen Kollektionen von zyklischen Dienen und von Dienophilen, wobei durch die Reaktionspartner privilegierte Kernstrukturen miteinander kombiniert wurden. Ein signifikanter Teil der neuen Moleküle zeigte in einem globalen Test, der die Beeinträchtigung der Proliferation von Säugerzellen maß, biologische Aktivität. Zwei Profilierungs-Methoden, Verfolgung der zellulären Impedanz und extensive zelluläre Bildanalyse, wurden eingesetzt, um Hinweise auf die Arten der Bioaktivitäten der positiven Verbindungen zu erhalten. Obwohl die Ergebnisse dieser Experimente beträchtliche Streuungen zeigten, war es in zwei Fällen möglich, die zellulären Prozesse zu identifizieren, mit denen die aktiven Verbindungen interferierten. In einem Fall wurde die Inhibition der Tubulin-Polymerisation beobachtet, im anderen Fall konnte eine Störung der Proteasom-Funktion bestätigt werden. Die synthetisierten Verbindungen sind nur ein Beispiel für Moleküle, die eine permanente Dreidimensionalität besitzen. Die erzielten Ergebnisse sprechen für eine weitere Untersuchung dieser Region des „chemischen Raums“ durch Erzeugung größerer und strukturell vielfältigerer Sammlungen derartiger Verbindungen und verwandter Moleküle. Ferner könnten andere Synthesewege, die zu alternativen Typen dreidimensionaler Verbindungen führen, entworfen und auf bioaktive Moleküle untersucht werden.

1. Introduction

Drug discovery is an important research area to obtain new chemical entities which can be lead structures for successful drug candidates. The aspect of drug discovery is gaining importance year by year, for example, by the evolution of resistance to existing anticancer[1-4] and antimicrobial agents.[5-8] In addition, for emerging infectious diseases such as Influenza A, Dengue fever and West Nile disease etc. there is an essential requirement to find new drugs.[9] However, the drug discovery rate is almost the same as in the last 50 years, which is below the required level.[10] This can be seen, for example, by the numbers of drugs approved by the FDA since 1993,[11] as shown in Fig. 1. Therefore, there is a dire need to synthesize or isolate new drug candidates.

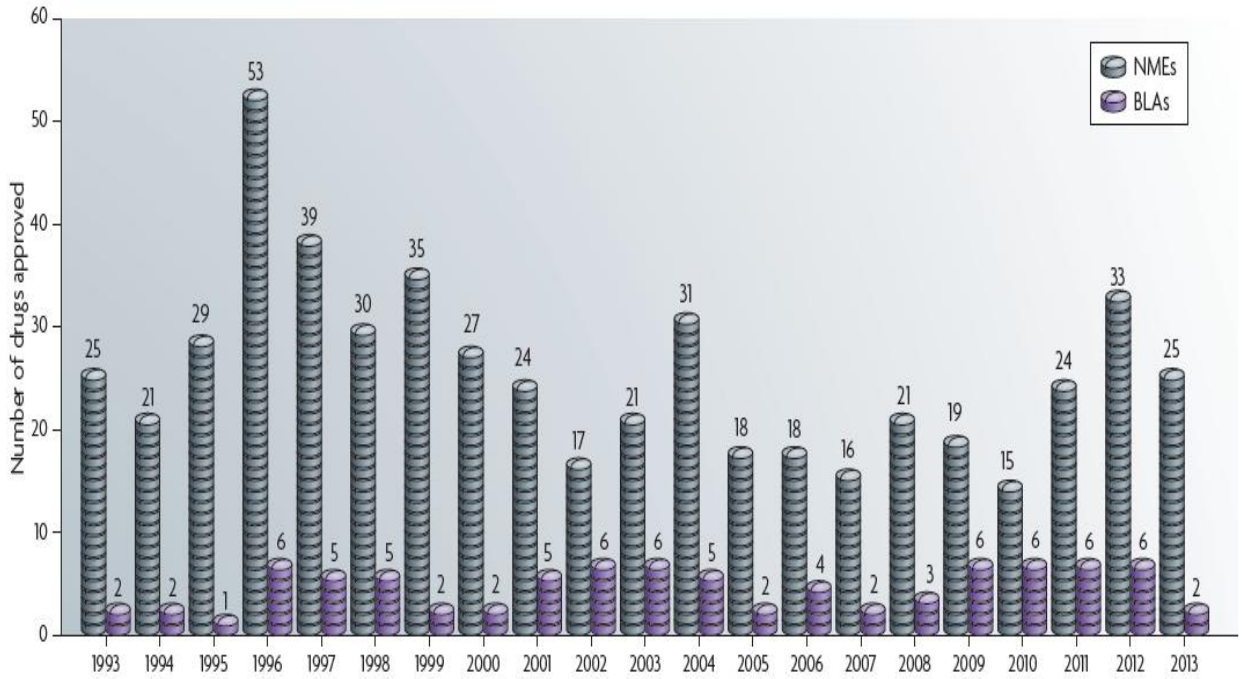

Fig. 1: New molecular entities (NMEs) and biologics license applications (BLAs) approved by the center for drug evaluation and research since 1993. (Adapted from Ref. 11)

1.1. Source and strategies in drug discovery

The general ways of contribution to the development of new drug candidates are isolation and/or synthesis.

Isolation of molecules from the extracts of natural resources like plants, microorganisms etc. provides natural compounds, which have typically evolved in nature for a particular biological function. They served remarkably as source of drugs including antibacterials and cytotoxic agents for cancer.[12] Despite of these positive results, natural products have some limitations in drug discovery which are worth mentioning. Even though nature created these complex molecules in order to interact with biological targets, the complications involved in the isolation, purification and the frequently required subsequent chemical derivatization of these compounds often severely limits their availability. Consequently, large collections of discrete natural products are not available for use in high-throughput screening and the lead optimization process.[13,14]

On the other hand, chemical synthesis is also a principal source for the discovery of new entities. This includes, on one end, the total synthesis of natural products that are otherwise difficult to obtain or to derivatize, and on the other end, the generation of drug-like organic molecules. Natural products have diverse and often complex molecular architectures. These challenges revealed gaps in the methods of organic synthesis, providing inspiration to fill them with novel methodologies and routes.[15] The possibility to optimize pharmacokinetic and pharmacodynamic properties by chemical synthesis is also an advantage in providing leads for drug discovery.

The evolution of modern methods in stereoselective organic synthesis and methodologies developed from solution chemistry[15] to solid phase chemistry[16-20] has

provided the means to generate not only compounds for a specific target, but also collections of structurally diverse compounds. Therefore it is possible to follow different synthetic strategies in drug discovery.

On one extreme there is target-oriented synthesis (ToS).[21] ToS means the synthesis of compounds destined to interact with a known target. This furthermore requires the knowledge of the interaction site through which the target exerts its biological effect and which should be addressed by the drug molecule. Very helpful is the knowledge of its three-dimensional structure in order to be able to carry out molecular docking studies with candidate compounds. Apparently, identification of a specific interaction site on a macromolecule and the elucidation of its three-dimensional structure are often complex and time-consuming. Even if this knowledge is available, the design of a molecular shape able to efficiently and specifically disturb this interaction is anything but a straightforward endeavor. The reasons include the flexibility of protein structure, the shortcomings of available programs for molecular docking and the limitations of the chemical tool box itself. Thus, for example, only 1 or 2 CH_2 units can be added where 1.5 would be required to obtain a positioning of the ligand that would yield a strong interaction.

The other end of the synthetic strategies is generation of diverse small molecule libraries, which are then screened against a variety of potential cellular target molecules. The libraries may be synthesized with different types of approaches such as diversity-oriented synthesis (DoS),[21] biology-oriented synthesis (BioS),[22] and fragment-based drug discovery (FBDD).[23]

1.2. Compound collections and hit-rate problem

Technological advances facilitated the proficient synthesis of libraries containing thousands of compounds efficiently and allowed to screen large collections to identify lead candidates.[24-26] However, these phenotypic screenings and biochemical assays often resulted in unsatisfactory outcome in terms of specificity and efficiency of the obtained hits. In other words, such synthetic compound collections suffer from low hit rates.[27] Mainly, their synthetic strategies are chemistry-driven. Compounds that are easy to synthesize are the major contributors for most compound collections. Thus, compounds are produced in view of quantity rather than quality by combining more reactive, but biologically undesirable functional groups. Clearly, strategies for the chemical synthesis of compound libraries should be more structure-driven, i.e., they should address structural features that distinguish drugs and bioactive compounds from compounds in general.

1.3. Criteria for the synthesis of structure-driven compound libraries

There have been attempts[28a,b] to predict the druglikeness of molecules considering molecular descriptors proposed by Lipinski[29] and combining them with computational methods, but no generally applicable means of differentiating drug-like compounds from non-drug-like compounds exists. Eventually, a simple method employing five physico-chemical parameters, molecular weight, topological surface area, rotatable bonds and hydrogen bond donors and acceptors was introduced by Lipinski as the “Rule-of-Five” (RO5) concept and got widespread popularity in the drug discovery and development field. The medicinal chemist’s community became increasingly aware of the value of considering calculated physical properties. These properties are examined thoroughly and compound collections are filtered by the ‘RO5’ as they

progress from hits through leads to drugs. However, it proved insufficient to determine the pharmacologically relevant properties for druglikeness with the descriptors mentioned. Therefore parameters related to structure, like shape and rigidity are also to be considered and additional methods to identify distinguishing features between drugs and other organic molecules are required.

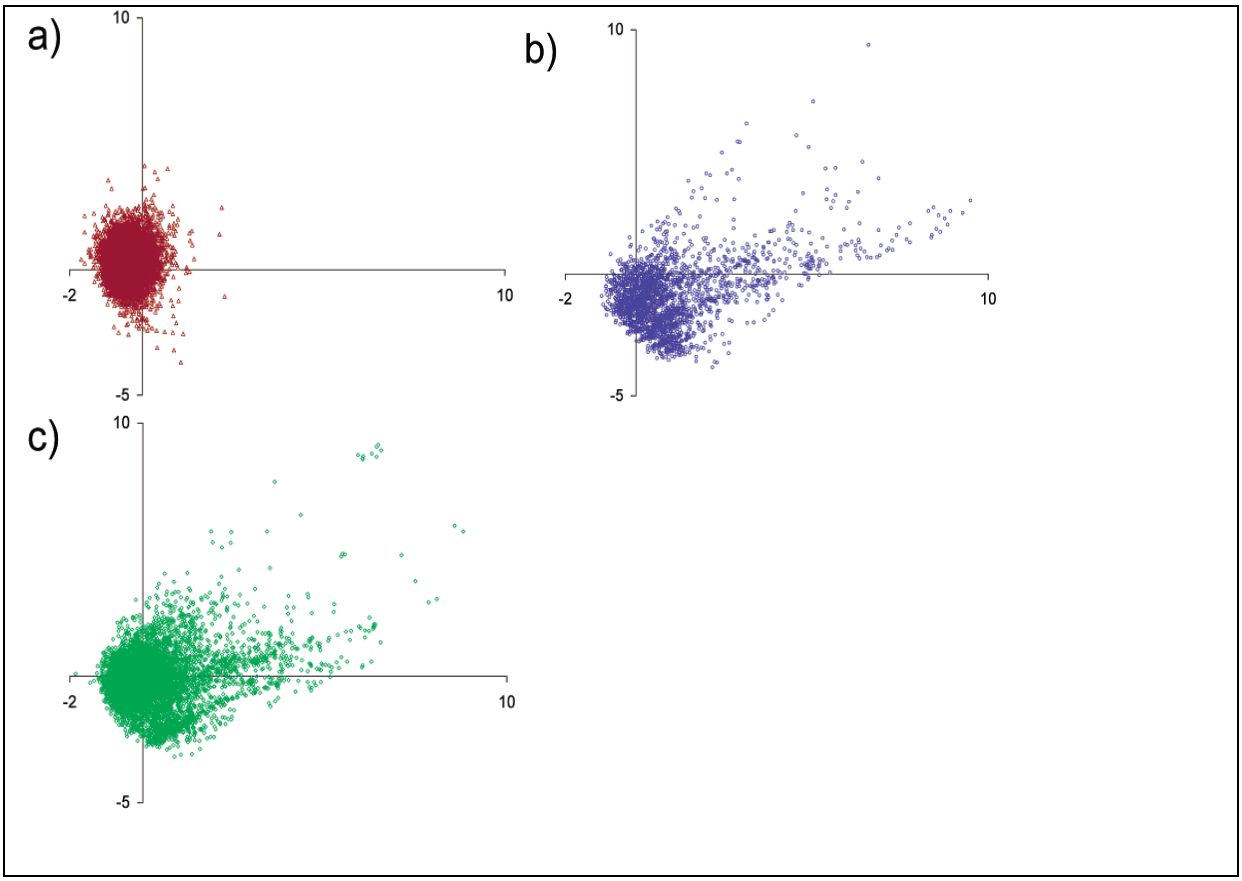

Fig. 2:. Comparison of three different classes of molecules was analyzed on the basis of a variety of molecular properties. Databases contained compounds from combinatorial chemistry (a), natural products (b) and drugs (c). A statistical approach known as principal component analysis was applied to the data to yield a two-dimensional representation of the distribution of these compounds in the chemical space. Plots of the first two principal components, which explain about 54% of the variance in the properties analyzed, are shown. Combinatorial compounds cover a limited region in the space specified by these principal components. (Adapted from Ref. 30)

Comparisons of synthetic molecules with those of drugs and natural products can reveal features lacking in the first group. This would give hints about how to increase the quality in the small molecule libraries and thereby address the hit-rate problem. Feher and Schmidt[30] performed a comparison between three classes of compounds, marketed drugs, compounds originating from combinatorial synthesis and natural products, based on variety of simple descriptors to identify how these classes populate the n-dimensional chemical space, where 'n' designates the number of descriptors or parameters or properties used in the comparison. A result of this analysis is shown in Fig. 2. It indicates that the structural diversity of combinatorial compounds is substantially lower than that of either drugs or natural products. The former are restricted to only a confined region of the chemical space.

In the following years, several proposals and approaches were reported concerning the definition of chemical space and the chemical space occupied by existing chemical entities.[31-34] These studies also suggest an unexplored medicinally relevant space which awaits the synthesis of respective molecules. This unexplored chemical space was recently defined by Reymond and co-workers with an enumeration of 166.4 billion virtual molecules, considering molecular shape as one of the descriptors.[35] Their study revealed that the majority of the synthesized molecules possessing reported biological activities and being clinically approved compounds were distributed in space regions characteristic for flat molecules (rod or disc shapes). Very few compounds were found in the space harbouring three-dimensional structures (spheres), as shown in Fig. 3. These results were consistent with other publications. Thus, Sauer et al. reported that the majority of the molecules synthesized in medicinal chemistry are either linear or planar structures and only a minority possesses three-dimensional structures.[36]

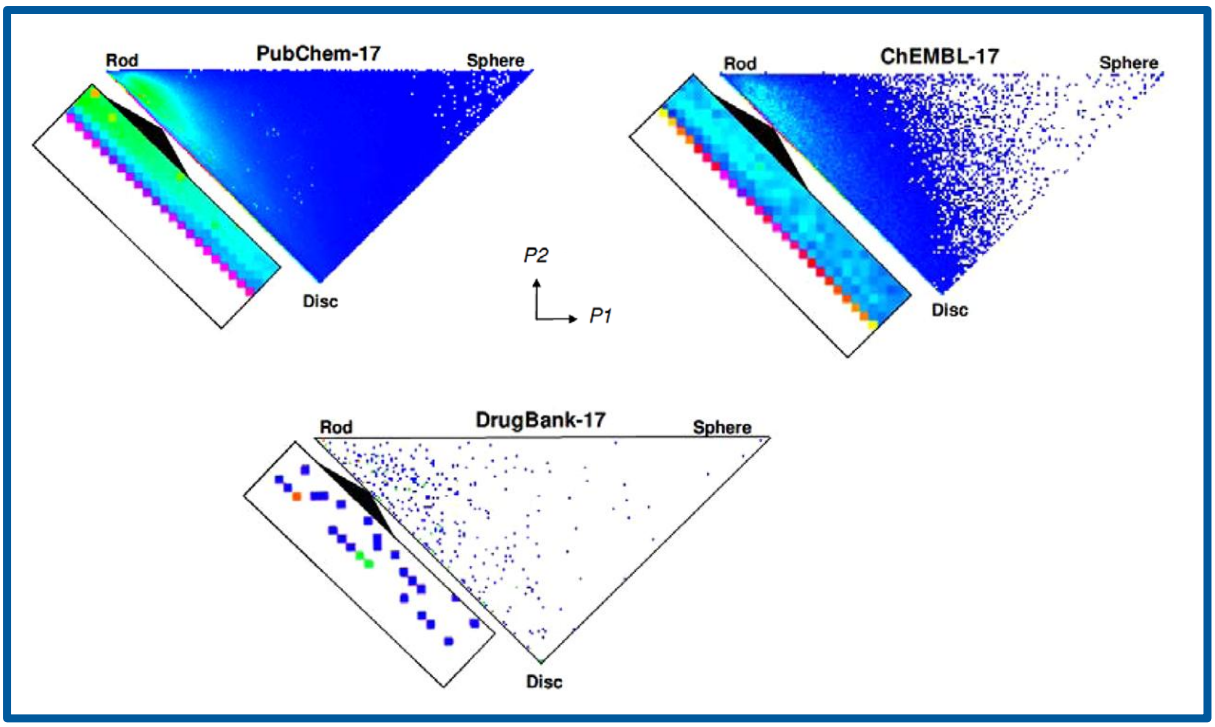

Fig 3:. Frequency of molecules with different shape in different databases. Molecular shape analyzed by the "principal moments of inertia". P1 and P2 are the normalized ratios of the principal moment of inertia. Occupancy of the P1, P2 plane is coloured from blue (1cpd/pixel) to purple (maximal value). Public compound archives PubChem, ChEMBL and DrugBank, the latter containing only approved drugs were considered for the analysis. The inserts show a magnified view of the lower left edge of each triangle. In all collections the lower left edge representing either rod or disc like structures is predominantly occupied whereas at the other end of the space, compound population is very low. In case of stereoisomers of compounds, only one isomer was considered for the analysis. (Adapted from Ref. 35)

Furthermore, a detailed study of the comprehensive medicinal chemistry database of 5120 molecules revealed that only very few synthesized compounds have a three-dimensional scaffold.[37] However, it was reported that molecules with a significant three-dimensional portion are known to have higher success rates in drug development.[38a,b] This may be rationalized by the following considerations. A permanent three-dimensional structure gives a molecule a rigid skeleton. The rigid nature of a small molecule can play vital role in binding to macromolecules. They can form

hydrogen bonds and hydrophobic interactions with proteins or other partners with low entropic losses in comparison to a flexible ligand with the same interaction pattern.[39] The presence of a rigid scaffold and very few rotatable bonds is frequently observed in bio-active molecules.[30] Therefore, compounds with a permanent three-dimensional structure may exploit the thermodynamic advantages attained by the rigidity in increased binding enthalpy and selectivity. Moreover, rigidity of a ligand may induce plasticity in the cellular target to attain maximum binding affinity.[40] For these reasons, an “escape from flatland” has been suggested as a valuable strategy to search for bioactive compounds.[38a]

1.4. The synthetic pathway devised for the generation of three-dimensional molecules

The above mentioned features of three-dimensional structures encouraged us to throw focus on the synthesis of three-dimensional compounds in order to explore a novel region of the chemical space for drug-like molecules.

Out of the many strategies to obtain three-dimensional molecules, we decided on a chemo-enzymatic route that starts from “privileged” core structures to yield bridged bicyclic compounds as end products. Privileged scaffolds are core structures frequently found in bioactive compounds.[41] The devised synthetic pathway is shown in Fig. 4. It comprises the following steps.

i) Conversion of aromatic or hetero-aromatic compounds into cyclic *cis*-dienediols via enzyme-catalyzed microbial oxidation.

ii) Protection of hydroxy groups, if required.

iii) [4+2] cycloaddition between the cyclic dienediols and dienophiles.

iv) Deprotection of hydroxy groups.

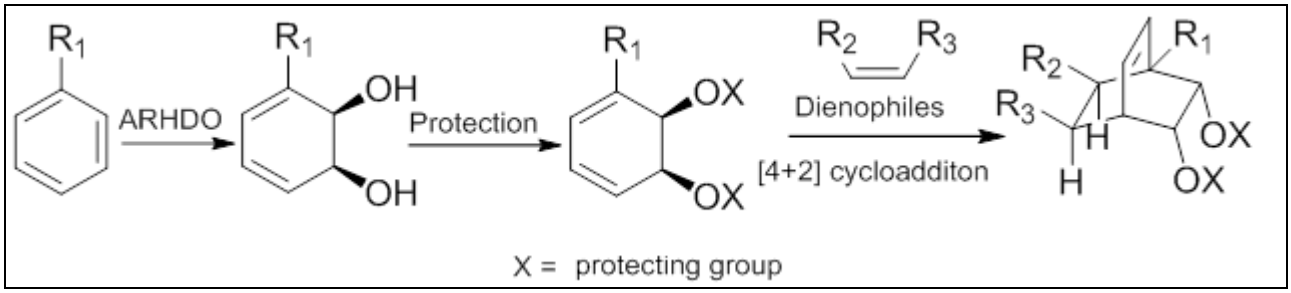

Fig. 4: Devised chemo-enzymatic route to synthesize three-dimensional compounds. ARHDO: Arylhydroxylating dioxygenase. Only one of the possible stereoisomers is shown.

1.4.1. Enzymatic formation of cyclic cis-dienediols

Cyclic dienediols may conveniently be obtained from aromatic compounds by enzymatic dioxygenation. The respective biocatalysts, aryl-hydroxylating dioxygenases (ARHDO), are bacterial enzymes that use molecular oxygen to activate the aromatic nucleus. This oxidation can be carried out with whole cells, either of mutant strains, deficient in a further metabolism of the generated dienediols, or of appropriate recombinant strains. This biocatalytic transformation involves the highly endothermic disruption of aromaticity and the introduction of two hydroxy groups, *cis* to each other on vicinal carbons, and of a diene ring structure[42] with defined stereochemistry. In 1973, Kobal *et al*. used such dienediols for the first time as a precursor in an organic reaction.[43] These molecules contain a remarkable combination of mutually connected functionalities that make them interesting as synthons for further diversification (Fig. 5).[44]

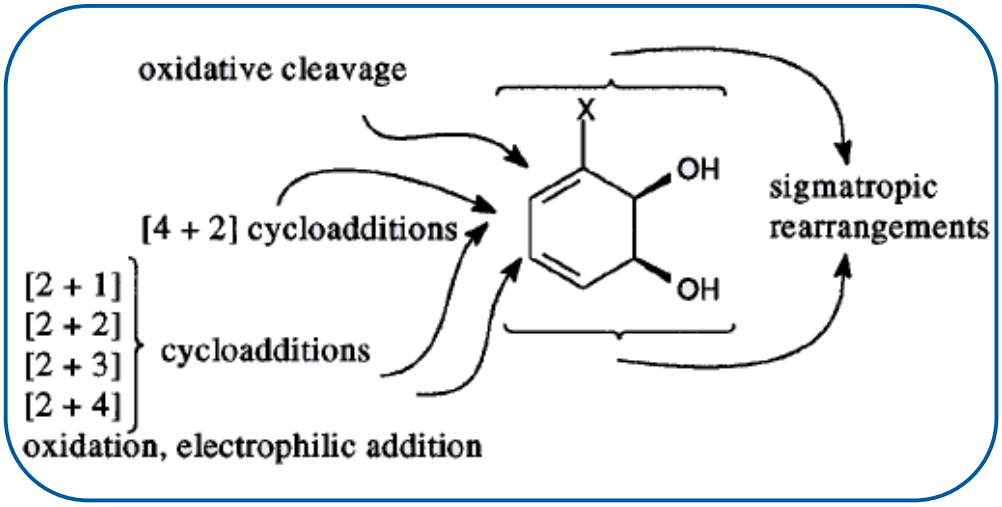

Fig. 5: Different reaction possibilities of *cis*-dienediols. (Adapted from Ref. 44).

1.4.2. The [4+2] Cycloaddition or Diels-Alder Reaction

For our purpose to synthesize three-dimensional molecules, the [4+2] cycloaddition or Diels-Alder reaction with the conjugated diene unit in the *cis*-dienediols, was of particular interest.

Since the invention in 1928, the Diels-Alder reaction is one of the well-investigated and widely used reactions in synthetic organic chemistry. It involves two reaction partners, a diene and dienophile, and is used for the construction of cyclic, polycyclic and hetero-cyclic compounds. New C-C, C-N or C-O bonds are formed, mostly under mild and simple reactions conditions in a single-step conversion. A bridged bicyclic skeleton may be obtained with either one or two cyclic reaction part-ners. The formation of two regio-isomers, the *endo* and *exo* forms of the resultant cycloadduct are therefore possible. However, in most instances the reaction is highly stereospecific and leads to the *endo* product. The diene skeleton present in the *cis*-diendiols is known to be reactive in cycloadditions. A first Diels-Alder reaction with

such a molecule was reported in 1973 by Kobal *et al*. in an attempt to confirm the stereochemistry of a dihydrodiol.[43]

In this work, two types of reaction partners for the dienediols were considered for the generation of the bridged bicycles. Either dienophiles containing privileged structures, for example, chalcone or flavanoid structures, or molecules possessing physico-chemical parameters favourable for druglikeness.

1.5. Outline of the thesis work

In the course of this thesis work, the following tasks were planned to be carried out.

I. Synthesis of a collection of dienophiles as precursors for the cycloaddition reaction.
II. Generation of a collection of bridged bicyclic compounds by Diels-Alder reactions between the dienophiles and dienediols supplied by a commercial source or by the lab of Bernd Hofer.
III. Assessments of how many of the bridged bicycles if any possess general bioactivity.
IV. For compounds positive in step III, characterization of the type of bioactivity with the aid of two different profiling methods, namely cellular impedance measurement and high content analysis with automatic microscopic imaging.
V. For compounds positive in step IV, verification of the profiling results by specific biological assays.

Questions to be answered in the course of this work include

I. Is it possible to obtain bioactive compounds by the devised synthetic route?

II. Do the bioactive compounds obtained show preferences for certain cellular processes?

III. Can the results of the profiling methods be confirmed by the specific bioactivity assays?

2. Results and Discussion

2.1. Chemistry

The generation of a mini library of bridged bicyclic compounds was pursued by a chemo-enzymatic pathway, shown in Fig. 4. One of the dienediols was from a commercial source; the others were supplied by the laboratory of Dr. Bernd Hofer. Therefore, the first part of this thesis starts with the second step of the above-mentioned pathway, a [4+2] cycloaddition or Diels-Alder reaction. This required the synthesis of most of the dienophile reaction partners (see below). Subsequently bridged bicyclic compounds were synthesized. Compound purification was done by flash column chromatography unless stated otherwise. The analytical techniques routinely used (unless stated otherwise) for the assessment of compound purity and structure were NMR and mass spectrometry.

2.1.1. Synthesis of dienophiles

From the chemical point of view, the dienophiles considered as reaction partners fall into two groups, maleimide-based and quinone-based dienophiles. Some of the dienophiles were from commercial sources, but the majority was synthesized as part of this thesis. An overview showing all of these dienophiles is given in Fig. 6. The reactions carried out for the synthesis of dienophiles, are described in the following chapters.

2.1.1.1. Synthesis of *N*-aryl or -alkyl maleimides

For the synthesis of *N*-aryl or -alkyl maleimides dienophile reaction partners, different substituted aromatic or aliphatic amines were reacted with maleic anhydride to produce *N*-aryl maleimides. The latter contain two electron-withdrawing groups on the

dienophile which enhances their reactivity in cycloaddition reactions. Seven maleimide derivatives were prepared as shown in Scheme 1. Maleic anhydride (1) was reacted with the aromatic or aliphatic amines (2) in diethylether or in ethyl acetate at RT to afford the corresponding aryl-oxoaminobutenoic acid intermediate (3) in excellent yield. Subsequent cyclization with sodium acetate and acetic anhydride at 80 ^{o}C[45] afforded *N*-aryl or –alkyl maleimides in moderate to good (40-65%) yields. Two more *N*-aryl- and *N*-alkyl-substituted maleimides were bought from a commercial source (shown in Fig. 6).

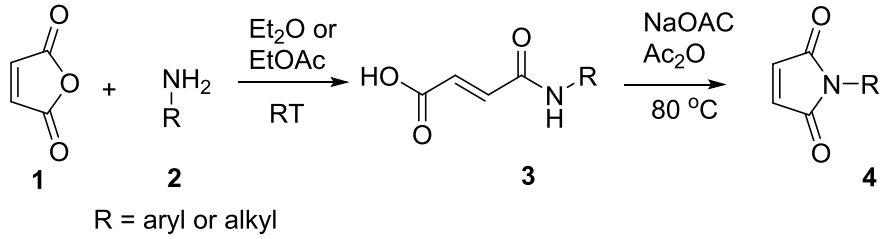

Scheme 1: Reaction scheme for the synthesis of *N*-aryl or -alkyl maleimides

2.1.1.2. Synthesis of 4'-aminochalcone-based maleimides

Chalcones or 1,2-diphenyl-2-propen-1-ones are Michael acceptors and comprise an important natural product group belonging to the flavonoid family.[46] They have been reported to have wide variety of biological activities.[47] Therefore, the dienophile collection was further enlarged by the synthesis of 4-aminochalcone-based maleimides as described by Jha *et al*..[48] This is depicted in Scheme 2. The reaction between 4'-aminoacetophenone (5) and maleic anhydride (1, Scheme 1) produced 4'-acetyl-*N*-maleanilinic acid as intermediate (7). Claisen-Schmidt condensation between this compound and various substituted aryl aldehydes (8) afforded the 4'-aminochalcone-maleimic acids (9). Dehydration of the latter with sodium acetate and acetic anhydride yielded the desired chalcone-maleimide derivatives (10). Due to activation by

its electron-withdrawing neighbouring groups, it is the C-C double bond of the maleimide unit, not of the chalcone, that later will participate in the [4+2] cycloadditions.

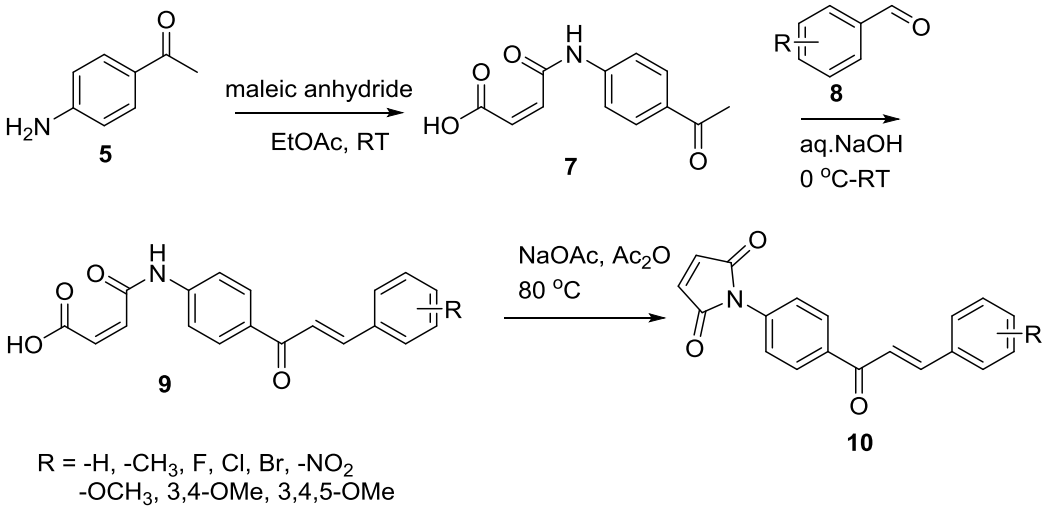

Scheme 2: Synthetic pathway for the preparation of 4'-aminochalcone-based maleimides.

2.1.1.3. Synthesis of 4'-aminocinnamate-based maleimides

As the substituted and unsubstitued *trans*-cinnamic acids and their derivatives possess a variety of biological activities,[49a,b] three 4'-aminocinnamate-based maleimides were included in the dienophile collection.

2.1.1.3.1. Synthesis from methyl-p-aminocinnamate

Trans-p-aminocinnamic acid was first esterified with methanol under acidic conditions to obtain methyl-*p*-aminocinnamate (11). As shown in

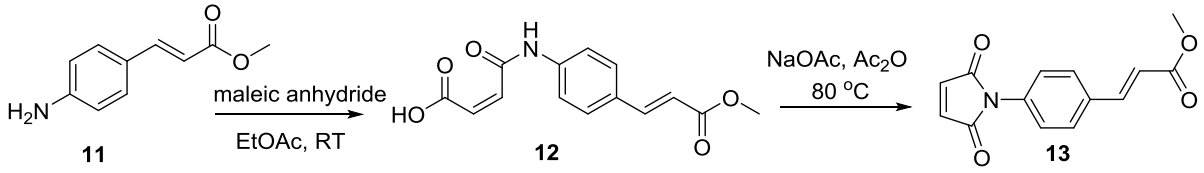

Scheme 3, this was then reacted with maleic anhydride to obtain the oxoaminobuten-

ioc acid intermediate (12). Cyclization with sodium acetate and acetic anhydride resulted in methyl-4'-aminocinnamate-maleimide (13).

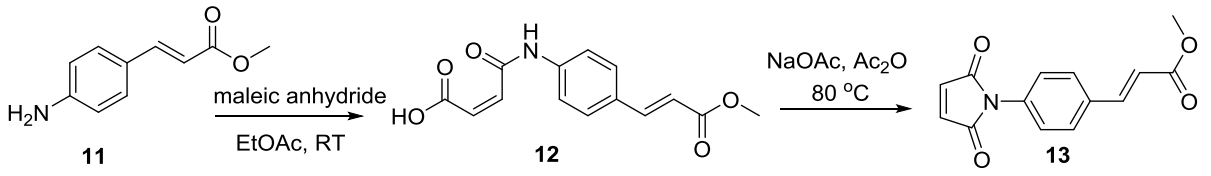

Scheme 3: Synthetic route for the preparation of 4'-amino methylcinnamate-based maleimide.

2.1.1.3.2. Synthesis from 4-aminomethylcinnamic acid

An alternate route using the free acid (Scheme 4) was taken into consideration because of the possibility to diversify the maleimide in the last step by different esterifications. As shown in

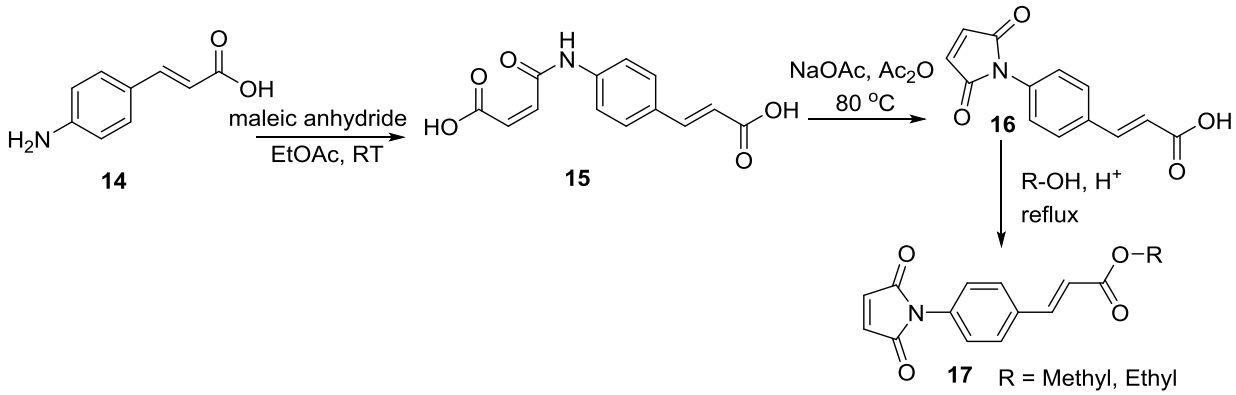

Scheme 4, *trans*-*p*-aminocinnamic acid was first reacted with maleic anhydride in ethyl acetate at RT to form the oxoaminobutenoic acid intermediate (15). Dehydration of the intermediate with sodium acetate and acetic anhydride yielded 4'-aminocinnamic acid-based maleimide 16. Reactions to form the intermediate (15) and the latter cyclization to get compound (16) proceeded equally well as with the ester (11, Scheme 3). Esterification of the acid 16 with methanol or ethanol under acidic conditions yielded the respective alkyl-4'-aminocinnamte-maleimides. The products possessed the expected *E*- configured double bond. This was shown by the *trans*-specific coupling constants in ^{1}H NMR spectroscopy.

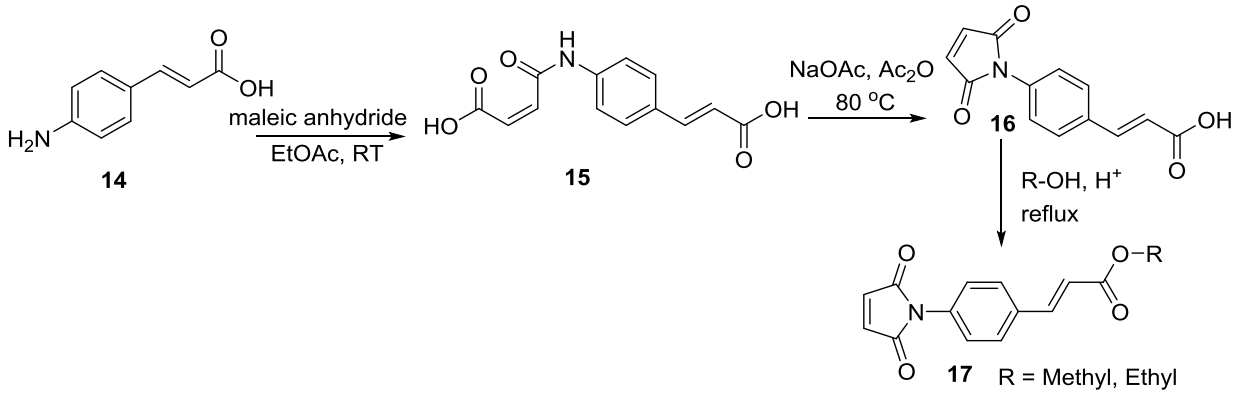

Scheme 4: Alternate route for the synthesis of -4'-amino alkylcinnamatebased-maleimides

2.1.1.4. Synthesis of a chromone-based maleimide

Chromones are one of the major classes of naturally occurring compounds. Chromone is the core structure of flavonoids. Thus, it is not surprising that chromones have been reported to posses multiple biological activities.[50] Therefore, a chromone-based maleimide was synthesized as shown in scheme 5. First, commercially available 7-amino-2-methylchromone (18) was reacted with maleic anhydride (Scheme 1) followed by cyclization to afford a chromone-maleimide compound (20) with good yield (70%).

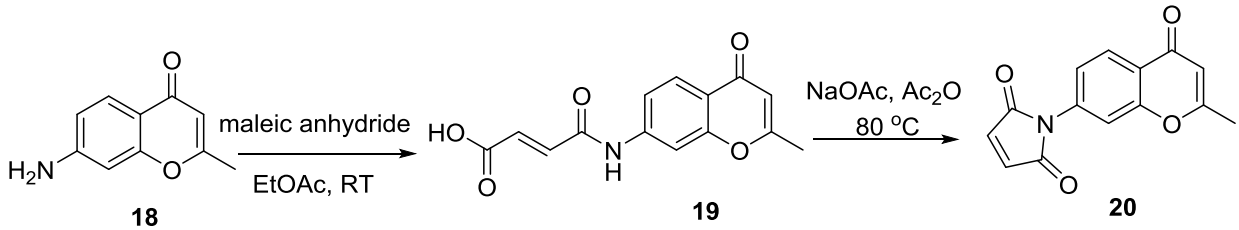

Scheme 5: Reaction scheme for the preparation of 7-maleimido-methyl chromone

2.1.1.5. Synthesis of amino-*N*-alkanoic acid-based maleimides

Further diversification of maleimide dienophiles was attempted by reacting maleic anhydride with aminoalkanoic acids,[51] as depicted in Scheme 6. These products were later not reacted at preparative scale with the dienediols, because their reactivity in cycloaddition reactions was found to be sluggish.

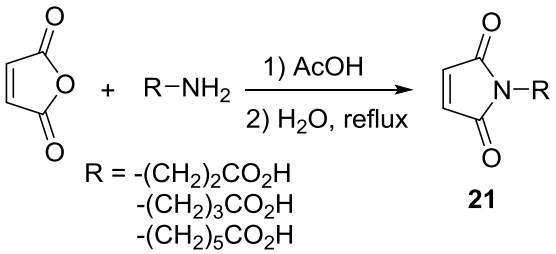

Scheme 6: Synthesis for amino-*N*-alkanoic acid-based maleimides

2.1.1.6. Overview of the dienophiles

All dienophiles used in subsequent cycloadditions are shown in Fig. 6. Five were from commercial sources (see legend); the others were synthesized as described in the preceding chapters. In these reactions, reactivities and yields were similar to data reported in the literature.[52,53,54] The chromone-based maleimide D22 and the chalcone-based maleimide D20 were not previously described in the literature.

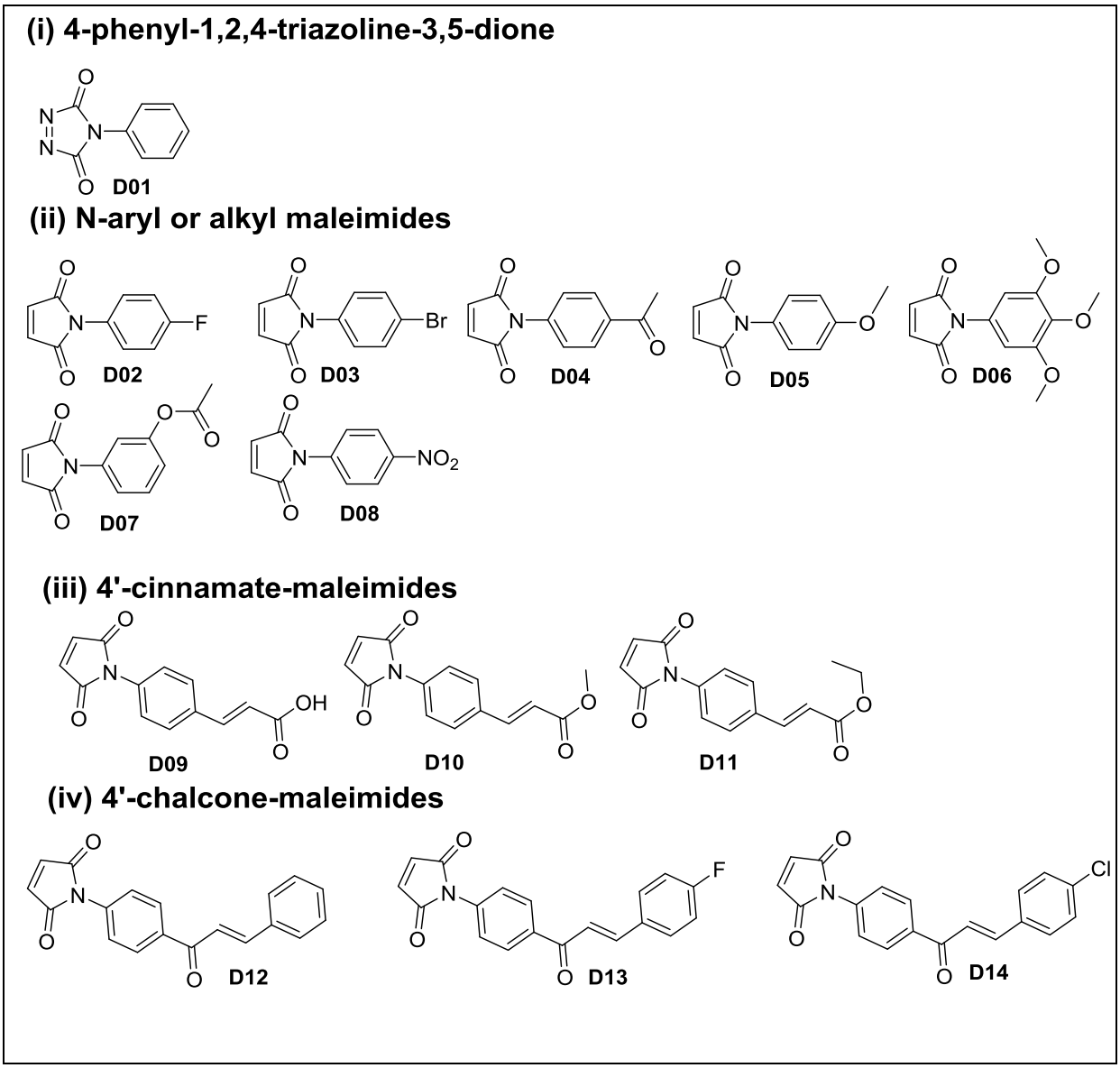

Figure continued on next page…

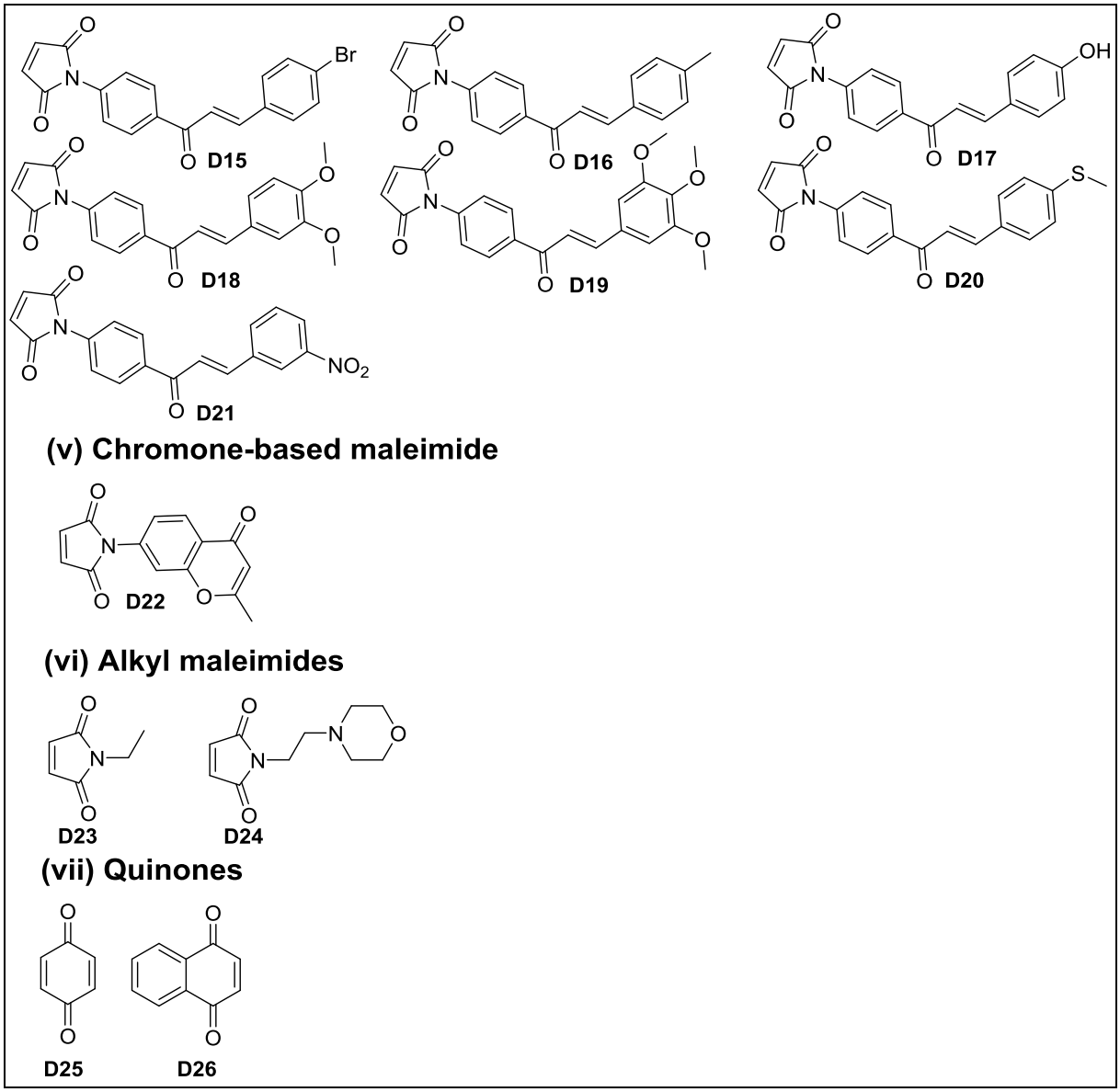

Fig. 6: Overview of structures of dienophiles synthesized in the course of this thesis or obtained commercially (D01, D03, D23, D25 and D26).

2.1.2. Synthesis of bridged bicyclic compounds

Bridged bicyclic compounds are a class of molecules that possess a permanent three-dimensional structure. A collection of bridged bicyclic compounds was synthesized by means of the Diels-Alder reaction as outlined in the introduction (Fig. 4). In

order to optimize the reaction conditions for the cycloaddition reactions, experiments were started with a simple diene, 1,3-cyclohexadiene, and commercially available dienophiles like benzoquinone, naphthoquinone, substituted maleic anhydrides, *N*-aryl and -alkyl maleimides. The reactions with *N*-aryl and alkylsubstitued maleimides afforded products in considerably good yields. These reactions proceeded well in chloroform as solvent at reflux conditions. Therefore the identical conditions were considered for the reactions with dienediols 22 and 23.

2.1.2.1. Synthesis of bridged bicyclic compounds from (1*S*-*cis*)-3-bromo-3,5-cyclohexadiene-1,2-diol (22)

In order to establish the reaction conditions for the Diels-Alder reaction with a protected dienediol, the first round of experiments was carried out with a commercial dienediol, (*1S*-*cis*)-3-Bromo-3,5-cyclohexadiene-1,2-diol (Scheme 7, 22), which was available in gram quantities.

2.1.2.1.1. Protection of (*1S*-*cis*)-3-bromo-3,5-cyclohexadiene-1,2-diol (22)

It was reported that synthetic applications involving *cis*-diol metabolites often require protection of the hydroxy groups.[55] Therefore the two hydroxy groups of the dienediol were reacted at low temperatures with 2,2-dimethoxypropane to form an acetonide (23), as shown in Scheme 7.[56] This was obtained in excellent yield (90%) after rapid purification by flash column chromatography. A dimerization of acetonides (protected diol) was reported upon storage at -30 ºC in pure form.[57] Therefore the compound was prepared in 100 milligram quantity, diluted in dichloromethane to approximately 10M and stored at -70 ºC until it was used in further reactions. Dimerization (approximately 25 %) was observed even at -70 ºC after several weeks.

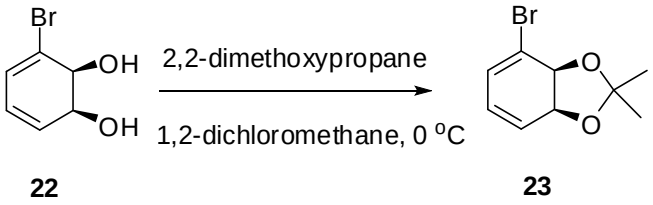

22 **23**

Scheme 7: Protection of hydroxy groups with 2,2-dimethoxy propane

2.1.2.1.2. [4+2] cycloaddition reactions with the protected diol, (*1S-cis*)-3-bromo-3,5-cyclohexadiene-1,2-diol (23)

The acetonide (23) was reacted with all maleimido-dienophiles shown in Fig. 6 except for D08, D12, D14, D16, D25, and D26, to afford bridged bicyclic structures in a simple one-step reaction. Reaction progress was monitored by thin layer chromatography (TLC). The rates of these reactions, when performed at RT, were sluggish, thus affording long reaction times (4-7 days). Refluxing the solution of the protected dienediol (23) and a dienophile in chloroform resulted in good yields of a mixture of two products in an approximate ratio of 3:2 with some exceptions, which are described later (see 2.1.2.3). The NMR characterization showed that they were isomers of the expected product. Their ratio was similar to data given in previous reports.[57] Both isomers were separated well, with an R_f difference of 0.3. They were purified by flash silica gel column chromatography and characterized by proton and carbon NMR spectroscopy. As expected, the dienophile was added to the dienediol (23) in a stereoselective manner to give only *endo* isomers. The major adduct was the result of an *endo*-addition of the dienophile *syn* to the isopropylidenedioxy ring face of the diene, and the minor adduct was formed by an *endo*-addition to the *anti*-face of the diene, as depicted in scheme 8.[57,58] These structures were identified by two dimensional NMR spectroscopy with NOE data. In case of the *endo-syn* isomer, a through-space interaction was found between one of the methyl groups of the isopropylidine

ring and the methine protons of the maleimide moiety. For the *endo-anti* isomer, a similar proximity was observed between the methine protons of the maleimide ring and the protons on the carbons bonded to the two oxygens of isopropylidine ring.

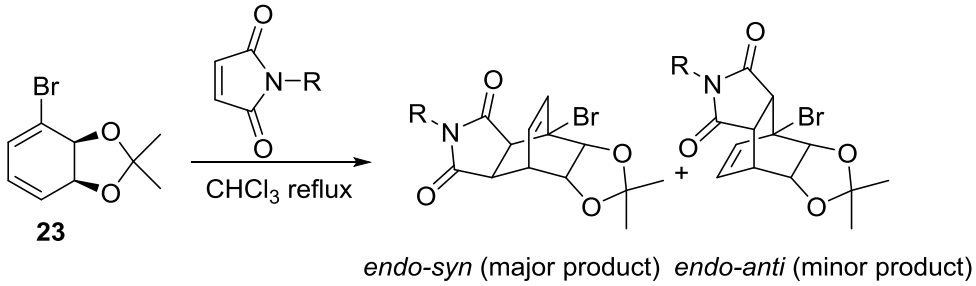

Scheme 8: Isomers formed in cycloadditions between dienediol 23 and various dienophiles. *Syn* and *anti* are assigned with respect to isopropylidine ring.

2.1.2.1.3. Deprotection of the acetonide group

In the specific interactions between small molecules and their cellular targets, hydrogen bond donors and acceptors play a major role to provide binding strength and specificity.[59] The removal of the acetonide group provides two additional free hydroxy groups that possess both hydrogen bond donor and acceptor capability. To deprotect the cycloadducts, compounds were refluxed under acidic conditions like aqueous trifluoroacetic acid and amberlyst acidic resin, as previously reported.[60a,b] However, all reactions resulted in poor yields (less than 30%).

2.1.2.1.4. [4+2] cycloaddition reactions with unprotected (*1S-cis*)-3-bromo-3,5-cyclohexadiene-1,2-diol (22)

Because of the poor yields in deprotection, Diels-Alder reactions were attempted without prior protection of the hydroxy groups. Cycloadditions were performed with the dienediol 22 and the entire collection of dienophiles (Fig. 6). Progress of the re-

actions was monitored by TLC. The first reactions were done under the same conditions stated above, but the reactions proceeded at very slow rates and required 2-4 days. Therefore conditions were changed to toluene reflux with a temperature increase of 40 ºC. This alleviated the product formation and significantly reduced the reaction time (24 h). These conditions were applied for all of the dienophiles. Cycloaddition products from all dienophiles were obtained successfully in moderate to good yields in the range of 40-70%, except with quinone-based dienophiles (D25, D26). The reaction profiles, as analyzed by TLC were clean, showing the two isomers and a low percentage of undesired products. The isomers ratio with all dienophiles was discussed later (see 2.1.2.3). The TLC separation of the two unprotected isomers was good with a R_f value of 0.6 for the *endo-syn* and of 0.3 for the *endo-anti* isomer. The quinone-based dienophiles D25 and D26 were reacted under conditions reported for a similar cycloaddition reaction with identical dienophiles[61a,b,c] i.e., refluxing in tetrahydrofuran and water (9:1) to obtain the cycloadducts. No compound was isolated from the reaction with D15 because of the product instability.

Cycloaddition reactions with prtotected and unprotected *cis*-dienediols were first reported by Gillard and Burnell.[58] They reacted *cis*-cyclohexa-3,5-diene-1,2-diol with two dienophiles. The yield with both protected and unprotected dienediols was similar to what was obtained with dienediols 22 and 23 in the current work. According to Gillard and Burnell, the protected dienediol showed higher reactivity than the unprotected one under identical conditions. However, with dienediols 22 and 23 the reactivity observed towards several dienophiles was the same under identical reaction conditions.

An overview of the structures of all cycloaddition products obtained from di-enediols 22 and 23 is shown in Fig. 7. It also includes cycloadducts that had been subjected to additional modification reactions which are described later (2.1.3). All bridged bicyclic compounds shown were not previously reported.

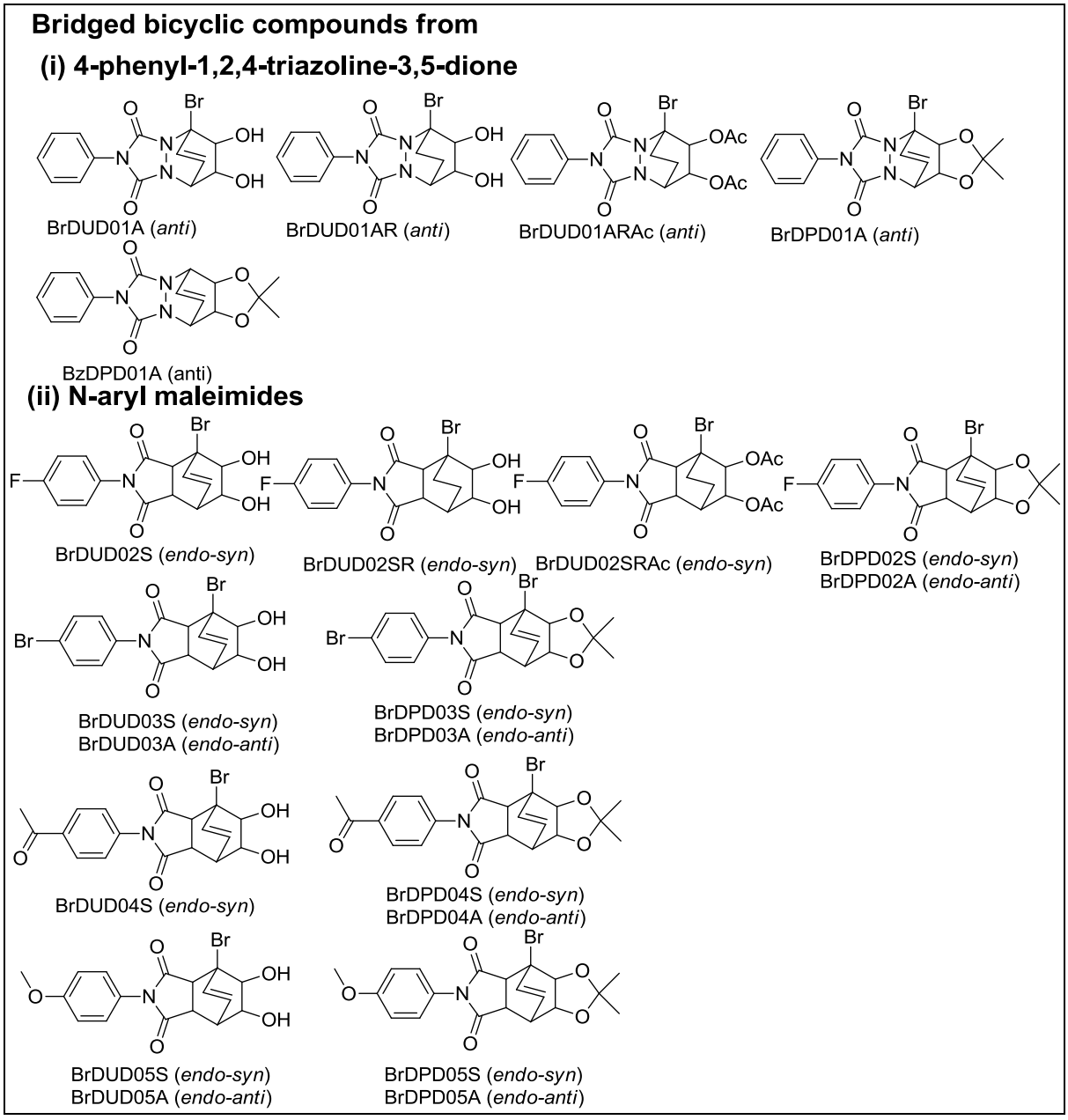

Fig continued on next page…

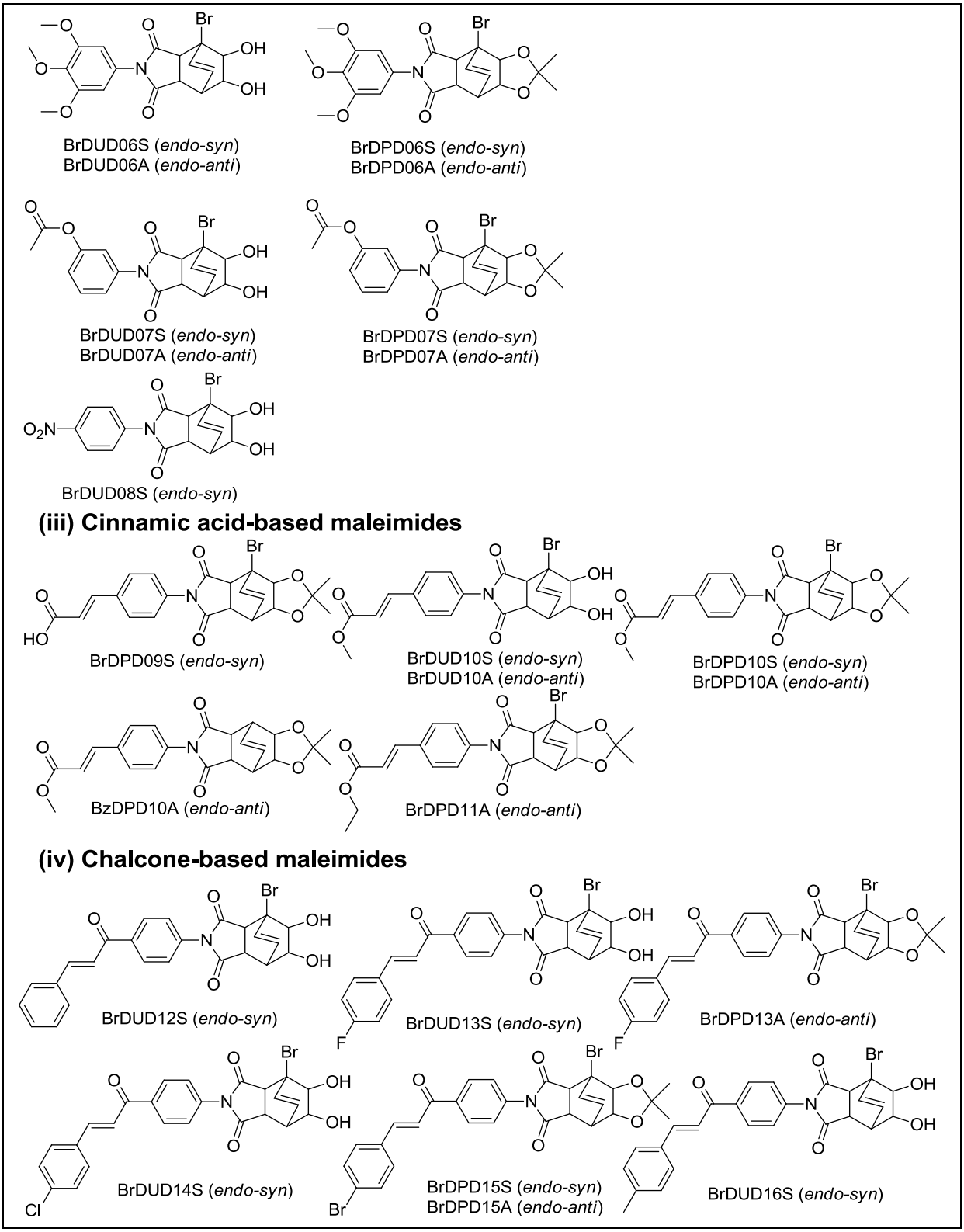

Figure continued on next page…

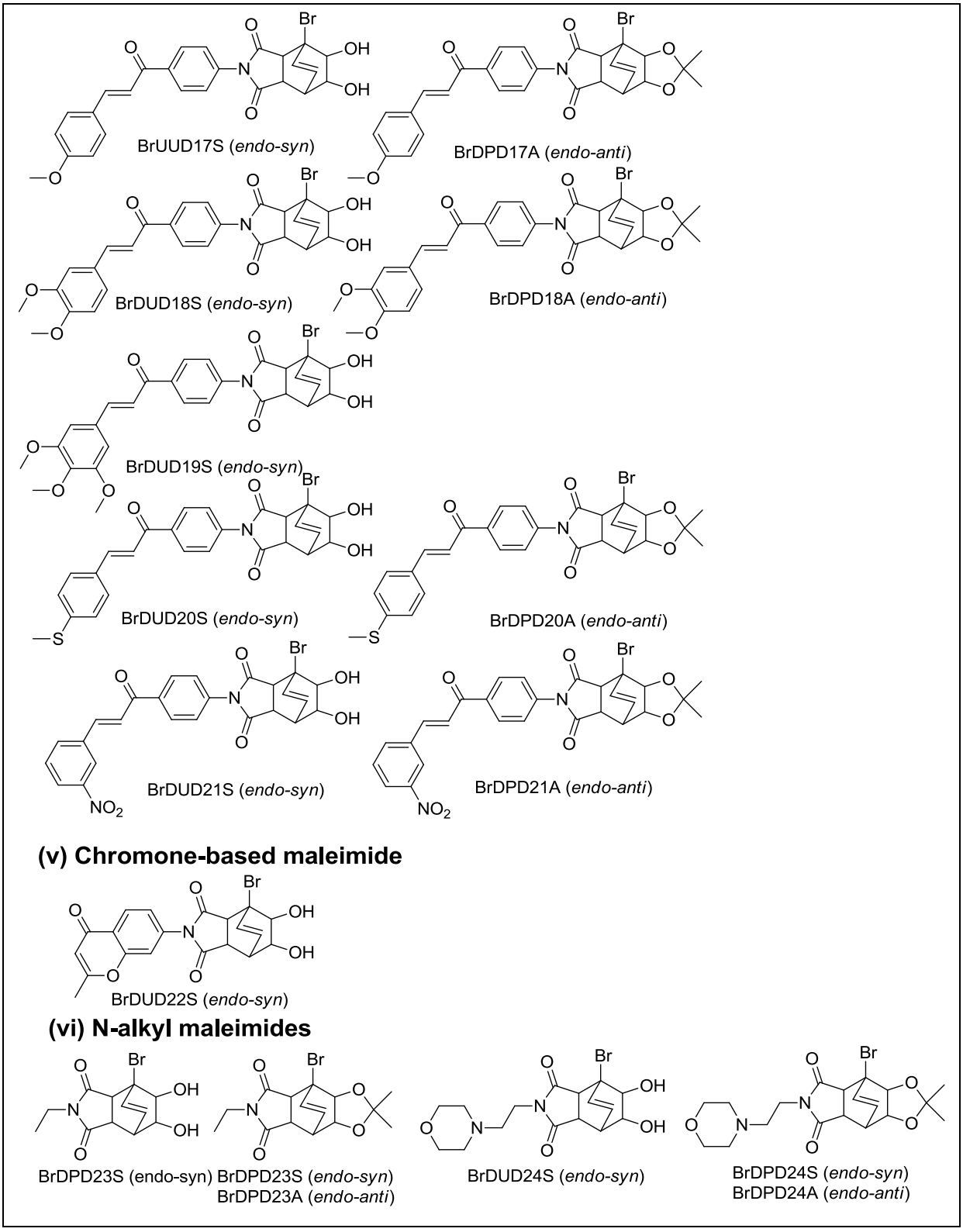

Figure continued on next page…

(vii) Quinone-based maleimides

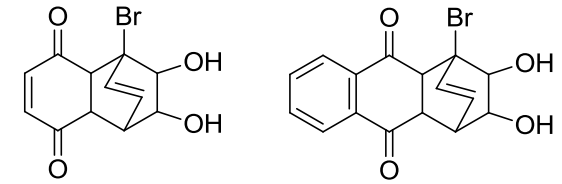

BrDUD25S (*endo-syn*) BrDUD26S (*endo-syn*)

Fig. 7: Structures of bridged bicyclic compounds obtained from cycloaddition reaction between dienediols 22, and/or 23 (Scheme 7) and our collection of dienophiles (Fig. 6). This overview also shows same additionally modified molecules (see 2.1.3). Structures are ordered by the number given to the dienophile. The compound codes shown contain the following information. The first three letters are the dienediol abbreviations used, BrD for dienediol 22 and BzD for the debrominated dienediol 22. 'P' or 'U' stands for protected or unprotected, respectively. This is followed by the dienophile number. The next letter represents the stereochemistry of the structure, either *–syn (S)* or *–anti (A).* Occasionally this is followed by R for reduction of the C-C double bond in one of the bridges or Ac for acetyl protection of the hydroxy groups.

2.1.2.2. Synthesis of bridged bicyclic compounds from hetero-aryl benzenes

Many privileged structures are hetero-aromatic scaffolds. Therefore, such hetero-aryl structures were selected as starting material for the synthesis of a second series of bridged bicyclic compounds.

2.1.2.2.1. Synthesis of *cis*-dienediols from hetero-aryl benzenes

Five hetero-aryl-substituted benzenes were converted to corresponding *cis*-dienediols with recombinant bacterial cells that efficiently synthesize an aryl-hydroxylating dioxygenase enzyme. The respective dienediol structures are shown in Fig. 8. As can be seen, dienediol formation was always directed towards the ortho

and para positions of the homo-aromatic ring, whereas the hetero-aryl substituent remained unchanged.

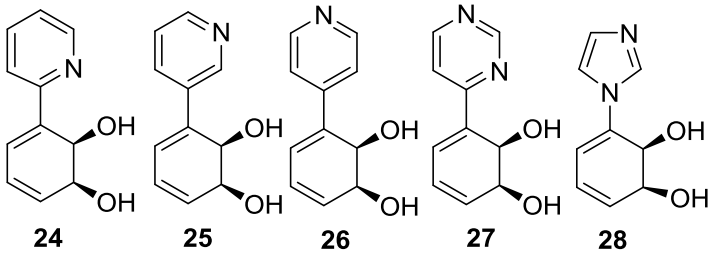

Fig. 8: Structures of hetero-aryl dienediols dienediols

After purification these compounds were obtained in quantities around 100 mg. They were supplied by the laboratory of Bernd Hofer.[62] Because of the limited amounts, cycloaddition reactions with these dienediols could only be carried out with a small number of the available dienophile partners.

2.1.2.2.2. Selection of dienophiles for the cycloadditions with hetero-aryl dienediols

Nine dienophiles were selected for the synthesis of cycloadducts with hetero-aryl dienediols. This was based on reactivity and yields with dienediols 22 and 23 and on the results of the biological activity screening of the first collection of bridged bicycles (see 2.2.1). With respect to biological activity as measured in the cytotoxicity assay, a threshold IC_{50} value around 15 µg/mL was set for the selection. But this was not strictly obeyed for the sake of structural diversity. Six of the selected dienophiles (D13, D17, D18, D19, D20 and D21, see Fig. 6), were chalcone-based maleimides and the rest were N-(3,4,5-trimethoxy phenyl)maleimide (D06) and 4-phenyl-1,2,4-triazoline-3,5-dione (D01).

2.1.2.2.3. Cycloadditions with hetero-aryl dienediols

Because of the problems with deprotection of the bridged bicyclic products derived from the protected dienediol 23, all cycloadditions were carried out with unprotected hetero-aryl dienediols. The first cycloaddition reactions with the selected dienophiles were performed with dienediol 28 (Fig. 8), which was available in relatively high amount amongst the in-house generated dienediols. Reactions were carried out with three of the selected dienophiles (D06, D10 and D17) under the same conditions used for dienediols 22 and 23. However, the progress of the reactions was very slow. Even after 4-6 days of refluxing, only about 10% of the desired product, but many by-products were observed by LC-MS. Therefore reaction trials were carried out. They were limited to only one dienophile (D10) because of its high reactivity. Different solvents like tetrahydrofuran and dioxane were used, but there was no improvement in the conversion. Thereafter, the reaction was carried out in a sealed tube with chloroform as solvent at 100-120 ºC for 3 days, but no substantial improvement was observed in the product formation. However the product with the dienophile D10 (Fig. 9, ImDUD10S), was synthesized on preparative scale, following the sealed tube reaction conditions. The yield was rather low (22%), but sufficient for isolation by preparative HPLC. Only one compound was obtained after purification, and NMR spectroscopy showed that the isolated product was in the *endo-syn* configuration, as expected from the previous reaction products of the unprotected dienediol 22.

Because of these disappointing results, several attempts were undertaken with dienediol 28 by employing microwave irradiation. In the past few years cycloaddition reactions in many cases have greatly benefited from the focused microwave irradiation, if they normally require elevated reaction temperatures for lengthy times

and high pressure. The short reaction time associated with microwave activation avoids decomposition of reagents and products. It also prevents polymerization of dienes and dienophiles.[63a,b] Microwave conditions with different reaction times in a sealed vessel were tried with dienediol 28, but there was no significant change in yield.

In order to check the reactivity of the other dienediols in the cycloaddition, reactions were performed with dienediol 27. The same conditions were used as mentioned above with chloroform as solvent at elevated temperature in a sealed vessel. This time the products were obtained in relatively high yield (40-60%) with all of the selected dienophiles and were isolated.

Dienediol 25 was reacted with the nine dienophiles under similar conditions. The reactivity of this dienediol was slightly lower than that of the dienediol 27. Accordingly, the yields of the cycloaddition products were only in the range of 30-45%. Eight compounds were purified. The only exception was the product from the reaction with D18 (Fig. 6) which was not isolated because of multiple product formation.

Finally dienediol 26 was reacted with two dienophiles D01, D17 (Fig. 6) and 24 was reacted only with D01, because of their limited availability. The reactivity of both of these dienediols was similar to that of dienediol 25.

Altogether, 21 bridged bicyclic compounds were synthesized with the five hetero-aryl dienediols (Fig. 9). The predominant products formed were always the *endo-syn* isomers with approximate ratios of 9:1, except for dienophile D01. For D01 isolated isomers were in the *endo-anti* configuration. Only the major isomers were isolated for further use. They were purified by flash chromatography and characterized by NMR and high resolution mass spectrometry.

Bridged bicyclic compounds from

(i) (1*S*,2*R*)-3-(pyridin-2-yl)cyclohexa-3,5-diene-1,2-diol

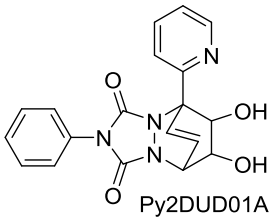

(ii) (1*S*,2*R*)-3-(pyridin-3-yl)cyclohexa-3,5-diene-1,2-diol

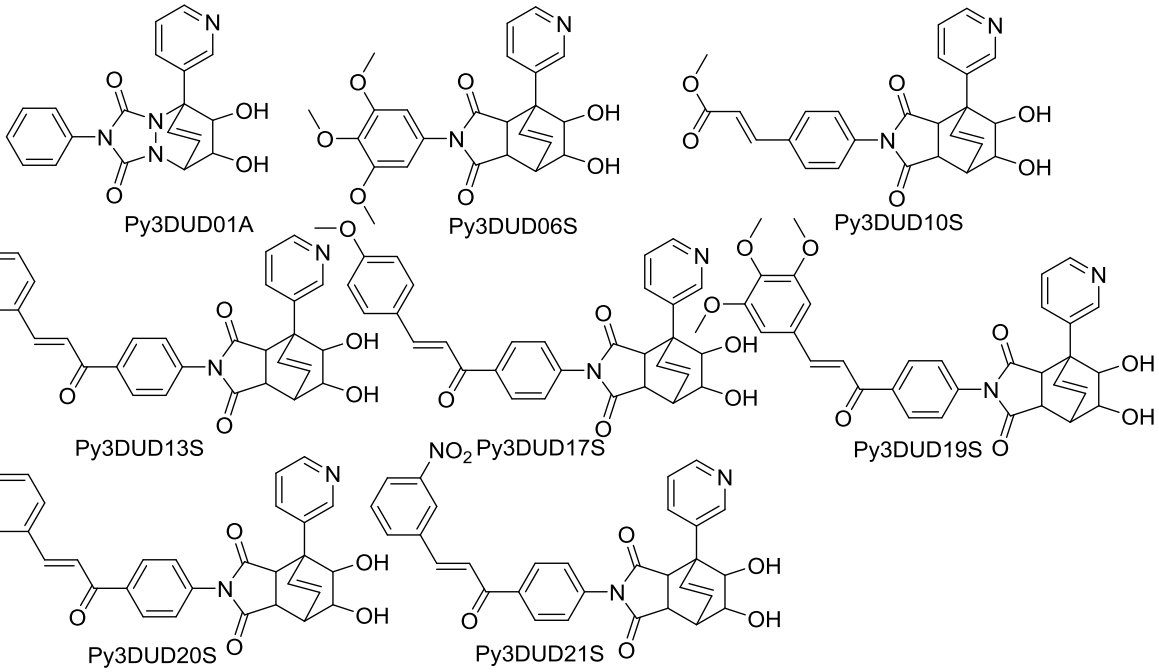

(iii) (1*S*,2*R*)-3-(pyridin-4-yl)cyclohexa-3,5-diene-1,2-diol

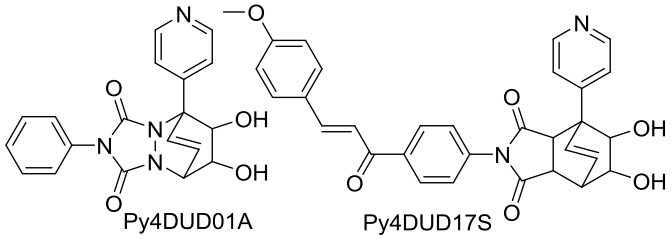

(iv) (1*S*,2*R*)-3-(pyrimidin-4-yl)cyclohexa-3,5-diene-1,2-diol

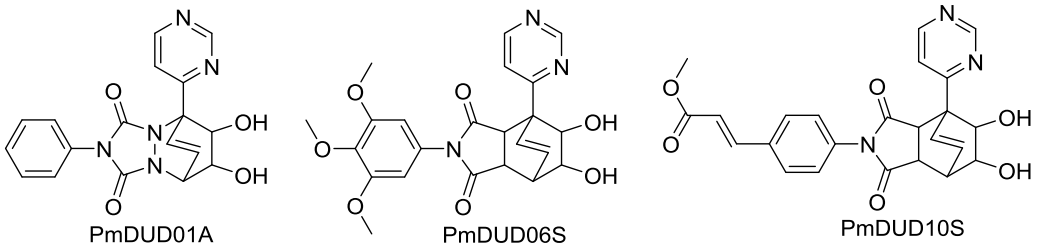

Figure continued from previous page…

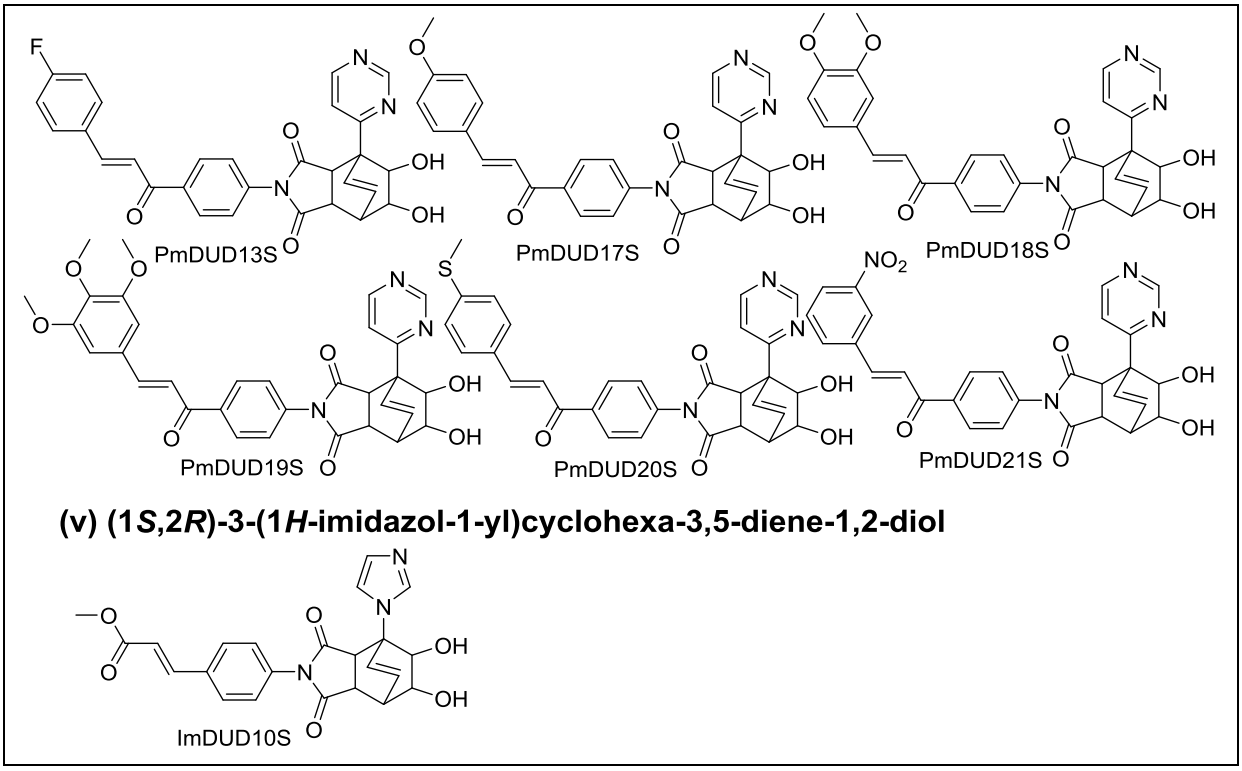

Fig. 9: Structures of the cycloaddition products obtained from the reaction between hetero-aryl dienediols and nine selected dienophiles. All isolated isomers were *endo-syn*, except for dienophile D01, where all isolated isomers were in the *endo-anti* configuration. The structures are ordered according to the dienediol number. Details of compound codes are given in the legend of Fig. 7. Dienediol abbreviations are Py2D, Py3D, Py4D, PmD and ImD for dienediols 25 to 28 (**Fig. 8**).

2.1.2.2.4. Reactivity of the hetero-aryl dienediols

The lower reactivity of the hetero-arylsubstituted dienediols in the cycloaddition reactions, in comparison to the dienediol 22, may be explained by the electron distribution between the diene and the hetero-aromatic ring attached to the dienediols. In terms of molecular orbital theory, in a normal electron-demand Diels-Alder reaction, electron-donating groups on the diene skeleton increase the energy of its highest occupied molecular orbital (HOMO), thereby leading to a smaller energy gap with the lowest unoccupied molecular orbital (LUMO) of the electrophilic dienophile. Electron-withdrawing groups show the opposite effect and decrease the reactivity of the diene. Therefore, the extended conjugation system present in the hetero-aryl rings at-

tached to the dienediol strongly withdraws electrons from the diene even when the heterocyclic nitrogens are not directly attached to the diene, thus making it more stable towards the reaction. In dienediols 22 and 23, the bromine is less electron-withdrawing than the aromatic heterocycles. Thus, compounds 22 and 23 are more reactive than their hetero-aryl counterparts.

2.1.2.3. Preferences in isomer formation in the cycloaddition reactions

The protected dienediol 23, when reacted with the dienophiles of the collection, in most cases yielded *endo-syn* and *endo-anti* isomers in a 3:2 ratio. However, there were some significant exceptions. In the reactions with dienophiles D10 and D11 (Fig. 6), the two isomers were produced in a 1:2 ratio and the cycloaddition with dienophile D23 yielded a 2:3 ratio. The typically observed preference for the *syn* isomer agrees with literature data on Diels-Alder reactions with the acetonides of dienediols, which reported similar preferences for this isomer.[58,64,65] However, no explanations were given for this selectivity. Typically, acetonides of dienediols show a strong preference for formation of the *anti* adduct.[64,65] The *syn* priority seems to be a special case that is observed with maleimides as dienophiles.[65] A strong *syn* selection is generally noticed when the diol groups of the dienes are not protected (my results discussed below).[64,65] This is ascribed to the formation of H-bonds between the diol and the dienophile which direct the latter to the *syn* face.[64] We propose a similar effect also for protected diols. The two oxygens are still available as H-bond acceptors. Hydrogens at double- or triple-bonded carbons possess certain acidity. In the case of maleimide, this is expected to be enhanced by the vicinal oxygens. Therefore, the formations of weak bonds of these lowly acidic hydrogens to the acetonide oxygens may exert a weak directing effect towards the *syn* face. When comparing the struc-

tures of the dienophiles that yielded a lower preference for the *syn* isomer (D10, D11, D23) to the structures of related dienophiles, that showed a higher *syn* preference (e.g. D09, D24), a straightforward explanation for these differences was not apparent.

The strongest deviation from the *syn* preference was noticed with D01, which exclusively yielded the *anti* isomer. This is in agreement with literature data[43,64] and is probably explained by a strong electrostatic repulsion between the lone electron pairs of the acetonide oxygens and of the triazolidinone nitrogens upon approach of the dienophile at the *syn* face. [58,64]

Isomer ratios showed much less variations in the reactions with unprotected dienediols, the one derived from bromobenzene as well as those derived from the heteroaromatics. Here, all dienophiles, with the single exception of D01, yielded *syn* and *anti* isomers in a ratio of approximately 9:1. Therefore, the stereochemical outcome of these cycloadditions can be interpreted, as just mentioned, by electrostatic repulsions in the case of D01 and by H-bonding in all other cases.

2.1.3. Structural modifications of bicyclic compounds

Because of their available quantity, four compounds were considered for further modification by introduction of small structural changes. Small changes would allow to correlate potential differences in biological activity with single structural features. The modifications were introduced with single-step reactions.

2.1.3.1. Debromination

A radical debromination reaction was performed with the acetonides of two compounds, BrDPD10A and BrDPD01S, as shown in Scheme 9, using tributyltin hydride and AIBN.[66] The desired compounds were obtained in 60-70% yields after purification.

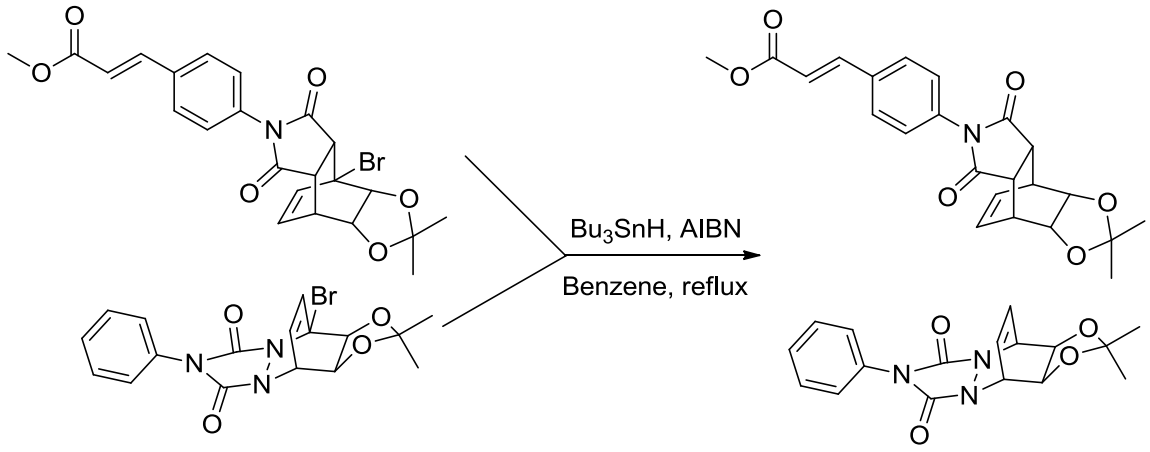

Scheme 9: Free-radical-mediated debromination

2.1.3.2. C-C double bond reduction

.In two unprotected compounds (BrDUD02S and BrDUD01A), the double bond present in the unsubstituted bridge was reduced by hydrogenation with activated palladium, as shown in Scheme 10, to afford the desired compound with 85% yield.[67] Subsequently, the free hydroxy groups were protected with acetyl functionality to obtain compounds with different substitutions on the free hydroxy groups. Acetylation protects hydroxy groups without introducing an extra five-membered ring on the bicyclic core structure.

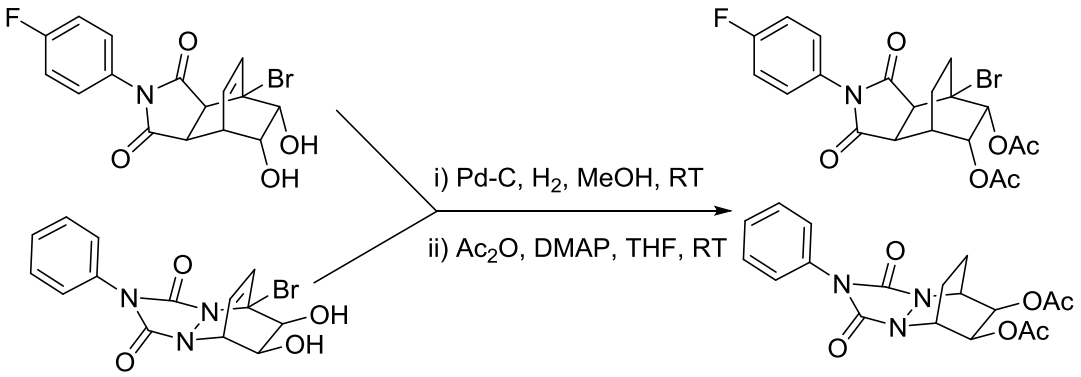

Scheme 10: Reduction of the etheno-bridge double bond.

2.2. Biology

2.2.1. Screening for the microbial growth inhibition

Because of the increasing antibiotic resistance of microbial strains, resulting in increased numbers of difficult-to-treat microbial infections, a highly desired, but hard to obtain biological activity is the ability to inhibit microbial growth. The agar diffusion assay is a classical method to determine such activity. The bacteria or fungi to be assayed are suspended in liquefied soft agar which is then poured uniformly onto an agar plate. A paper disc, to which a solution of the compound of interest is applied, is placed on the surface of the agar. The compound diffuses through the disk into the agar. After incubation, halos are observed where the compound concentration is greater than or equal to the one required to inhibit growth. This halo is termed zone of inhibition and its diameter is used to estimate the microorganism's sensitivity to that particular compound.[68]

All of the synthesized cycloadducts were used in the assay. A sensitive Gram-positive bacterial strain *Micrococcus luteus,* and a yeast strain, *Hansenula anomala,*

were used as microorganisms. None of the compounds showed any zone of inhibition with both of the microbial strains.

2.2.2. Screening for growth inhibition of mammalian cells

A cell proliferation test was used for the general screening of the synthesized bicyclic compounds for biological activity. To this end, a colorimetric cell viability assay (MTT assay) was performed with a mouse connective tissue cell line, L929 (fibroblast). In this screening, biological activity is determined as a compound-cell interaction that reduces the number of viable cells.[69] It must be kept in mind that neither this nor any other assay is able to detect all types of bioactivity. Moreover, the obtained viability values vary from one cell type to another. Thus, these are solely specific for the cells used in the test.

In this assay cells were incubated with the test compounds for 5 days. After the incubation period, the number of viable cells was determined by adding a solution of a tetrazole dye, 3-(4,5-dimethylthiazol-2-yl)-2,5-diphenyltetrazolium bromide (MTT). The celluar oxidoreductase enzymes present in viable cells reduce the MTT to the insoluble purple-colored-formazan. Thus, the intensity of the purple color reflects the number of viable cells. In this way half maximal inhibitory concentration values (IC_{50}) of the screened compounds were determined and used as a rough quantification of their bioactivity. The results obtained with bridged bicycles derived from bromobenzene and hetero-aryl benzenes are shown in Tables 1 and 2, respectively.

Table 1: Bioactivity values of bridged bicyclic compounds derived from bromobenzene as determined in a cell viability assay. Standard deviations are indicated. Compound structures are found in Fig. 7.

Compound	IC_{50} (µg/mL)	Compound	IC_{50} (µg/mL)
Compounds from N-phenyl tetrazolidinone		**Compounds from chalcone-based maleimides**	
BrDUD01A	15±2.8	BrDUD12S	19±1.4
BrDUD01AR	25±0.7	BrDUD13S	24±2.8
BrDUD01ARAc	>40	BrDPD13S	12±1.06
BrDPD01A	24±2.8	BrDPD13A	5±0.35
BzDPD01A	10±4.9	BrDUD14S	18±0.7
Compounds from *N*-aryl and –alkyl maleimides		BrDPD15S	12±0.7
		BrDPD15A	12±1.4
BrDUD02S	>40	BrDUD16S	3.5±0.14
BrDUD02SR	>40	BrDUD17S	7±0.35
BrDUD02SRAc	>40	BrDPD17S	20±2.1
BrDPD02A	>40	BrDPD17A	5±0.21
BrDPD02S	>40	BrDUD18S	10±2.8
BrDUD03S	>40	BrDPD18A	10±1.06
BrDPD03S	>40	BrDUD19S	2.5±0.14
BrDPD03A	>40	BrDUD20S	12±2.1
BrDUD04S	>40	BrDPD20S	17±1.06
BrDPD04S	>40	BrDPD20A	14±1.06
BrDPD04A	>40	BrDUD21S	17±0.7
BrDUD05S	>40	BrDPD21A	19±1.4
BrDUD05A	>40	BrDUD22S	>40
BrDPD05S	>40	BrDUD23S	>40
BrDPD05A	>40	BrDPD23S	>40
BrDUD06S	20±1.4	BrDPD23A	>40
BrDUD06A	>40	BrDUD24S	>40
BrDPD06S	>40	BrDPD24S	>40
BrDPD06A	>40	BrDPD24A	>40
BrDUD07S	>40	**Compounds from quinone-based maleimides**	
BrDUD07A	>40		
BrDPD07S	>40	BrDUD25A	7±1.4
BrDPD07A	>40	BrDUD26S	14±0.7
BrDUD08S	16±1.06		
BrDUD08A	>40		
Compounds from cinnamate-based maleimides			
BrDPD09S	12±2.1		
BrDUD10S	>40		
BrDUD10A	>40		
BrDPD10S	18±0.7		
BrDPD10A	6±1.06		
BzDPD10A	7±2.5		
BrDPD11A	>40		

The first set of compounds (Table 1) is significantly larger than the second and enables correlations between small differences in molecular structures and bio-activity values.

As can directly be seen in Table 1, compounds synthesized with cinnamate-based maleimides and chalcone-based maleimides generally showed higher bio-activities than the *N*-aryl and –alkyl maleimide based compounds. More specifically, such differences were also observed in the comparisons of the IC_{50} values of pairs of compounds that are identical except for the absence or presence, respectively, of the α,β-unsaturated keto moiety. For example, compound BrDUD06S (Table 2), showed an IC_{50} value of 20 µg/mL, but its analogue with a chalcone backbone, compound BrDUD19S exerted the same effect at an almost 10-fold lower concentration (2.5 µg/mL). Protection of the diol hydroxy groups resulted in no clear tendency. Both, increases and decreases in activity were observed. When hydroxy groups were protected, the *anti*-isomer always showed higher bioactivity than the *syn*-isomer. This may be seen, for example, in the case of compounds BrDPD17A and BrDPD17S. Amongst the cycloadducts with chalcone backbone, different substitutions of the terminal phenyl ring result in different IC_{50} values. The 3,4,5-trimethoxy and 4-methyl substitutions (BrDUD19S and BrDUD16S) yielded particularly low IC_{50} values of 2.5 or 3.5 µg/mL, respectively. Modifications like debromination (BzDPD01A, BzDPD10A), reduction of C-C double bond (BrDUD01AR, BrDUD02SR) and acetyl protection of hydroxy groups (BrDUD01ARAc, BrDUD02SRAc) of the bicyclic compounds showed no significant influence on their bioactivity.

In the collection of molecules synthesized from hetero-aryl dienediols, all compounds possed unprotected hydroxy groups and all, with the exception of the one derived from D01, were *endo-syn* isomers.

Table 2: Bioactivity values of bridged bicyclic compounds derived from hetero-aryl benzenes as determined in a cell viability assay. Standard deviations are indicated. Compound structures are found in Fig. 9. Values of the respective molecules derived from bromobenzene (unprotected dienediol 22) are included for comparison.

Dienophiles used for synthesis	**IC_{50} vlaues (µg/mL)**					
	Dienediols used for synthesis					
	22	**24**	**25**	**26**	**27**	**28**
D01	15±2.8	30±3.5	25±4.2	30±1.4	35±4.9	NP*
D06	20±1.4	NP	>40	NP	29±2.83	NP
D10	>40	NP	22±3.53	NP	36±1.43	28±5.6
D13	24±2.8	NP	20±0.7	NP	15±2.1	NP
D17	7±0.35	NP	20±1.4	NP	35±4.9	NP
D18	10±2.8	NP	NP	NP	NP	>40
D19	2.5±0.14	NP	7±0.7	NP	18±0.35	NP
D20	12±2.1	NP	20±2.8	NP	20±0.35	NP
D21	17±0.7	NP	18±5.3	NP	22±1.4	NP

*NP-compound not prepared

Among these relatively small numbers of compounds, it is impossible to draw general conclusions with respect to the influence of specific structural features. However, when comparing the cycloaddition products derived from hetero-aryl dienediols with their counterparts derived from the bromo-substituted dienediols (Table 2), the former in most cases showed higher IC_{50} values than the latter. It is also noteworthy that, among the former compounds, again a compound which possesses

the 3,4,5-trimethoxy substitution at the aromatic ring (Py3DUD19S) exhibited the lowest IC_{50} value (7 µg/mL).

The total fraction of bridged bicyclic compounds that displayed biological activity in this assay was about 26%, taking an IC_{50} of 15 µg/mL as threshold value.

2.2.3. Bio-activity profiling

After having verified biological activity in a mammalian cell line for an appreciable fraction of the synthesized bridged bicyclic compounds, it was of interest to obtain suggestions about with which cellular processes the molecules interfere. To this end, two general bioactivity profiling methods were applied.

I) Measurement of cellular impedance

II) High content image analysis

Altogether, 30 compounds were selected for these profilings; the 16 most active of the bromobenzene-derived molecules (Table 1) and the 14 most active of the hetero-arylbenzene derived molecules (Table 2).

2.2.3.1. Cellular impedance measurement

Biological profiling via impedance measurement of cell cultures is a label-free real-time monitoring technique of cell perturbation. Cellular impedance is the opposition of cells to alternating current when voltage is applied. Typically the time course of impedance is measured over several days, yielding so-called time-dependent cellular response profiles (TCRP). The change of cellular impedance over time is sensitive to cellular phenomena like adhesion, proliferation, morphological changes, apoptosis and many intracellular interactions. For interpretation of the results, the TCRPs of test compounds with unknown mode of action are compared to those obtained

from reference compounds for which the phenomena with which they interfere are known. Mathematical analysis of these TCRPs by a spline-fitting method and construction of a distance matrix using the basis spline coefficients as descriptors, yields distance metrics with numerical values (Euclidean distance) between the reference compounds and the compounds under investigation. Hierarchical clustering using the distance matrix derived from the spline fitting of TCRPs was used to visualize similiarities of the curves represented as a dendrogram. A heatmap representation of the Z-transformed basis spline coefficient was used to represent the deviation of the basis spline coeficient for each TCRP from the mean. Compounds which cluster together might have a similar mode of action.

To carry out such impedance measurements, cells are incubated and treated with the test compounds in a micro-titre plate (E-plate) with embedded gold electrodes at the bottom of each well. The incubation period can be up to 5 days.[70] L929 cells were used for this assay, because they are known to grow in micro-titre plates with good adhesion, which is an important criterion for the impedance measurement. According to the experience in our laboratory, compounds are added to the cells at IC_{90} concentrations as obtained from the cell viability assay (2.2.2).

As any clustering algorithm works with certain rules, the dendrograms obtained give not always correct representations of TCRP similarities. Therefore, we used the exact numerical values (Euclidean distance) of the curve distances for the evaluation. The smaller this value is, the higher is the similarity between the compared curves. The respective distance matrices of the experiments are given in the Appendix.

2.2.3.1.1. Cellular Impedance profiling with compounds derived from (1*S*-*cis*)-3-bromo-3,5-cyclohexadiene-1,2-diol (22) and protected (1*S*-*cis*)-3-bromo-3,5-cyclohexadiene-1,2-diol (23)

As the compounds derived from hetero-aryl dienediols were synthesized later, the first impedance experiments were carried out with the 16 compounds selected from the cycloadditions with unprotected and protected, respectively, dienediols 22 and 23. The heat map obtained in the first experiment is shown in Fig. 10a.

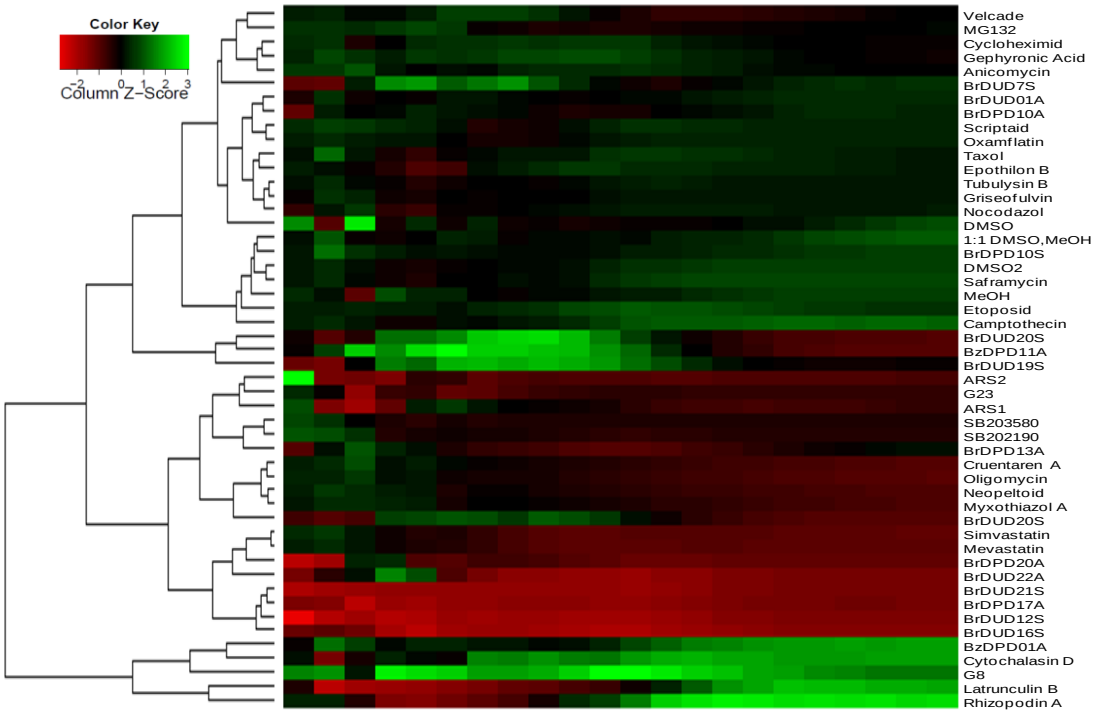

Fig. 10a: A heat map deduced from the cellular impedance measurement of 16 cycloadducts derived from dienediols 22 and 23, co-clustered with a heat map of 24 reference compounds. On the y-axis, TCRP similarity is indicated by a dendrogram representation. On the x-axis, time-segmented curve descriptors defined by cubic smoothing of spline-fitted TCRPs are shown for the measurement time of 120 h. The 'z' score indicates the standard deviation from the mean value of the descriptors. For the structures of the bridged bicycles see Fig. 7.

From the distance matrices (see Appendix), compounds with relatively close proximity to reference compounds were identified. Two compounds, BrDP20A (dis-

tance of 1.15), BrDU22S (distance of 1.7) were relatively close to the reference compounds for respiratory-system inhibition and two compounds, BrDUD17S (distance of 2.04), BrDUD19S (distance of 2.01) were moderately close to translation inhibitors. Three compounds (BrDUD01A, BrDPD10A and BrDPD10S) were in proximity to both assayed histone deacetylase (HDAC) inhibitors, scriptamid and oxamflatin (distance of 0.56-0.9) and to the tubulin polymerization inhibitors griseofulvin and tubulysin (distance of 0.7-1.2). The other compounds showed no close similarity to the reference compounds.

The experiment was repeated with the same compounds under identical conditions to verify the reproducibility of the results.

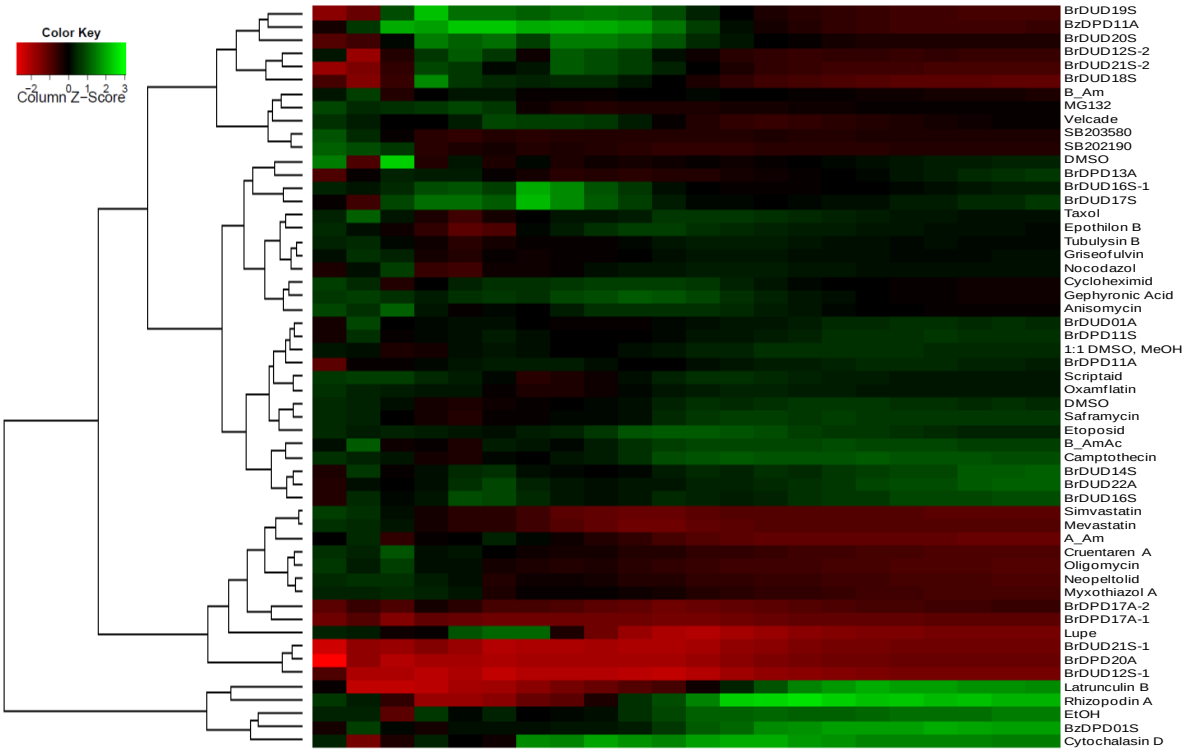

Fig. 10b. Heat map cluster from a repetition of the experiment of Fig. 10a.

The results of the repetition experiment were not in good correlation with the first experiment. Only three compounds, which were close to the HDAC inhibiting

reference compounds, showed similar results as in the first assay. Among the other compounds, one compound (BrDPD17A) was similar (distance of 0.98) to mevastatin and simvastatin, which are known cholesterol biosynthesis inhibiting compounds, and two compounds (BrDUD12S and BrDUD14S) were close (distance of 1.1, 1.4) to respiratory-chain inhibiting reference compounds.

2.2.3.1.2. Cellular impedance measurements with compounds derived from unprotected hetero-aryl dienediols

The 14 selected bridged bicyclic compounds synthesized from hetero-aryl dienediols were profiled under the same assay conditions used in the above two experiments.

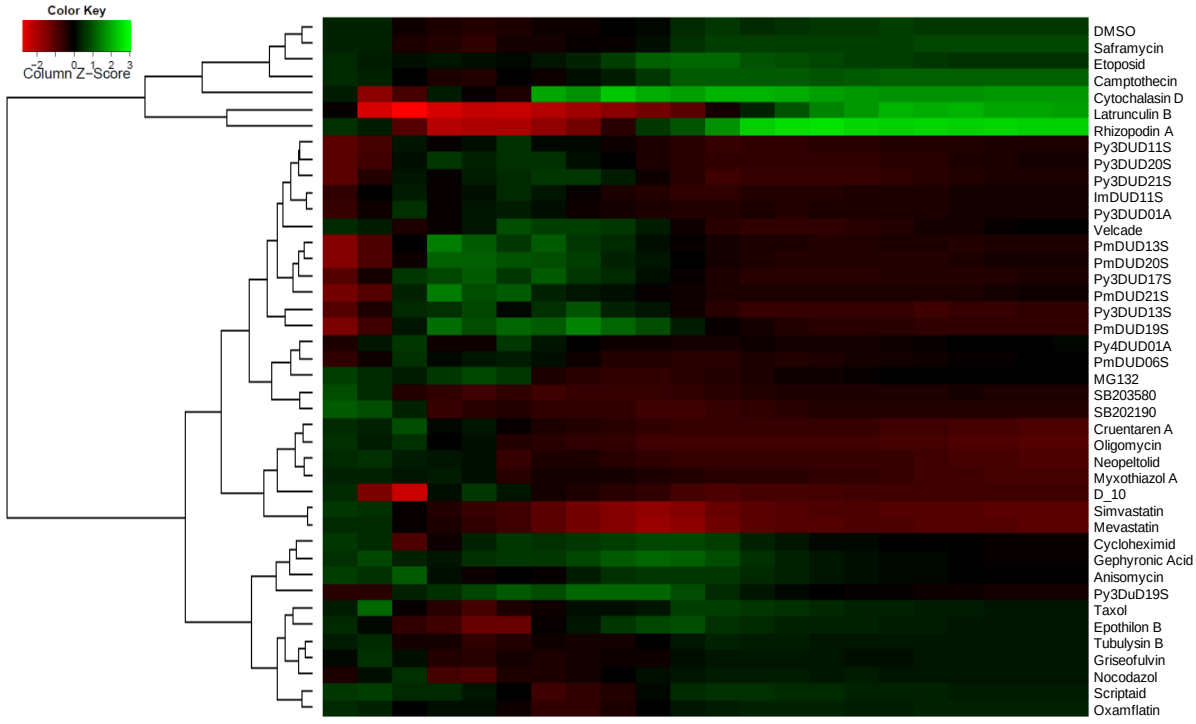

Fig. 11a. A heat map deduced from the cellular impedance measurement of 14 cycloadducts derived from unprotected hetero-aryl dienediols, co-clustered with 24 reference compounds. For further explanations see legend of Fig 10a.

The numerical values in distance matrices resulting from the first assay (see Appendix) indicated that 12 out of 14 compounds showed the highest TCRP similari-

ties (distance of 0.5-1.0) with the known proteasome inhibitors MG132 and Velcade. Of these molecules, some (Py3DUD01A, PmDUD06S, PmDUD20S and ImDUD10S) also displayed TCRP similarities with the curves for inhibitors of translation (distance of 0.8-1.0), tubulin polymerization (distance of 0.6-0.7) and *p*-38 MAP kinase (distance of 0.87). Among the remaining two compounds one (PmDUD19S) was close to translation inhibitors (distance of 1.2) and the other one (Py3DUD19S) clustered with a transcription inhibitor (distance of 0.8). The compounds were reexamined under identical conditions (Fig. 11b).

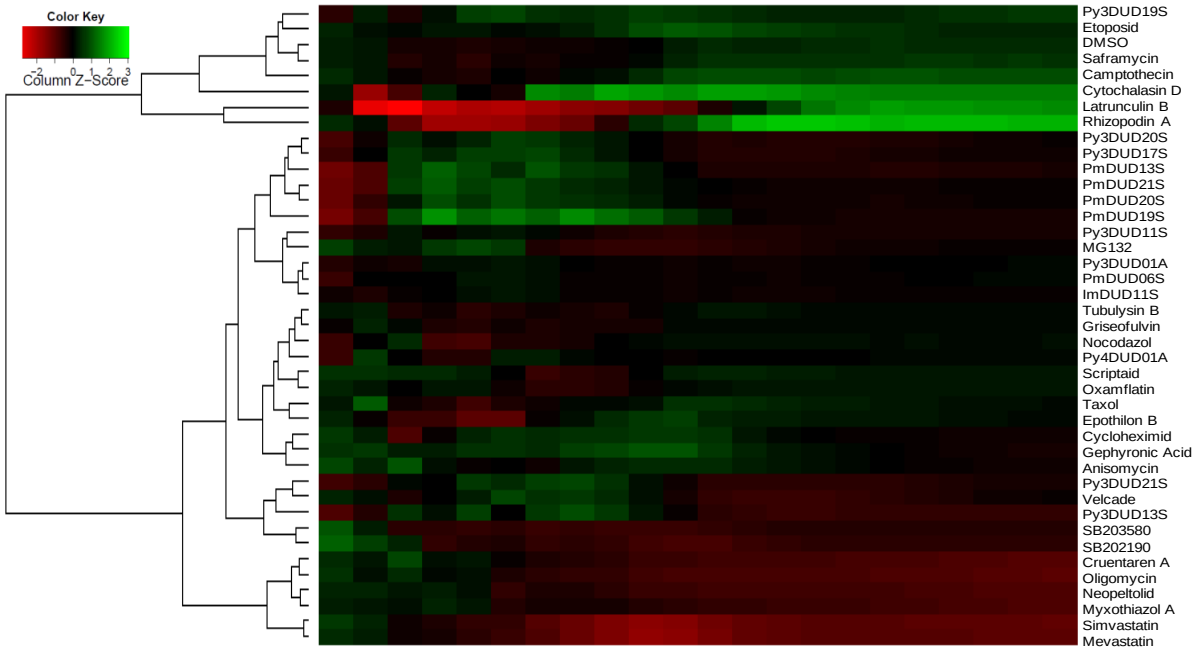

Fig. 11b. Heat map cluster from a repetition of the experiment of Fig.11a.

The outcome of the repetition experiment was fairly consistent with the first experiment according to the distance values (see Appendix). Thus, 12 out of 14 compounds were close (distance of 0.6-0.9) to the proteasome inhibitors, Velcade and MG-132. Three compounds (Py3DUD01A, Py3DUD10S and ImDUD10S) from these 12 were also close (distance of 0.8-1.0) to p-38 MAP kinase inhibitors. Of the

two remaining two compounds, one (Py3DUD19S) was in the proximity of translation inhibiting compounds (distance of 0.84) and the other one (Py3DUD13S) was close to (distance of 0.9) respiratory-chain inhibiting compounds. Both experiments suggested for the majority of the compounds to be able to inhibit the proteasome.

2.2.3.2. High content image analysis

High content image analysis (HCIA) is a bioactivity profiling method that uses the visualization of physiological alterations of cells with fluorescent markers. Analysis is done by high-throughput automated imaging of multi-labeled cells and statistical analysis of sub-cellular image localization and pattern.[71a,b] This multi-dimensional analysis method yields high information content. This method was established in our laboratory and assay conditions were optimized as described by Diestel et al..[72] Similar procedures and conditions were adopted to perform the assay in this work (for details see Materials and Methods). The cells used are KB 3–1 (human cervical cancer cell line) or A–498 (human kidney cancer cell line). Incubations are done with test compounds and with reference compounds for which the cellular targets are known. This is done in a micro-titre plate for overnight. Subsequently, cells are fixed and stained with primary antibodies for the protein of interest and complementary secondary antibodies that carry a fluorescent reporter. Images of labeled cells are recorded at four different sites in each well with the help of automated microscope. An example of captured images from one of the experiments is shown in Fig. 12.

These images are analyzed with segmentation by specifying parameters like stained area, intensity etc. Image analysis information is quantified with defined descriptors (see Table 5, 8 and 9 in Materials & Methods) to produce numerical data.

Mining of the numerical data results in correlation coefficient values and different visual representation like heat map with dendrogram.

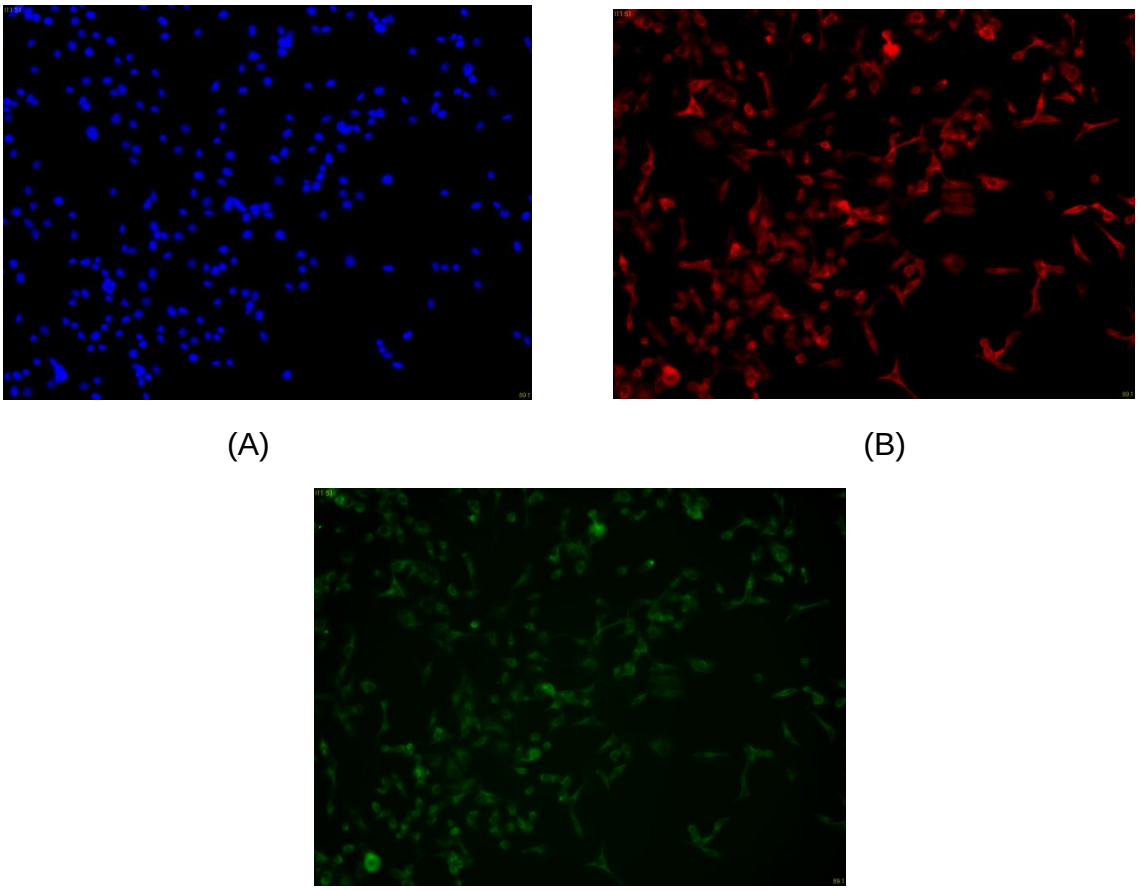

(A) (B)

(C)

Fig. 12. Example images of KB 3–1 cells labeled with (A) DAPI staining of the nucleus (blue); (B) an antibody against the endoplasmic reticulum and a fluorescent rabbit anti-rat IgG (red); (C) an antibody against cytokeratin and a fluorescent anti-mouse IgG (green); the images were captured by the automated microscope.

All of the 30 compounds selected from both sets of syntheses (see 2.2.3), together with 63 reference molecules were simultaneously subjected to this profiling technique. After image acquisition and analysis, the data were compiled in different output forms. One type of the output is in the form of a heat map, associated with a dendrogram to show the proximities between test and reference compounds. The result of the first experiment, as shown in this form, is depicted in Fig. 13a. As men-

tioned earlier (refer 2.2.3.1) these dendrograms do not accurately display all distances. Therefore the numerical correlation values for the exact similarity between two compounds, calculated by the Euclidean squared method, were considered for the evaluation. The values for the 30 most similar reference compounds are given in the Appendix. The closer these values to one, the higher the similarity between two compounds.

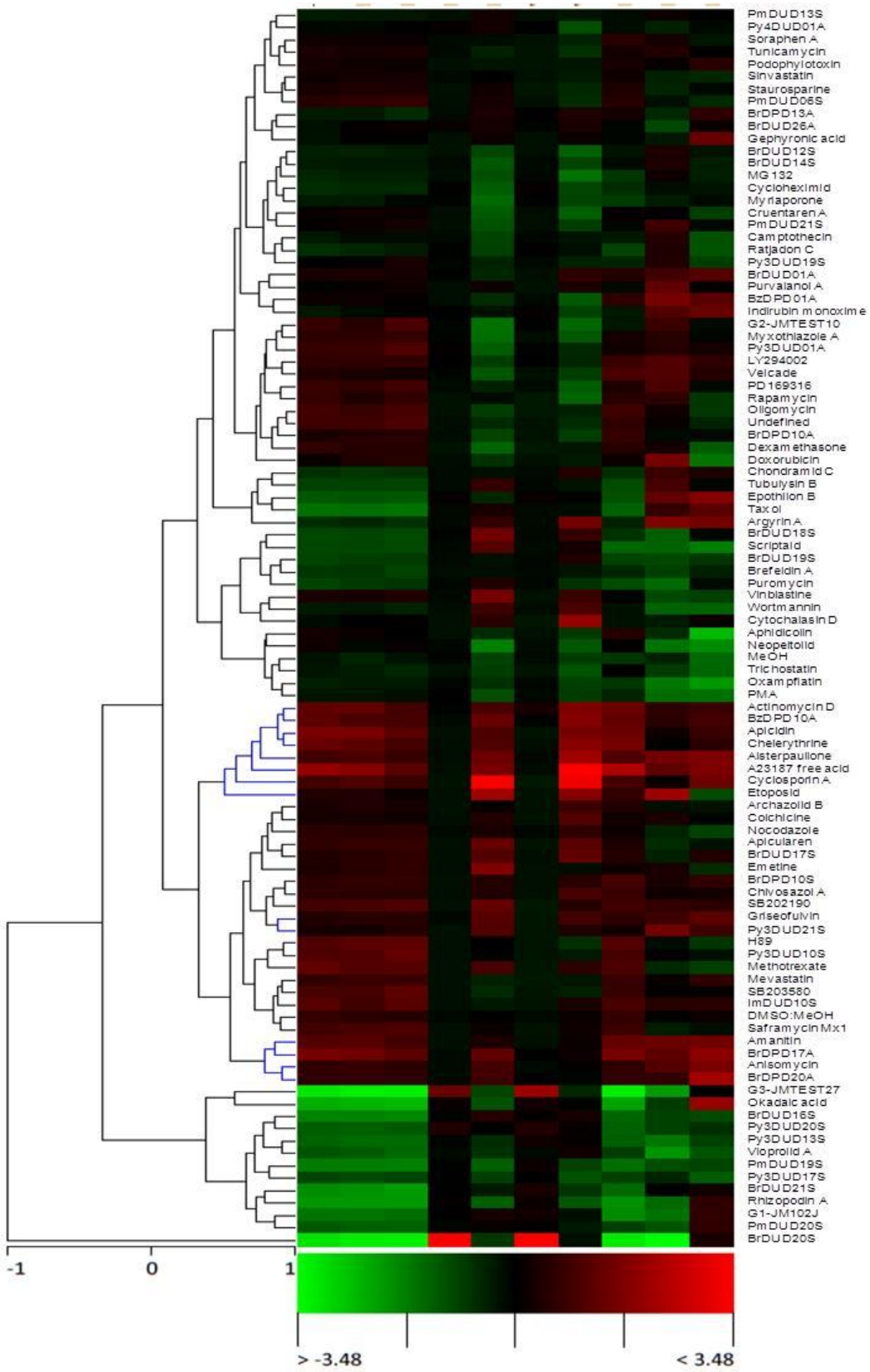

Fig. 13a. A heat map and dendrogram obtained from the high content image analysis with 30 bridged bicyclic compounds and 64 reference compounds.

The numerical data obtained from the above experiment (see Appendix), showed that some test compounds gave good correlation values with more than one reference. Eighteen (BrDUD01A, BzDPD01A, BzDPD10A , BrDUD16S, BrDUD17S, BrDPD17A, BrDUD18S, BrDUD19S, BrDPD20A, BrDUD26S, Py3DUD01A, Py3DUD10S, Py3DUD20S, Py3DUD21S, PmDUD06S, PmDUD19S, and ImDUD10S) showed similarity (correlation values of 0.8-0.93) with inhibitors of different kinases, 14 (BrDUD01A, BrDPD10S, BrDPD13A, BrDUD12S, BrDUD14S, BrDPD17A, BrDUD19S, BrDPD20A, BrDUD26S, Py3DUD13S, Py3DUD17S, Py3DUD20S, Py3DUD21S and PmDUD20S) were close (correlation values of 0.8-0.9) to translation inhibitors, 12 compounds (BrDUD01A, BzDPD01A, BzDPD10A, BrDPD10S, BrDPD13A, BrDPD17A, BrDUD17S, BrDPD20A, BrDUD21S, Py3DUD21S PmDUD20S and PmDUD13S) showed similarity (correlation values of 0.77-0.85) to tubulin polymerization inhibiting compounds and 12 compounds (BzDPD01A, BrDPD10A, BrDPD13A, BrDUD18S, BrDUD19S, Py3DUD13S, Py3DUD17S, Py3DUD19S, Py3DUD20S Py4DUD01A, PmDUD20S and PmDUD21S), were close to Golgi appratus-destroying compounds (correlation values of 0.8-0.9) Thus, for several of the test molecules, there were indications for more than one bioactivity. For example, out of 18 compounds similar to kinase inhibitors, some were also close to tubulin polymerization inhibitors.

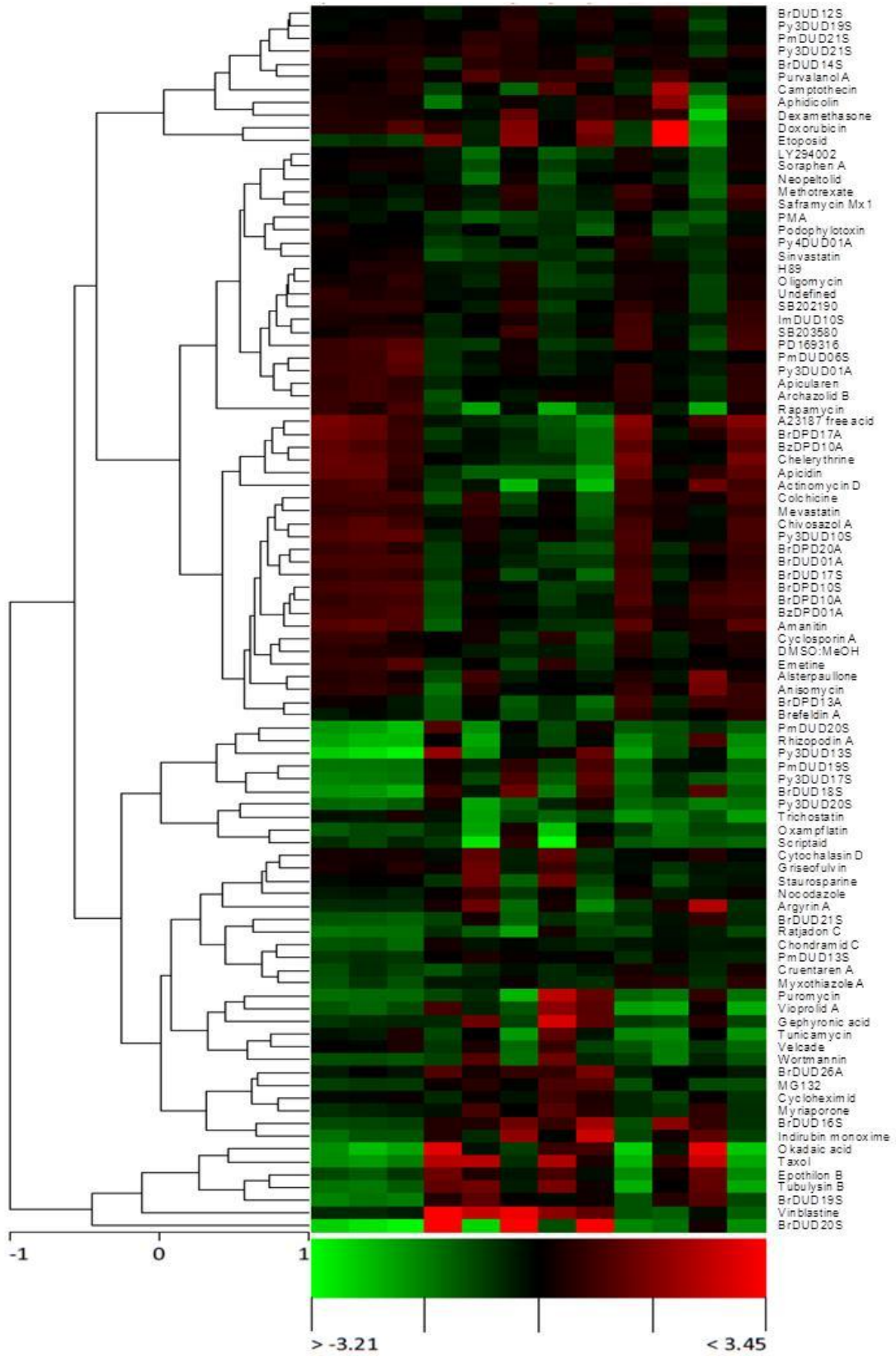

Fig. 13b. Heat map cluster from a repetition of the experiment of Fig. 13a.

The results of the first experiment were not well reproduced, as may be seen by comparing Figs. 13a and 13b. The majority of the compounds (BrDUD01A, BrDPD10A, BzDPD10A, BrDUD12S, BrDUD14S, Py3DUD01A, Py3DUD19S, Py3DUD21S, Py4DUD01A, PmDUD06S, PmDUD21S and ImDUD10S) showed close proximity with different kinase-inhibiting compounds (correlation values of 0.75-0.88) and 9 compounds (BrDUD01A, BzDPD01A BzDPD10A, BrDPD10S, BrDUD17S, BrDPD20A, Py3DUD10S, Py3DUD21S and PmDUD13S) showed similarity to actin polymerization-related compounds (correlation values of 0.74-0.87).

2.2.3.3. Comparison of cellular Impedance measurement and high content image analysis results

The results acquired from both profiling techniques were compared to select compounds with the highest probability for interference with a particular cellular process. These compounds subsequently should be subjected to specific biological assays in order to verify the suggested activity. According to the evaluation of the high content analysis, the predominant prediction was transcription inhibition and actin polymerization inhibition, in contrast to the impedance measurement results. The impedance profiling suggested proteasome inhibitory activity for many compounds. All of them came from the compound collection obtained from hetero-aryl dienediols. Surprisingly, high content image analysis never pointed to this target. For only one compound, both profiling techniques suggested the same phenotype, namely MAP-kinase pathway inhibition.

2.2.3.4. Selection of compounds for specific biological assays from impedance measurement and high content image analysis

Because of the differing results between the two profiling methods, compounds were selected separately, based on the following threshold values: ≤1 for impedance measurement and ≥ 0.8 for high content image analysis. For impedance measurement 2.26% of all distance values were under the set limit, for high content screening 0.87% of all correlation values were above the indicated threshold. There was a partial overlap in the assigned compounds. However, assignments typically were for different cellular processes. There was only one case (compound ImDUD10S) to which both methods assigned the same activity, inhibition of the MAP kinase pathway.

Additional criteria for the assays to be carried out were availability of reagents, complexity and laboratory experience with the assay. Thus, eventually four different assays were carried out involving 28 compounds, which corresponded to 17 different compounds (see Table 3).

Table 3. List of selected compounds and specific biological assays from the cellular impedance measurement and high content analysis

Actin polymerization inhibition Assay	**Tubulin polymerization inhibition Assay**	**HDAC inhibition Assay**	**Proteasome inhibition Assay**
BrDUD01A	BrDUD01A	BrDUD01A	PmDUD06S
BrDUD10S	BrDPD10A	BrDPD10A	PmDUD13S
BrDUD17S	BrDUD18S	BzDPD10A	PmDUD21S
BrDUD18S	BrDUD19S		Py3DUD01A
PmDUD13S	PmDUD06S		Py3DUD10S
PmDUD20S	Py3DUD01A		Py3DUD17S
Py3DUD10S	Py3DUD21S		Py3DUD20S
Py3DUD21S	ImDUD10S		Py3DUD21S
			ImDUD10S

2.2.4. Specific biological assays

A number of specific biological assays were carried out in order to verify the potential bioactivities suggested by the two profiling techniques, impedance measurement and high content image analysis. The selection of the respective compounds was described under 2.2.3.4.

2.2.4.1. Assay for inhibition of actin-polymerization

The globular protein actin dynamically forms helical microfilaments, which are involved in important cellular processes like motility, cell division, cytokinesis, vesicle and organelle movement etc. It maintains cell adhesion and cell shape.[73] Actin polymerization inhibitors interrupt the filamenting process, thereby causing cell death.[74] As shown in Table 3, eight compounds were selected to assay inhibition of actin po-

lymerization. Ptk2 cells (potooro kidney, epithelium-like) were used for this assay because of their robust adherence towards several washing steps and their flat morphology for clear visualization of labeled protein structures. The cells were incubated overnight with the test compounds at two different concentrations, which were the IC_{50} and IC_{70} determined in the MTT test (see 2.2.2.). Cells were fixed and subsequently stained with Alexa Fluor 488 phalloidin to visualize the actin protein structure. The cells were examined under the fluorescence microscope. Rhizopodin, which is a known actin polymerization inhibitor, was used as positive control. One of the compounds, Py3DUD21S, showed a detectable effect on the cytoskeleton of the cells by disturbing its tight structure (Fig. 14). However, some stress fibers were still observed (shown by red arrows in Fig. 14), which are characteristic actin structures. Therefore, a clear effect on actin polymerization could not be confirmed in this assay.

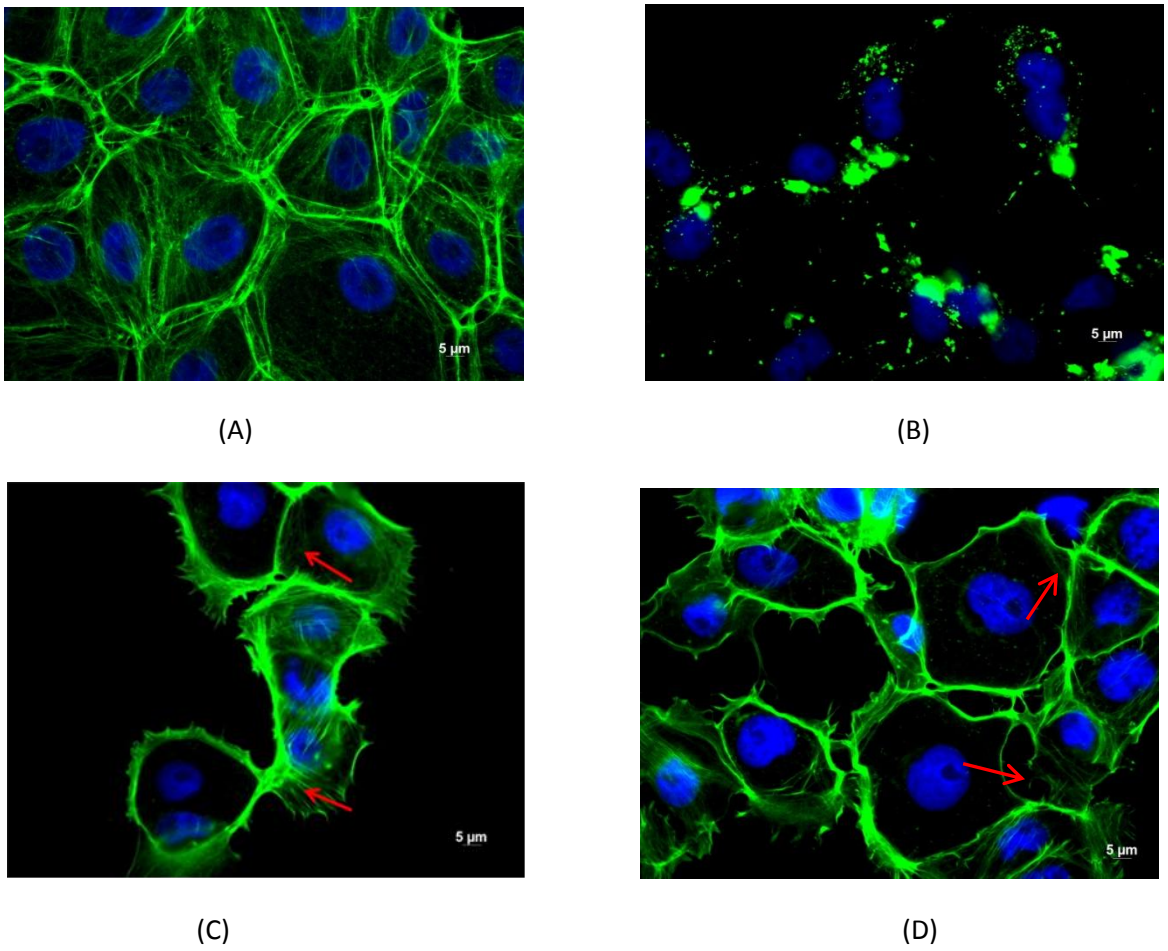

(A) (B)

(C) (D)

Fig. 14. Assay for inhibition of actin polymerization. PtK2 cells were treated with (A) the solvent DMSO as a negative control, (B) Rhizopodin as positive control, (C) and (D) compound Py3DUD21S in concentrations of 18 µg/mL, and 23 µg/mL, respectively. Cells were labeled with DAPI (blue), Alexa Fluor 488 phalloidin (green). Red arrows indicate stress fibers, which are typical actin structures.

2.2.4.2. Assay for inhibition of tubulin polymerization

Tubulin is a globular polypeptide of 50 KDa. In a reversible reaction it polymerizes to form microtubules, which play a vital role in growth, division, and cytoskeletal organization of normal and tumor cells. Tubulin-polymerization-affecting compounds attack microtubules by interfering with the dynamics of tubulin polymerization and depolymerization, resulting in apoptotic cell death.[75a,b] Eight compounds (listed in Table 3) were selected for the tubulin inhibition assay. Ptk2 cells were incubated overnight

with the test compounds at concentrations of 18 and 23 µg/mL, which were the IC_{50} and IC_{70} determined in the MTT test (see 2.2.2). Nocodazole, a known inhibitor of tubulin polymerization, was used as positive control. The cells were fixed and subsequently stained with a primary antibody against α-tubulin, followed by a complementary labeled antibody, anti-mouse IgG, to visualize the tubulin structure. Additionally, the cell nucleus was labeled with DAPI. The cells were examined under the fluorescence microscope. One of the eight compounds, Py3DUD21S, showed an effect on the tubulin structure of the cells at 23 µg/mL (IC_{70}). To determine the concentration-dependence of this effect, the assay was repeated with concentrations below the IC_{70}. As shown in Fig. 15, the compound caused a slight disruption of the tubulin structure at 19 µg/mL and a strong disruption 21 µg/mL (indicated by red arrows in Fig. 15). As these two concentrations are rather similar, the assay was repeated to verify this steep concentration-dependence. The result was well reproduced. The enhancement in activity, with a small concentration difference of 2 µg/mL, may be due to a cytotoxic effect of the compound on the cells used.

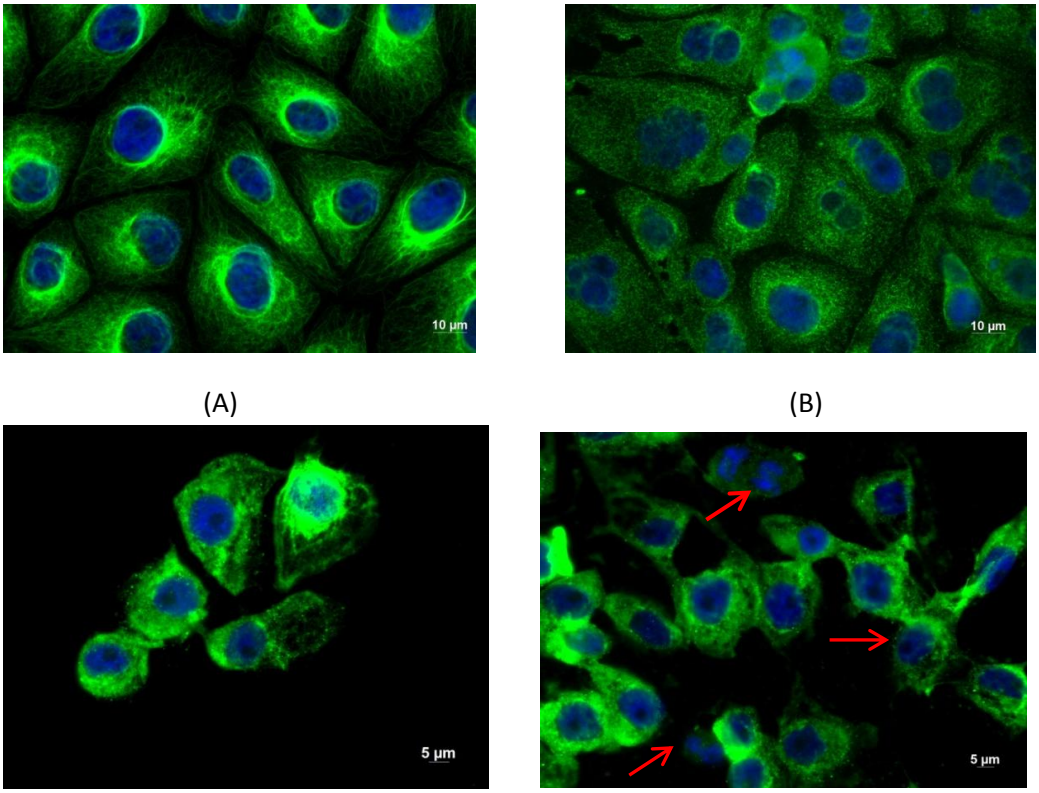

Fig. 15. Assay for the inhibition of tubulin polymerization. Microscopic images of compound-treated PtK2 cells are shown. Cells were labeled with an antibody against α-tubulin and anti-mouse IgG (green) and with DAPI (blue). (A) cells with solvent control (DMSO), (B) cells with nocodazole (0.16 µM) as positive control, (C) and (D) cells treated with 19 µg/mL or 21 µg/mL, respectively, of compound Py3DUD21S. Red arrows point to the disruption of tubulin structures.

2.2.4.3. Histone deacetylase (HDAC) inhibition Assay

The reversible acetylation of histones is a vital process, which is critical for the regulation of gene expression via transcription in eukaryotic cells. Histone deacetylase (HDAC) removes acetyl groups from lysine residues of histone proteins. The resulting positive charges increase the histone affinity towards DNA and thereby block the access of positive transcription factors. This down-regulates gene expression. HDACs are involved in a number of human disease states, namely several cancers, neurological disorders, and aging.[76]

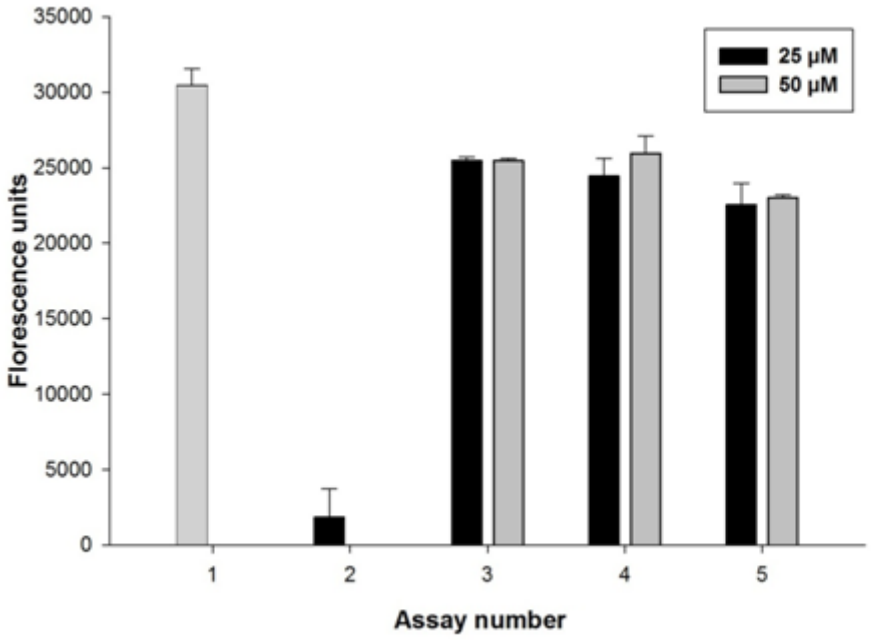

Fig. 16. Fluorometric HDAC inhibition assay. The measured fluorescence is directly proportional to the deacetylation activity of the sample. Assay 1 shows the blank with only cell lysate with HDAC and assay 2 shows the positive control, Trichostatin. Assays 3-6 show the results with the compounds, BrDUD01A, BrDPD10A and BzDPD10A. Standard deviations are indicated.

Three compounds (shown in Table 3) were assayed for potential HDAC inhibitory activity. HDAC activity is assayed by a two-step process. In the first step deacetylation of the acetylated lysine side-chain of a peptide, coupled with a fluorescent reporter, 7-amino-4-methylcoumarin (AMC) is catalyzed by a HDAC-containing HeLa cell lysate. In the next step, to quantify this reaction, trypsine is added to catalyse the cleavage of the deacetylated substrate to release fluorescent AMC. The decrease in emitted fluorescence is directly proportional to the activity of the test compound.[77] The HeLa cell lysate with peptide substrate was incubated with the test compounds for 30 min in a tissue culture plate. The trypsin reagent was added to generate the fluorescence emitter. A known HDAC inhibitor, trichostatin A, was used as positive

control. A plot of the fluorescence signals at different concentrations of the compounds is shown in Fig. 16. The results did not show an HDAC inhibition and did not confirm the suggestions of both profiling techniques, impedance measurement and high content image analysis.

2.2.4.4. Proteasome inhibition assay

The proteasome, a multicatalytic complex, is responsible for most of the intracellular protein degradation, including proteins that regulate cell cycle and apoptosis. Inhibition of the proteasome results in accumulation of unwanted proteins and leads to cell death.[78a,b] Nine of the profiled compounds, shown in Table 3, were selected to verify proteasome inhibition. The assay performed measures the proteolytic activity associated with the proteasome via bioluminescence. KB 3–1 cells were used in this assay because of their good adherence and growth. A proteasome substrate peptide that was conjugated with a luminogenic reporter group, aminoluciferin, was added to the KB 3–1 cells. The cellular proteasome cleaves the peptide to release the aminoluciferin. The luminescence signal is proportional to proteasome activity. The cells were incubated with the test compounds for 2 h. Thereafter, the proteasome substrate was added and the generated luminescence was measured. A known proteasome inhibitor, MG-132, was used as positive control. All compounds were used at two concentrations, 25 and 50 µg/mL. One out of the nine compounds, PmDUD21S, showed significant inhibition. The assay was repeated with different amounts of this compound to determine the concentration-dependency of the effect (Fig. 17). This clearly confirmed the inhibitory effect at concentrations of 25 µg/mL or above.

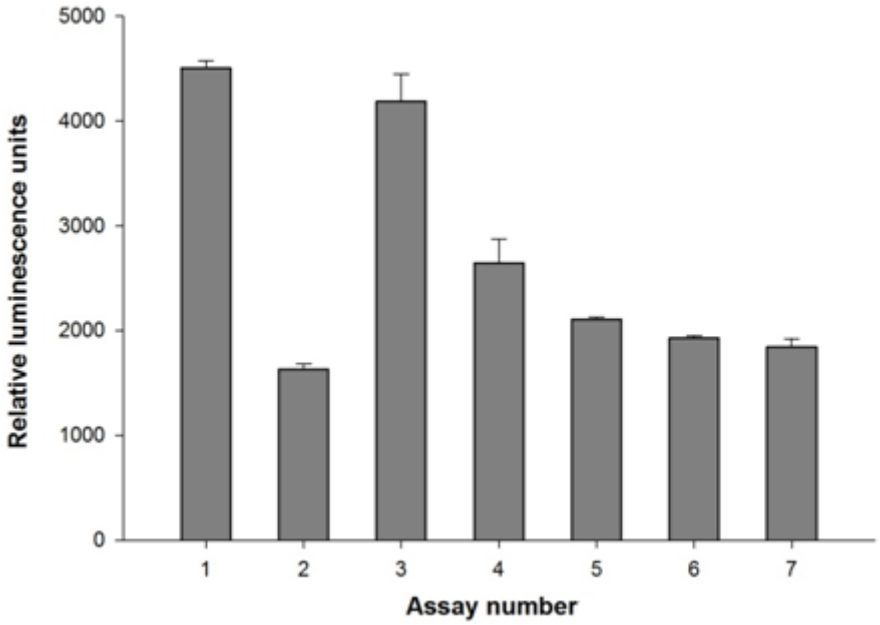

Fig. 17. Bioluminescent proteasome inhibition assay. Proteolysis is proportional to the relative luminescence units (RLU) determined. Column 1 shows the solvent control, DMSO and MeOH in a 1:1 ratio (v/v). Column 2 shows MG-132 as positive control (4 µM). Columns 3-7 show the effects of compound PmDUD21S at 20, 25, 30, 35, 40 µg/mL concentrations. Standard deviations are indicated.

3. Conclusions

3.1. Chemistry

In order to carry out Diels-Alder reactions with dienediols, a protection of the hydroxy groups is not generally required. However, protection exerts a considerable influence on the stereoselectivity in the cycloaddition reactions. The presence of free hydroxy groups typically strongly favours formation of the *syn* isomer. Thus, no protection of the diol moiety is recommended, if this is the desired isomer. The opposite recommendation holds, if the *anti* isomer is to be obtained in higher yields.

The reactivity of heteroaryl-substituted dienediols in [4+2] cycloaddition was significantly lower than that of the bromo-substituted dienediol. Conditions for the cycloadditions with heteroaryl dienediols have not yet been described. From the experience of this work, suitable reaction conditions are working at elevated temperatures (100-120 ºC) in a sealed vessel.

The distribution between *syn* and *anti* isomers in the cycloadducts was largely in accordance with literature data. Thus, also after protection of the *syn*-directing diol moiety, the predominant isomer obtained with maleimide-derived dienophiles was in most cases the *syn* product. A maleimide-specific directing effect, involving H-bond formation, is proposed to explain this finding.

3.2. Biology

It was possible to obtain a significant fraction of bioactive compounds through the described synthetic route, leading to bridged bicyclic compounds.

With the bioactivity profiling methods and conditions used, it was difficult to identify specific activities for active compounds. Possible reasons include the, in my

hands, limited reproducibility of the results as well as limitations in the number and kind of available reference compounds.

In spite of these problems and with a limited number of assays, that could be carried out, two types of bioactivity predictions of the profilings were confirmed: i) interference with the polymerization of tubulin and ii) inhibition of the proteasome.

The bridged bicyclic compounds synthesized in this work are just one example for molecules possessing a permanent three-dimensional structure. Following the devised synthetic route and principles, larger and structurally more diverse collections of bridged bicycles and related molecules may be generated with the aid of solid-phase chemistry. Moreover, other synthetic pathways, leading to different types of three-dimensional compounds, may be developed and explored.

4. Materials and Methods

4.1. Materials

4.1.1. Instruments/Equipment

Automatic Microsope	ImageXpress Micro (Molecular Devices)
Bacterial cell incubator	Memmert
Cell counter	Cedex XS (Innovatis)
Centrifuges	5810R (Eppendorf)
Eucoryatic cell incubator	CO2-Auto-Zero (Heraeus)
Fluorescence microscope	Axioplan (Zeiss) with camera Axiocam (Zeiss) ca
Incubator (Impedance measurement)	MIDI 40, CO_2 incubator (Thermo Fischer Scientific)
Impedance recorder	RTCA single plate (Roche/Acea Biosciences)
Laminar airflow	Maxisafe 2020 (Thermo Fisher Scientific)
Light microscope	Axiovert 35 (Zeiss)
Microlitre plate reader	Infinite M200 pro (Tecan)
Microlitre plate washer	BioTek, 405-select TS
Microlitre pipettes	Research und Reference (Eppendorf)
Pipetting robot with pintool	Biomek FXP Laboratory Automation Workstation (Beckman Coulter)
Shaker	Titramax 1000 (Heidolph)
Vacum pump	Vacusafe comfort (Integra Biosciences)

4.1.2. Softwares

ChemBio Draw, ACD Labs (for NMR analysis), AxioVision 3.1, SigmaPlot 12.3, Microsoft Office 2010.

4.1.3. Antibodies/Dyes

Primary Antibodies

Alexa Fluor 488 Phalloidin	Invitrogen
Anillin Antibody (Rabbit)	Bethyl Laboratories
Anti-Calmodulin (Mouse)	Invitrogen
Anti-c-Fos (Rabbit)	Sigma
Anti-phospho-CREB (Rabbit)	Sigma
DAPI dihydrochloride	Sigma
GRP94 (Rat)	Dianova
Monoclonal anti-p53, Clone BP53-12 (Mouse)	Sigma
Monoclonal anti-Pan Cytokeratin, Clone C-11 (Mouse)	Sigma
Monoclonal anti-Splicing Factor SC-35, Clone SC-35 (Mouse)	Sigma
Monoclonal anti-α-Tubulin, Clone B-5-1-2 (HCA), Clone DM1A (Mouse)	Sigma
Phospho-p38 MAPK (Thr180/Tyr182) Antibody (Rabbit)	New England Biolabs
Phospho-p44/42 MAPK (Thr202/Tyr204) Antibody (Mouse)	New England Biolabs

Secondary Antibodies

Atto 488 anti-rabbit (Goat)	Sigma
Alexa Fluor 488 anti-rat (Rabbit)	Invitrogen
Atto 594 anti-mouse (Goat)	Sigma

4.1.4. Culture media

For bacterial cultures EBSS,[79] and for hyphal fungi M90[80] medium was used. All media components were purchased from Becton Dickinson, Fluka, Merck, Roth or Sigma and Gibco. Media was prepared by mixing the following components at RT.

EBSS (pH 7.0): Peptone (5 g/l)
Proteosepeptone (5 g/l)
Meat extract (1 g/l)
Yeast extract (1 g/l)
HEPES (10 g/l)

M90 (pH 5.6): Malt extract (30 g/l)
Peptone (3 g/l)

For the agar media (agar diffusion tests), 15 g/L agar was added. The media were prepared in distilled H_2O and autoclaved immediately. The autoclaved media were then stored at 4 °C.

5.1.5. Media for cell cultures

Eukaryotic cells used for the assays with their respective media are given in the Table 4.

Table 4. Media used for different cell lines

Cell line	Medium	Manufacturer	Supplements
PtK2	MEM	Gibco	- 1x Non-essential amino acids (Gibco) - 1x GlutaMAX (Gibco) - 10 % FBS (Lonza)
L-929, KB-3-1	DMEM	Lonza	10 % FBS (Lonza)

4.1.6. Assay kits

Histone Deacetylase Assay, Fluorometric	Sigma
Proteasome-Glo^{TM} Assay	Promega

4.1.7. Microorganisms and cell lines

The microorganisms and eukaryotic cells used for the bioactivity assays are listed below in the Tables 5 and 6.

Table 5. Microorganisms and their sources

Microorganisms	Abbreviation	Source	Type
Micrococcus luteus	Mcl	HZI collection	Gram-positive bacterium
Hansenula anomala	Hna	DSMZ 70263	Yeast

Table 6. Mammalian cell lines with their source, origin and morphology

Cell line	**Source**	**Species**	**Origin**	**Morphology**
L-929	DSMZ ACC2	Mouse	Connective tissue	Fibroblast
KB 3–1	DSMZ ACC158	Human	Cervical cancer	Epithelium-like
PtK2	ATCC CCL-56	Potoroo	Kidney	Epithelium-like

4.2. Methods

4.2.1. Chemistry

4.2.1.1. Chromatography

A. TLC

TLC was performed on pre-coated aluminum sheets, silica gel 60 F_{254} with concentrating zone 20 x 2.5 cm (Merck). Zones were detected by fluorescence quenching with irradiation at 254 nm and/or staining using a solution of Vaughn's reagent 9.6 g $(NH_4)_6 MO_7O_{24}$ 4 H_2O and 0.4 g $Ce(SO_4)_2$ 4 H_2O in 200 mL 7 M H_2SO_4) followed by heating with a heat gun until the solution was dried.

B. Column chromatography/flash chromatography

This was done with flash silica gel (J. T. Baker) having pore size of 60 Å. Column size and silica gel quantity was selected according to a previous report.[81]

C. Preparative HPLC

A Merck-Hitachi (L-6200A) pump with UV detector (L-7400) was used with 1% trifluoroacetic acid in acetonitrile and water as eluent for purification. A Phenomenex Luna C18 RP column (250 mm length) with 20 mm diameter was used.

4.2.1.2. Microwave reactions

The reactions were performed in a sealed reaction vessel of an MLS START 1500 microwave synthesizer with an output power of 500 W. Reactions were carried out with time intervals of 10-15 minutes with TLC monitoring.

4.2.1.3. NMR spectrometry

Spectral data was recorded with instruments Bruker DPX-Bruker AV II-300 (300.1 MHz for 1H NMR, 13C NMR with 75.5 MHz, T = 296 K), AV III-400 (400.1 MHz for 1H NMR, 13C NMR with 100.6 MHz, T = 296 K), Bruker DRX-400 (400.1 MHz for 1H NMR, 13C NMR with 100.6 MHz, T = 300 K), and Bruker AV II-600 (600.1 MHz for 1H NMR; 13C NMR with 150.3 MHz). The chemical shifts δ are given in ppm and referenced to the internal solvent standard. Multiplicities of NMR signals are indicated as follows: s (singlet), d (doublet), t (triplet), m (multiplet), dd (doublet of doublets), dt (doublet of triplets) and br. s (broad singlet).

4.2.1.4. Synthetic procedures

All non-aqueous reactions were conducted in dried glassware under drying tube. All yields refer to isolated compounds after the final purification process, unless otherwise stated. For all purified compounds, the purity was estimated by ^{1}H NMR spectrometry. The purity of the compounds was always above 85%.

4.2.1.4.1. General procedure for the preparation of *N*-aryl or -alkyl maleimides (D2, D4-D8, D23 and D24)

Appropriate aryl or alkyl amine (2**,** 5.8 mmol) was added to the solution of maleic anhydride (1, 5.1 mmol) in ethyl acetate (15 mL) and stirred at RT for 1 h. The resultant solid precipitate was filtered and dried under vacuum to get the intermediate, *N*-substituted aminobutenoic acid (3). A mixture of NaOAc (2.55 mmol) and acetic anhydride (25.5 mmol) was heated to 80 ºC in an oil bath until all NaOAc had dissolved. The intermediate (3) was added to this solution and stirred at 80 ºC. After 1 h, the reaction was cooled to RT and diluted with ice cold-water (15 mL). The aqueous layer was extracted with ethyl acetate (2 x 15 mL). The organic layers were

combined and dried over Na_2SO_4. The organic layer was evaporated at 30 ºC under reduced pressure. The obtained crude compounds were purified by column chromatography using petroleum ether and ethyl acetate as eluents to obtain compounds in 40-65% yield. Compounds were characterized by ^{1}H NMR and ^{13}C NMR spectrometry.

1-(4-fluorophenyl)-1*H*-pyrrole-2,5-dione (D02)

^{1}H NMR (500 MHz, $CDCl_3$): *δ* 6.85 (s, 2H), 7.15 (dd, *J* = 9.00, 8.24 Hz, 2H), 7.28–7.33 (m, 2H); ^{13}C NMR (126 MHz, $CDCl_3$): *δ* 116.1, 116.3, 127.2, 127.9, 134.3, 160.9, 162.8, 169.4.

1-(4-acetylphenyl)-1*H*-pyrrole-2,5-dione (D04)

^{1}H NMR (500 MHz, $CDCl_3$): *δ* 2.61 (s, 3H), 6.88 (s, 2H), 7.48–7.59 (m, 2H), 8.00–8.09 (m, 2H); ^{13}C NMR (126 MHz, $CDCl_3$): *δ* 26.7, 125.4, 129.2, 134.5, 135.6, 136.0, 169.0, 197.0.

1-(4-methoxyphenyl)-1*H*-pyrrole-2,5-dione (D05)

^{1}H NMR (500 MHz, $CDCl_3$): *δ* 3.85 (s, 3H), 6.85 (s, 2H), 6.97–7.02 (m, 2H), 7.22–7.27 (m, 2H); ^{13}C NMR (126 MHz, $CDCl_3$): *δ* 55.5, 114.5, 123.8, 127.6, 134.2, 159.0, 169.9.

1-(3,4,5-trimethoxyphenyl)-1*H*-pyrrole-2,5-dione (D06)

^{1}H NMR (500 MHz, $CDCl_3$): *δ* 3.84 (s, 9H), 6.52 (s, 2H), 6.84 (s, 2H); ^{13}C NMR (126 MHz, $CDCl_3$): *δ* 56.3, 60.9, 104.1, 126.7, 134.2, 137.9, 153.5, 169.7.

3-(2,5-dioxo-2,5-dihydro-1*H*-pyrrol-1-yl)phenyl acetate (D07)

^{1}H NMR (700 MHz, $CDCl_3$): *δ* 2.29 (s, 3H), 6.83 (s, 2H), 7.10 (ddd, *J* = 8.23, 2.21, 0.97 Hz, 1H), 7.19 (t, *J* = 2.15 Hz, 1H), 7.26–7.29 (m, 1H), 7.42–7.47 (m, 1H); ^{13}C NMR (176 MHz, $CDCl_3$): *δ* 21.1, 119.0, 120.9, 122.8, 129.7, 132.2, 134.3, 150.8, 169.1.

1-(4-nitrophenyl)-1*H*-pyrrole-2,5-dione (D08)

^{1}H NMR (500 MHz, $CDCl_3$): *δ* 6.92 (s, 2H), 7.64–7.71 (m, 2H), 8.29–8.36 (m, 2H); ^{13}C NMR (126 MHz, $CDCl_3$): *δ* 124.5, 125.5, 134.6, 137.1, 146.3, 168.5.

1-(2-morpholinoethyl)-1*H*-pyrrole-2,5-dione (D24)

^{1}H NMR (300 MHz, $CDCl_3$): *δ* 2.42–2.49 (m, 4H), 2.52 (t, *J* = 6.40 Hz, 2H), 3.59–3.68 (m, 6H), 6.68 (s, 2H); ^{13}C NMR (126 MHz, $CDCl_3$): *δ* 36.0, 53.1, 56.3, 67.2, 134.1, 168.2.

4.2.1.4.2. General procedure for the preparation of 4'-amino chalcone-based maleimides (D12-D20)

A solution of the appropriate aromatic aldehyde (8**,** 1.5 mmol) in ethanol (1 mL) was cooled in an ice bath to 0 ºC, after which a precooled solution of sodium hydroxide in water (2.3 mmol in 2 mL) was added dropwise with stirring. A precooled mixture of oxoaminobutenoic acid (7**,** 1.3 mmol), and sodium hydroxide (2.6 mmol) in water (2 mL) was added dropwise to the stirring solution of the aryl aldehyde over a period of 15 min with stirring. The reaction mixture was stirred at RT for 14 h, acidified with 2N hydrochloric acid and stirred for another 1h. The resultant precipitate was filtered, washed with water and vacuum dried. The completely dried solid intermediate (9) was added to the mixture of NaOAc (0.7 mmol) and acetic anhydride (7.7 mmol),

which was preheated to 90 ºC for 20 min. The resultant reaction mixture was stirred at 90 ºC. After 1 h, the reaction was allowed to cool to RT and quenched with ice-cold water (5 mL). The aqueous layer was extracted with ethyl acetate (2 x 15 mL), and the combined organic layers were dried over Na_2SO_4 and concentrated under reduced pressure. The crude compound was purified by column chromatography using dichloromethane as eluents. Compounds were characterized by ^{1}H NMR and ^{13}C NMR spectrometry and their yields were in 40-60%.

1-(4-cinnamoylphenyl)-1*H*-pyrrole-2,5-dione (D12)

^{1}H NMR (500 MHz, $CDCl_3$): *δ* 7.19 (s, 3H), 7.37–7.43 (m, 5H), 7.46 (d, *J* = 15.72 Hz, 1H), 7.61–7.64 (m, 2H), 7.78 (d, *J* = 15.8, 1H), 8.03–8.07 (m, 2H); ^{13}C NMR (126 MHz, $CDCl_3$): *δ* 121.6, 126.3, 128.5, 129.1, 129.3, 134.6, 135.2, 136.0, 137.9,145.6,169.1,189.6.

(*E*)-1-(4-(3-(4-fluorophenyl)acryloyl)phenyl)-1*H*-pyrrole-2,5-dione (D13)

^{1}H NMR (500 MHz, $CDCl_3$): *δ* 6.90 (s, 2H), 7.08–7.15 (m, 2H), 7.43 (d, *J* = 15.72 Hz, 1H), 7.54–7.59 (m, 2H), 7.61–7.66 (m, 2H), 7.78 (d, *J* = 15.56 Hz, 1H), 8.08–8.13 (m, 2H); ^{13}C NMR (126 MHz, $CDCl_3$): *δ* 116.2, 116.3, 121.5, 125.5, 129.4, 130.4, 131.1, 134.5, 135.3, 137.0, 144.0, 169.0, 189.3.

(*E*)-1-(4-(3-(4-chlorophenyl)acryloyl)phenyl)-1*H*-pyrrole-2,5-dione (D14)

^{1}H NMR (500 MHz, $CDCl_3$): *δ* 6.91 (s, 2H), 7.36–7.42 (m, 2H), 7.48 (d, *J* = 15.56 Hz, 1H), 7.53–7.60 (m, 4H), 7.76 (d, *J* = 15.72 Hz, 1H), 8.07–8.13 (m, 2H); ^{13}C NMR (126 MHz, $CDCl_3$): *δ* 122.2, 125.5, 129.3, 129.4, 129.7, 133.3, 134.5, 135.4, 136.7, 136.9, 143.8, 169.0, 189.2.

(*E*)-1-(4-(3-(p-tolyl)acryloyl)phenyl)-1*H*-pyrrole-2,5-dione (D16)

^{1}H NMR (300 MHz, $CDCl_3$): *δ* 2.39 (s, 3H), 6.87–6.90 (m, 2H), 7.19–7.27 (m, 2H), 7.46 (d, *J* = 15.82 Hz, 1H), 7.50–7.59 (m, 4H), 7.80 (d, *J* = 15.64 Hz, 1H), 8.06–8.15 (m, 2H); ^{13}C NMR (75 MHz, $CDCl_3$): *δ* 21.58, 120.83, 125.44 128.58, 129.37, 129.78, 132.06, 134.46, 135.11, 137.3, 141.33, 145.47, 169.01, 198.6.

(*E*)-1-(4-(3-(4-methoxyphenyl)acryloyl)phenyl)-1*H*-pyrrole-2,5-dione (D17)

^{1}H NMR (500 MHz, $CDCl_3$): *δ* 3.86 (s, 3H), 6.89 (s, 2H), 6.94 (d, *J* = 8.70 Hz, 2H), 7.39 (d, *J* = 15.72 Hz, 1H), 7.53–7.57 (m, 2H), 7.60 (d, *J* = 8.54 Hz, 2H), 7.80 (d, *J* = 15.56 Hz, 1H), 8.08–8.12 (m, 2H); ^{13}C NMR (126 MHz, $CDCl_3$): *δ* 55.5, 114.5, 119.5, 125.4, 127.5, 129.3, 130.4, 134.5, 135.0, 137.5, 145.3, 161.9, 169.0, 189.5.

(*E*)-1-(4-(3-(3,4-dimethoxyphenyl)acryloyl)phenyl)-1*H*-pyrrole-2,5-dione (D18)

^{1}H NMR (500 MHz, $CDCl_3$): *δ* 3.91–3.97 (m, 6H), 6.87–6.92 (m, 3H), 7.15 (d, *J* = 1.83 Hz, 1H), 7.23 (dd, *J* = 8.32, 1.91 Hz, 1H), 7.36 (d, *J* = 15.56 Hz, 1H), 7.53–7.57 (m, 2H), 7.76 (d, *J* = 15.56 Hz, 1H), 8.06–8.12 (m, 2H); ^{13}C NMR (126 MHz, $CDCl_3$): *δ* 56.0, 56.1, 110.2, 111.2, 119.9, 123.3, 125.4, 127.8, 129.3, 134.5, 135.0, 137.4, 145.6, 149.4, 151.7, 169.0, 189.6.

(*E*)-1-(4-(3-(3,4,5-trimethoxyphenyl)acryloyl)phenyl)-1*H*-pyrrole-2,5-dione (D19)

^{1}H NMR (500 MHz, $CDCl_3$): *δ* 3.88–3.93 (m, 9H), 6.85–6.87 (m, 2H), 6.90 (s, 2H), 7.37 (d, *J* = 15.56 Hz, 1H), 7.54–7.59 (m, 2H), 7.72 (d, *J* = 15.72 Hz, 1H), 8.07–8.12 (m, 2H); ^{13}C NMR (126 MHz, $CDCl_3$): *δ* 56.3, 61.0, 105.6, 121.4, 125.1, 129.4, 130.3, 134.5, 135.2, 137.3, 145.6, 153.6, 169.0, 189.7.

(*E*)-1-(4-(3-(4-(methylthio)phenyl)acryloyl)phenyl)-1*H*-pyrrole-2,5-dione (D20)

^{1}H NMR (500 MHz, $CDCl_3$): δ 2.51 (s, 3H), 6.89 (s, 2H), 7.22–7.28 (m, 2H), 7.46 (d, *J* = 15.72 Hz, 1H), 7.56 (d, *J* = 8.54 Hz, 4H), 7.78 (d, *J* = 15.56 Hz, 1H), 8.07–8.12 (m, 2H); ^{13}C NMR (126 MHz, $CDCl_3$): δ 15.2, 120.7, 125.5, 126.0, 128.9, 129.5, 131.3, 134.5, 135.1, 137.2, 142.7, 144.9, 169.0, 189.4.

(*E*)-1-(4-(3-(3-nitrophenyl)acryloyl)phenyl)-1*H*-pyrrole-2,5-dione (D21)

^{1}H NMR (500 MHz, DMSO-d_6): δ 7.24 (s, 2H), 7.56–7.62 (m, 2H), 7.73–7.79 (m, 1H), 7.89 (d, *J* = 15.72 Hz, 1H), 8.20 (d, *J* = 15.72 Hz, 1H), 8.26–8.39 (m, 4H), 8.80 (t, *J* = 1.91 Hz, 1H); ^{13}C NMR (126 MHz, DMSO-d_6): δ 123.1, 124.7, 124.8, 126.3, 129.4, 130.4, 134.9, 135.2, 135.9, 136.0, 136.6, 141.7, 148.5, 169.6, 188.3.

4.2.1.4.3. General procedure for the preparation of 4'-cinnamic-maleimides (D9-D11)

4-Amino-(*E*)-cinnamic acid (14, 3.1 mmol) was added to a solution of maleic anhydride (2.76 mmol) in ethyl acetate (5 mL) and stirred at RT for 2 h. The resultant precipitate was filtered and dried under vacuum. The dried intermediate (15) was added to a mixture of NaOAc (1.5 mmol) and acetic anhydride (15.3 mmol), which was preheated to 80 ºC and stirred at same temperature. After 1 h, the reaction mixture was diluted with ice-cold water (15 mL). The precipitated solid was filtered and washed with water. The obtained brown-coloured crude compound was purified by column chromatography using dichloromethane as eluent to yield the free acid (16). The acid (16, 0.12 m mol) was refluxed with a catalytic amount of sulfuric acid and molecular sieves (100 mg) in methanol or ethanol (5 mL) for overnight. Reaction was monitored by TLC and after completion of the reaction, the molecular sieves were filtered off and the solvent was evaporated from the reaction mixture under reduced pressure at

30 ºC. The remaining solid was neutralized with a saturated aqueous solution of $NaHCO_3$. The aqueous layer was two times extracted with equal volumes of ethyl acetate. The organic layers were combined, dried over Na_2SO_4.and the solvent was removed under reduced pressure at 30 ºC. The crude compound was purified by column chromatography using ethyl acetate and petroleum ether as eluents. Compounds were characterized by ^{1}H NMR and ^{13}C NMR spectrometry and their yields were in 45-60%.

(*E*)-3-(4-(2,5-dioxo-2,5-dihydro-1*H*-pyrrol-1-yl)phenyl)acrylic acid (D09)

^{1}H NMR (400 MHz, Acetone-d_6): δ 6.58 (d, J = 16.28 Hz, 1H), 7.06 (s, 2H), 7.46–7.51 (m, 2H), 7.71 (d, J = 16.28 Hz, 1H), 7.76–7.85 (m, 2H); ^{13}C NMR (101 MHz, Acetone-d_6): δ 120.0, 127.4, 129.4, 134.5, 135.4, 144.4, 167.5, 170.3.

Methyl (*E*)-3-(4-(2,5-dioxo-2,5-dihydro-1*H*-pyrrol-1-yl)phenyl)acrylate (D10)

^{1}H NMR (500 MHz, $CDCl_3$): δ 3.86 (s, 3H), 6.89 (s, 2H), 6.94 (d, J = 8.70 Hz, 2H), 7.39 (d, J = 15.72 Hz, 1H), 7.53–7.57 (m, 2H), 7.60 (d, J = 8.54 Hz, 2H), 7.80 (d, J = 15.56 Hz, 1H), 8.08–8.12 (m, 2H); ^{13}C NMR (126 MHz, $CDCl_3$): δ 51.8, 118.9, 126.0, 128.8, 132.9, 133.8, 134.4, 143.6, 167.2, 169.2.

Ethyl (*E*)-3-(4-(2,5-dioxo-2,5-dihydro-1*H*-pyrrol-1-yl)phenyl)acrylate (D11)

^{1}H NMR (300 MHz, $CDCl_3$): δ 1.34 (t, J = 7.16 Hz, 3H), 4.27 (q, J = 7.16 Hz, 2H), 6.44 (d, J = 16.01 Hz, 1H), 6.86 (s, 2H), 7.38–7.44 (m, 2H), 7.58–7.63 (m, 2H), 7.68 (d, J = 16.01 Hz, 1H); ^{13}C NMR (75 MHz, $CDCl_3$): δ 14.3, 57.3, 60.7, 118.9, 126.0, 128.7, 132.8, 133.7, 134.4, 143.4, 167.0, 169.1.

4.2.1.4.4. Procedure for the synthesis of chromone-based maleimide (D22)

7-Amino-2-methylchromone (18**,** 2.9 mmol) was added to a solution of maleic anhydride (1, 2.6 mmol) in ethyl acetate (10 mL). The mixture was stirred at RT for 1 h. The resultant solid precipitate was filtered and dried at RT under vacuum to get the intermediate, N-substituted aminobutenoic acid (19). A mixture of NaOAc (1.45 mmol) and acetic anhydride (14.5 mmol) was heated to 80 ºC in an oil bath until all NaOAc had dissolved. The intermediate (19) was added to this solution and stirred at 80 ºC. After 1 h, the reaction was cooled to RT and diluted with ice cold water (10 mL). The aqueous layer was extracted with ethyl acetate (2 x 10 mL). The organic layers were combined and dried over Na_2SO_4. The organic layer was evaporated at 30 ºC under reduced pressure and obtained crude compound was purified by column chromatography using ethyl acetate and petroleum ether as eluents to obtain compound D22 in 70% yield. It was characterized by NMR and mass spectrometry.

1-(2-methyl-4-oxo-4*H*-chromen-7-yl)-1*H*-pyrrole-2,5-dione (D22)

^{1}H NMR (300 MHz, $CDCl_3$): δ 2.38 (s, 3 H), 6.11–6.21 (m, 1H), 6.87–6.93 (m, 2H), 7.48 (dd, *J* = 8.67, 1.88 Hz, 1H), 7.56 (d, *J* = 1.70 Hz, 1H), 8.21–8.28 (m, 1H); ^{13}C NMR (75 MHz, $CDCl_3$): δ 20.61, 110.86, 114.34, 121.73, 122.4, 126.6, 134.5, 135.8, 156.5, 166.6, 168.7, 177.5; NSI-MS: *m/z* 256.0607 $(M+H)^+$

4.2.1.4.5. General procedure for the synthesis of amino-*N*-alkanoic acid maleimides (21)

Maleic anhydride (1**,** 10.2 mmol) was mixed with an appropriate amino acid (10.2 mmol) in acetic acid (10 mL) and the mixture was stirred at RT for 5 hours until a mono-coupled amide intermediate precipitated out. The intermediate was filtered and washed with water, followed by dissolution at reflux in water. Evaporation of water

under reduced pressure at 30 ºC and subsequent recrystalyzation in methanol gave the pure maleimide derivatives in good yields (55-70%). The compounds were characterized by ^{1}H NMR.

4.2.1.4.6. Procedure for the protection of (*1S-cis*)-3-bromo-3,5-cyclohexadiene-1,2-diol (22)

2,2-Dimethoxypropane (1.1 mmol) and a catalytic amount of p-toluenesulfonic acid were added to a pre-cooled solution of the dienediol (22**,** 0.52 mmol) in dichloromethane (4 mL). The reaction mixture was allowed to warm to RT and stirred until the reaction was complete (monitored by TLC). The reaction mixture was neutralized with triethylamine (0.2 mmol), and dichloromethane was evaporated under reduced pressure at 25 ºC. The crude compound was purified by flash column chromatography using ethylacetate and petroleum ether as eluents to obtain the pure compound in 90% yield.

TLC: 1:9 ethyl acetate, petroleum ether, R_f 0.7.

4.2.1.4.7. General procedure for [4+2] cycloadditions with protected (*1S-cis*)-3-bromo-3,5-cyclohexadiene-1,2-diol (23)

A mixture of the protected dienediol (23, 0.07 mmol) and a dienophile (0.08 mmol) in chloroform (4 mL) was refluxed under a drying tube for 2-4 days. Reaction progress was monitored by TLC. After the reaction was completed, the solvent was removed under reduced pressure at 25 ºC and the crude compound was purified by column chromatography using ethyl acetate and petroleum ether as eluents to afford cycloadducts in 40-70% yield. The compounds were characterized by ^{1}H NMR, ^{13}C NMR and mass spectrometry.

TLC: 1:1 ethyl acetate, petroleum ether, R_f 0.3-0.6.

4-bromo-2,2-dimethyl-7-phenyl-3a,4,10,10a-tetrahydro-6*H*-4,10-etheno[1,3]dioxolo[4,5-*d*][1,2,4]triazolo[1,2-*a*]pyridazine-6,8(7*H*)-dione

BrDPD01A (*anti*): ^{1}H NMR (300 MHz, $CDCl_3$): *δ* 1.36–1.44 (m, 6H), 4.64–4.79 (m, 2H), 5.18 (ddd, *J* = 5.56, 4.05, 1.32 Hz, 1H), 6.29 (ddd, *J* = 8.43, 5.79, 0.85 Hz, 1H), 6.58 (dt, *J* = 8.48, 1.32 Hz, 1H), 7.33–7.49 (m, 5H); ^{13}C NMR (75 MHz, $CDCl_3$): *δ* 25.5, 25.6, 51.9, 68.0, 74.9, 81.3, 112.5, 125.8, 128.3, 128.8, 129.2, 130.9, 134.8, 154.4, 154.9; NSI-MS: *m/z* 406, 408; HRMS (NSI): For $C_{17}H_{16}BrN_3O_4$+H $(M+H)^+$ *m/z* calcd., 406.0402; found, 406.0397.

4-bromo-6-(4-fluorophenyl)-2,2-dimethyl-3a,4,4a,7a,8,8a-hexahydro-5*H*-4,8-etheno[1,3]dioxolo[4,5-*f*]isoindole-5,7(6*H*)-dione

BrDPD02S (*endo-syn*): ^{1}H NMR (600 MHz, $CDCl_3$): *δ* 1.41 (s, 3H), 1.57 (s, 3H), 3.49–3.55 (m, 1H), 3.60–3.65 (m, 1H), 3.70–3.76 (m, 1H), 4.30 (dd, *J* = 8.25, 3.85 Hz, 1H), 4.39 (d, *J* = 8.44 Hz, 1H), 6.17 (dd, *J* = 8.44, 6.24 Hz, 1H), 6.39 (d, *J* = 9.54 Hz, 1H), 7.08–7.15 (m, 2H), 7.16–7.22 (m, 2H); ^{13}C NMR (101 MHz, $CDCl_3$): *δ* 24.4, 26.3, 36.6, 40.2, 44.2, 57.1, 75.1, 82.0, 113.4, 116.0, 116.3, 128.2, 128.3, 131.0, 137.1, 161.1, 163.5, 174.4, 176.6; NSI-MS: *m/z* 422, 424; HRMS (NSI): For $C_{19}H_{17}BrFNO_4$+H $(M+H)^+$ *m/z* calcd., 422.0403; found, 422.0398.

BrDPD02A (*endo-anti*): ^{1}H NMR (600 MHz, $CDCl_3$): *δ* 1.35 (s, 3H), 1.40 (s, 3H), 3.05 (dd, *J* = 8.44, 2.93 Hz, 1H), 3.12–3.17 (m, 1H), 3.55–3.60 (m, 1H), 4.40–4.48 (m, 2H), 6.07 (dd, *J* = 8.25, 6.42 Hz, 1H), 6.29 (d, *J* = 8.80 Hz, 1H), 7.10–7.15 (m, 2H), 7.16–7.22 (m, 2H); ^{13}C NMR (101 MHz, $CDCl_3$): *δ* 25.1, 25.4, 35.9, 42.2, 46.7, 57.7, 78.0, 83.7, 110.7, 116.1, 116.4, 128.2, 128.3, 129.7, 134.5, 160.7, 164.0, 172.4, 174.7; NSI-MS: *m/z* 422, 424; HRMS (NSI): For $C_{19}H_{17}BrFNO_4$+H $(M+H)^+$ *m/z* calcd., 422.0403; found, 422.0398.

4-bromo-6-(4-bromophenyl)-2,2-dimethyl-3a,4,4a,7a,8,8a-hexahydro-5*H*-4,8-ethenoo[1,3]dioxolo[4,5-*f*]isoindole-5,7(6*H*)-dione

BrDPD03S (*endo-syn*): ^{1}H NMR (300 MHz, $CDCl_3$): δ 1.41 (s, 3H), 1.57 (s, 3H), 3.49–3.57 (m, 1H), 3.59–3.66 (m, 1H), 3.70–3.76 (m, 1H), 4.26–4.33 (m, 1H), 4.34–4.43 (m, 1H), 6.16 (dd, *J* = 8.48, 6.59 Hz, 1H), 6.39 (d, *J* = 8.48 Hz, 1H), 7.07–7.15 (m, 2H), 7.52–7.61 (m, 2H); ^{13}C NMR (75 MHz, $CDCl_3$): δ 24.4, 26.3, 36.6, 40.3, 44.2, 57.5, 85.0, 82.0, 113.4, 127.5, 127.9, 128.0, 131.8, 132.3, 137.1, 174.1, 176.3; NSI-MS: *m/z* 481, 483, 485; HRMS (NSI): For $C_{19}H_{17}Br_2NO_4$+H $(M+H)^+$ *m/z* calcd., 481.9602; found, 481.9597.

BrDPD03A (*endo-anti*): ^{1}H NMR (300 MHz, $CDCl_3$): δ 1.35 (s, 3H), 1.40 (s, 3H), 3.01–3.08 (m, 1H), 3.15 (d, *J* = 8.29 Hz, 1H), 3.54–3.61 (m, 1H), 4.44 (s, 2H), 6.04–6.09 (m, 1H), 6.28 (d, *J* = 8.85 Hz, 1H), 7.07–7.14 (m, 2H), 7.53–7.61 (m, 2H); ^{13}C NMR (75 MHz, $CDCl_3$): δ 25.1, 25.4, 35.9, 42.3, 46.7, 57.6, 78.0, 83.7, 110.7, 122.8, 127.9, 129.7, 130.4, 132.4, 134.5, 172.1, 174.4; NSI-MS: *m/z* 481, 483, 485; HRMS (NSI): For $C_{19}H_{17}Br_2NO_4$+H $(M+H)^+$ *m/z* calcd., 481.9602; found, 481.9597.

6-(4-acetylphenyl)-4-bromo-2,2-dimethyl-3a,4,4a,7a,8,8a-hexahydro-5*H*-4,8-ethenoo[1,3]dioxolo[4,5-*f*]isoindole-5,7(6*H*)-dione

BrDPD04S (*endo-syn*): ^{1}H NMR (300 MHz, $CDCl_3$): δ 1.42 (s, 3H), 1.57 (s, 3H), 2.60 (s, 3H), 3.50–3.58 (m, 1H), 3.61–3.69 (m, 1H), 3.74 (s, 1H), 4.27–4.34 (m, 1H), 4.36–4.43 (m, 1H), 6.18 (dd, *J* = 8.57, 6.50 Hz, 1H), 6.41 (d, *J* = 8.48 Hz, 1H), 7.35–7.38 (m, 2H), 7.98–8.05 (m, 2H); ^{13}C NMR (75 MHz, $CDCl_3$): δ 24.4, 26.3, 26.7, 36.6, 40.3, 44.3, 57.4, 75.0, 82.0, 113.4, 126.4, 129.1, 131.0, 135.7, 136.9, 137.1, 174.0, 176.2, 197.0; NSI-MS: *m/z* 446, 448; HRMS (NSI): For $C_{21}H_{20}BrNO_5$+H $(M+H)^+$ *m/z* calcd., 446.0603; found, 446.0598.

BrDPD04A (*endo-anti*): ^{1}H NMR (300 MHz, $CDCl_3$): *δ* 1.36 (s, 3H), 1.40 (s, 3H), 2.60 (s, 3H), 3.05–3.11 (m, 1H), 3.18 (d, *J* = 8.48 Hz, 1H), 3.55–3.63 (m, 1H), 4.45 (s, 2H), 6.08 (dd, *J* = 8.57, 6.31 Hz, 1H), 6.31 (d, *J* = 8.48 Hz, 1H), 7.33–7.38 (m, 2H), 8.00–8.05 (m, 2H); ^{13}C NMR (75 MHz, $CDCl_3$): *δ* 25.1, 25.4, 26.7, 35.9, 42.3, 46.8, 57.6, 76.0, 83.7, 110.8, 126.4, 129.1, 129.8, 134.5, 135.4, 137.0, 172.0, 174.3, 197.0; NSI-MS: *m/z* 446, 448; HRMS (NSI): For $C_{21}H_{20}BrNO_5$+H $(M+H)^+$ *m/z* calcd., 446.0603; found, 446.0598.

4-bromo-6-(4-methoxyphenyl)-2,2-dimethyl-3a,4,4a,7a,8,8a-hexahydro-5*H*-4,8-etheno[1,3]dioxolo[4,5-*f*]isoindole-5,7(6*H*)-dione

BrDPD05S (*endo-syn*): ^{1}H NMR (300 MHz, $CDCl_3$): *δ* 1.41 (s, 3H), 1.53 (s, 3H), 3.49**–**3.57 (m, 1H), 3.58–3.65 (m, 1H), 3.69–3.75 (m, 1H), 3.80 (s, 3H), 4.26–4.33 (m, 1H), 4.36–4.42 (m, 1H), 6.16 (dd, *J* = 8.57, 6.31 Hz, 1H), 6.39 (d, *J* = 8.67 Hz, 1H), 6.89–6.98 (m, 2H), 7.06–7.15 (m, 2H); ^{13}C NMR (75 MHz, $CDCl_3$): *δ* 24.4, 26.3, 36.6, 40.2, 44.2, 55.5, 57.6, 75.1, 82.1, 113.3, 114.4, 124.3, 127.6, 130.1, 137.0, 160.0, 174.7, 176.9; NSI-MS: *m/z* 434, 436; HRMS (NSI): For $C_{20}H_{20}BrNO_5$+H $(M+H)^+$ *m/z* calcd., 434.0603; found, 434.0598.

BrDPD05A (*endo-anti*): ^{1}H NMR (300 MHz, $CDCl_3$): *δ* 1.35 (s, 3H), 1.40 (s, 3H), 2.99–3.07 (m, 1H), 3.09–3.18 (m, 1H), 3.50–3.63 (m, 1H), 3.81 (s, 3H), 4.39–4.50 (m, 2H), 6.06 (dd, *J* = 8.48, 6.22 Hz, 1H), 6.28 (d, *J* = 8.48 Hz, 1H), 6.87–7.00 (m, 2H), 7.05–7.15 (m, 2H); ^{13}C NMR (75 MHz, $CDCl_3$): *δ* 25.1, 25.4, 35.9, 42.2, 46.6, 55.6, 57.8, 78.1, 83.7, 110.7, 114.5, 124.1, 127.6, 129.7, 134.5, 159.8, 172.7, 175.0; NSI-MS: *m/z* 434, 436; HRMS (NSI): For $C_{20}H_{20}BrNO_5$+H $(M+H)^+$ *m/z* calcd., 434.0603; found, 434.0598.

4-bromo-2,2-dimethyl-6-(3,4,5-trimethoxyphenyl)-3a,4,4a,7a,8,8a-hexahydro-5*H*-4,8-etheno[1,3]dioxolo[4,5-*f*]isoindole-5,7(6*H*)-dione

BrDPD06S (*endo-syn*): ^{1}H NMR (400 MHz, $CDCl_3$): δ 1.42 (s, 3H), 1.57 (s, 3H), 1.73 (s, 1H), 3.49–3.58 (m, 1H), 3.59–3.66 (m, 1H), 3.73 (d, *J* = 8.14 Hz, 1H), 3.78–3.86 (m, 9H), 4.23–4.44 (m, 2H), 6.11–6.24 (m, 1H), 6.36–6.47 (m, 3H); ^{13}C NMR (75 MHz, $CDCl_3$): δ 24.4, 26.3, 36.7, 40.3, 44.2, 55.4, 56.3, 58.8, 77.2, 82.0, 103.2, 113.3, 126.9, 129.7, 136.5, 153.5, 174.0, 176.2; NSI-MS: *m/z* 494, 496; HRMS (NSI): For $C_{22}H_{24}BrNO_7$+H $(M+H)^+$ *m/z* calcd., 494.0814; found, 494.0809.

BrDPD06A *(endo-anti)*: ^{1}H NMR (400 MHz, $CDCl_3$): δ 1.35 (s, 3H), 1.40 (s, 3H), 3.03 (dd, *J* = 8.39, 2.80 Hz, 1H), 3.14 (d, *J* = 8.65 Hz, 1H), 3.53–3.61 (m, 1H), 3.76–3.87 (m, 9H), 4.38–4.50 (m, 2H), 6.08 (dd, *J* = 8.65, 6.61 Hz, 1H), 6.30 (d, *J* = 8.65 Hz, 1H), 6.39 (s, 2H); ^{13}C NMR (75 MHz, $CDCl_3$): δ 25.1, 25.4, 35.9, 42.2, 46.7, 56.3, 57.7, 60.9, 78.1, 83.7, 104.1, 110.7, 126.9, 129.7, 134.6, 153.5, 172.5, 174.7; NSI-MS: *m/z* 494, 496; HRMS (NSI): For $C_{22}H_{24}BrNO_7$+H $(M+H)^+$ *m/z* calcd., 494.0814; found, 494.0809.

3-(4-bromo-2,2-dimethyl-5,7-dioxo-3a,4,4a,5,7,7a,8,8a-octahydro-6*H*-4,8-etheno-[1,3]dioxolo[4,5-*f*]isoindol-6-yl)phenyl acetate

BrDPD07S (*endo-syn*): ^{1}H NMR (600 MHz, $CDCl_3$): δ 1.41 (s, 3H), 1.57 (s, 3H), 2.27 (s, 3H), 3.49–3.55 (m, 1H), 3.60–3.65 (m, 1H), 3.72 (d, *J* = 8.44 Hz, 1H), 4.29 (dd, *J* = 8.25, 3.85 Hz, 1H), 4.38 (d, *J* = 8.07 Hz, 1H), 6.13–6.18 (m, 1H), 6.38 (d, *J* = 8.80 Hz, 1H), 7.03–7.08 (m, 1H), 7.10–7.16 (m, 2H), 7.39–7.45 (m, 1H); ^{13}C NMR (75 MHz, $CDCl_3$): δ 21.1, 24.4, 26.3, 36.6, 40.2, 44.2, 57.5, 75.1, 82.0, 113.4, 119.6, 121.9, 123.4, 129.6, 131.0, 132.5, 137.1, 150.1, 168.9, 174.1, 176.2; NSI-MS: *m/z*

462, 464; HRMS (NSI): For $C_{21}H_{20}BrNO_6$+H $(M+H)^+$ *m/z* calcd., 462.0548; found, 462.0547.

BrDPD07A *(endo-anti)*: ^{1}H NMR (600 MHz, $CDCl_3$): *δ* 1.35 (s, 4H), 1.40 (s, 4H), 2.28 (s, 3H), 2.99–3.06 (m, 1H), 3.11–3.16 (m, 1H), 3.53–3.60 (m, 1H), 4.38–4.48 (m, 2H), 6.03–6.09 (m, 1H), 6.24–6.31 (m, 1H), 7.03–7.08 (m, 1H), 7.10–7.17 (m, 2H), 7.40–7.47 (m, 1H); ^{13}C NMR (75 MHz, $CDCl_3$): *δ* 21.1, 25.1, 25.4, 35.9, 42.2, 46.6, 57.7, 78.0, 83.7, 110.7, 119.7, 122.1, 123.4, 129.6, 129.7, 132.2, 134.5, 150.8, 168.9, 172.1, 174.3; NSI-MS: *m/z* 462, 464; HRMS (NSI): For $C_{21}H_{20}BrNO_6$+H $(M+H)^+$ *m/z* calcd., 462.0548; found, 462.0547.

(*E*)-3-(4-(4-bromo-2,2-dimethyl-5,7-dioxo-3a,4,4a,5,7,7a,8,8a-octahydro-6*H*-4,8-etheno[1,3]dioxolo[4,5-*f*]isoindol-6-yl)phenyl)acrylic acid

BrDPD09S (*endo-syn*): ^{1}H NMR (400 MHz, Acetone-d_6): *δ* 1.41 (s, 3H), 1.55 (s, 3H), 3.40**–**3.47 (m, 1H), 3.70 (dd, *J* = 8.65, 3.05 Hz, 1H), 3.80 (d, *J* = 8.65 Hz, 1H), 4.38–4.49 (m, 2H), 6.30 (dd, *J* = 8.39, 6.36 Hz, 1H), 6.42 (d, *J* = 8.65 Hz, 1H), 6.57 (d, *J* = 15.77 Hz, 1H), 7.26–7.33 (m, 2H), 7.69 (d, *J* = 15.77 Hz, 1H), 7.75–7.82 (m, 2H); ^{13}C NMR (101 MHz, Acetone-d_6): *δ* 24.6, 26.3, 37.6, 41.4, 45.6, 59.7, 76.0, 83.0, 113.6, 120.4, 128.0, 129.3, 132.4, 135.0, 135.4, 137.4, 144.2, 167.5, 175.0, 177.2; NSI-MS: *m/z* 474, 476*;* HRMS (NSI): For $C_{22}H_{20}BrNO_6$ $(M+H)^+$ *m/z* calcd.,474.0552; found, 474.0547.

Methyl-(*E*)-3-(4-(4-bromo-2,2-dimethyl-5,7-dioxo-3a,4,4a,5,7,7a,8,8a-octahydro-6*H*-4,8-etheno[1,3]dioxolo[4,5-*f*]isoindol-6-yl)phenyl)acrylate

BrDPD10S (*endo-syn*): ^{1}H NMR (400 MHz, $CDCl_3$): δ 1.41 (s, 3H), 1.57 (s, 3H), 3.54 (dt, *J* = 6.36, 3.43 Hz, 1H), 3.60–3.68 (m, 1H), 3.71–3.77 (m, 1H), 3.80 (s, 3H), 4.30 (dd, *J* = 8.14, 4.07 Hz, 1H), 4.36–4.43 (m, 1H), 6.17 (dd, *J* = 8.39, 6.36 Hz, 1H), 6.35–6.48 (m, 2H), 7.27 (d, *J* = 8.14 Hz, 2H), 7.58 (d, *J* = 8.65 Hz, 2H), 7.66 (d, *J* = 15.77 Hz, 1H); ^{13}C NMR (101 MHz, $CDCl_3$): δ 24.4, 26.3, 36.6, 40.3, 44.3, 51.9, 57.5, 75.1, 82.0, 113.4, 119.2, 126.7, 128.6, 131.0, 133.1, 134.8, 137.1, 143.5, 167.1, 174.2, 176.4; NSI-MS: *m/z* 488, 490; HRMS (NSI): For $C_{23}H_{22}BrNO_6$+H $(M+H)^+$ *m/z* calcd., 488.0709; found, 488.0703.

BrDPD10A (*endo-anti*): ^{1}H NMR (400 MHz, $CDCl_3$): δ 1.35 (s, 3H), 1.40 (s, 3H), 3.06 (dd, *J* = 8.39, 2.80 Hz, 1H), 3.12–3.19 (m, 1H), 3.56–3.61 (m, 1H), 3.80 (s, 3H), 4.39–4.51 (m, 2H), 6.07 (dd, *J* = 8.65, 6.10 Hz, 1H), 6.29 (d, *J* = 8.65 Hz, 1H), 6.44 (d, *J* = 16.28 Hz, 1H), 7.26–7.28 (m, 2H), 7.54–7.61 (m, 2H), 7.63–7.71 (m, 1H); ^{13}C NMR (101 MHz, $CDCl_3$): δ 25.4, 25.8, 36.3, 42.7, 47.1, 52.2, 58.0, 78.4, 84.1, 111.1, 119.7, 127.1, 129.0, 130.1, 133.2, 134.9, 135.3, 143.8, 167.5, 172.6, 174.8; NSI-MS: *m/z* 488, 490; HRMS (NSI): For $C_{23}H_{22}BrNO_6$+H $(M+H)^+$ *m/z* calcd., 488.0709; found, 488.0703.

Ethyl-(*E*)-3-(4-(4-bromo-2,2-dimethyl-5,7-dioxo-3a,4,4a,5,7,7a,8,8a-octahydro-6*H*-4,8-etheno[1,3]dioxolo[4,5-*f*]isoindol-6-yl)phenyl)acrylate

BrDPD11A (*endo-anti*): ^{1}H NMR (300 MHz, $CDCl_3$): δ 1.28–1.45 (m, 9H), 3.02–3.11 (m, 1H), 3.12–3.20 (m, 1H), 3.55–3.62 (m, 1H), 4.21–4.31 (m, 2H), 4.40–4.52 (m, 2H), 6.07 (dd, *J* = 8.57, 6.31 Hz, 1H), 6.29 (d, *J* = 8.67 Hz, 1H), 6.43 (d, *J* = 16.01 Hz, 1H), 7.22–7.30 (m, 3H), 7.58 (d, *J* = 8.48 Hz, 2H), 7.66 (d, *J* = 16.01 Hz, 1H); ^{13}C

NMR (75 MHz, $CDCl_3$): δ 14.3, 25.1, 25.4, 35.9, 42.3, 46.7, 57.7, 60.7, 78.0, 83.7, 110.7, 119.8, 126.7, 128.6, 129.7, 132.7, 134.5, 135.0, 143.1, 166.7, 172.2, 174.5; NSI-MS: *m/z* 502, 504; HRMS (NSI): For $C_{24}H_{24}BrNO_6$+H $(M+H)^+$ *m/z* calcd., 502.0865; found, 502.0860.

(*E*)-4-bromo-6-(4-(3-(4-fluorophenyl)acryloyl)phenyl)-2,2-dimethyl-3a,4,4a,7a,8,-8a-hexahydro-5*H*-4,8-etheno[1,3]dioxolo[4,5-*f*]isoindole-5,7(6*H*)-dione

BrDPD13S (*endo-syn*): ^{1}H NMR (300 MHz, $CDCl_3$): δ 1.42 (s, 3H), 1.58 (s, 2H), 3.51–3.59 (m, 1H), 3.63–3.70 (m, 1H), 3.73–3.80 (m, 1H), 4.27–4.35 (m, 1H), 4.37–4.44 (m, 1H), 6.20 (dd, *J* = 8.48, 6.59 Hz, 1H), 6.42 (d, *J* = 8.48 Hz, 1H), 7.06–7.15 (m, 2H), 7.34–7.45 (m, 3H), 7.58–7.67 (m, 2H), 7.77 (d, *J* = 15.82 Hz, 1H), 8.02–8.10 (m, 2H); ^{13}C NMR (75 MHz, $CDCl_3$): δ 24.4, 26.3, 36.7, 40.3, 44.4, 57.5, 75.0, 82.0, 113.4, 116.1, 116.4, 121.6, 126.4, 130.6, 130.4, 129.3, 131.1, 135.4, 137.1, 138.0, 144.2, 174.1, 176.3, 189.4; NSI-MS: *m/z* 552, 554; HRMS (NSI): For $C_{28}H_{23}BrFNO_5$+H $(M+H)^+$ *m/z* calcd., 552.0822; found, 552.0816.

BrDPD13A (*endo-anti*): ^{1}H NMR (300 MHz, $CDCl_3$): δ 1.36 (s, 3H), 1.41 (s, 3H), 3.00–3.24 (m, 2H), 3.55–3.66 (m, 1H), 4.40–4.51 (m, 2H), 6.05–6.15 (m, 1H), 6.27–6.38 (m, 1H), 7.11 (t, *J* = 8.57 Hz, 2H), 7.35–7.45 (m, 3H), 7.63 (dd, *J* = 8.76, 5.37 Hz, 2H), 7.77 (d, *J* = 15.82 Hz, 1H), 8.07 (d, *J* = 8.48 Hz, 2H); ^{13}C NMR (75 MHz, $CDCl_3$): δ 25.1, 25.4, 35.9, 42.4, 46.8, 57.6, 78.0, 83.7, 110.8, 116.2, 116.4, 121.5, 126.4, 129.3, 129.8, 130.4, 130.6, 134.6, 135.1, 138.2, 144.3, 172.1, 174.3, 189.3; NSI-MS: *m/z* 552, 554; HRMS (NSI): For $C_{28}H_{23}BrFNO_5$+H $(M+H)^+$ *m/z* calcd., 552.0822; found, 552.0816.

(*E*)-4-bromo-6-(4-(3-(4-bromophenyl)acryloyl)phenyl)-2,2-dimethyl-3a,4,4a,7a,8,-8a-hexahydro-5*H*-4,8-etheno[1,3]dioxolo[4,5-*f*]isoindole-5,7(6*H*)-dione

BrDPD15S (*endo-syn*): ^{1}H NMR (400 MHz, $CDCl_3$): δ 1.42 (s, 3H), 1.58 (s, 3H), 3.52–3.60 (m, 1H), 3.67 (dd, *J* = 8.65, 3.05 Hz, 1H), 3.74–3.81 (m, 1H), 4.22–4.44 (m, 2H), 6.19 (dd, *J* = 8.39, 6.36 Hz, 1H), 6.42 (d, *J* = 8.65 Hz, 1H), 7.37–7.59 (m, 7H), 7.73 (d, *J* = 15.77 Hz, 1H), 8.06 (d, *J* = 8.65 Hz, 2H); ^{13}C NMR (101 MHz, $CDCl_3$): δ 25.1, 25.4, 35.9, 42.2, 46.7, 57.8, 78.1, 83.8, 110.7, 114.5, 117.7, 120.2, 124.8, 125.5, 127.1, 127.6, 129.1, 129.7, 134.5, 159.8, 172.7, 174.5, 189.2; NSI-MS: *m/z* 612, 614, 616; HRMS (NSI): For $C_{28}H_{23}Br_2NO_5$+H $(M+H)^+$ *m/z* calcd., 612.0021; found, 612.0021.

BrDPD15A *(endo-anti)*: ^{1}H NMR (400 MHz, $CDCl_3$): δ 1.36 (s, 3H), 1.41 (s, 3H), 3.05–3.12 (m, 1H), 3.16–3.22 (m, 1H), 3.57–3.64 (m, 1H), 4.42–4.50 (m, 2H), 6.06–6.13 (m, 1H), 6.31 (d, *J* = 8.65 Hz, 1H), 7.35–7.58 (m, 7H), 7.73 (d, *J* = 15.77 Hz, 1H), 8.07 (d, *J* = 8.14 Hz, 2H); NSI-MS: *m/z* 612, 614, 616; HRMS (NSI): For $C_{28}H_{23}Br_2NO_5$+H $(M+H)^+$ *m/z* calcd., 612.0021; found, 612.0021.

(*E*)-4-bromo-6-(4-(3-(4-methoxyphenyl)acryloyl)phenyl)-2,2-dimethyl-3a,4,4a,-7a,8,8a-hexahydro-5*H*-4,8-etheno[1,3]dioxolo[4,5-*f*]isoindole-5,7(6*H*)-dione

BrDPD17S (*endo-syn*): ^{1}H NMR (600 MHz, $CDCl_3$): δ 1.42 (s, 3H), 1.58 (s, 3H), 3.53–3.58 (m, 1H), 3.66 (dd, *J* = 8.44, 2.93 Hz, 1H), 3.75–3.79 (m, 1H), 3.85 (s, 3H), 4.31 (dd, *J* = 8.07, 3.67 Hz, 1H), 4.40 (d, *J* = 8.07 Hz, 1H), 6.19 (dd, *J* = 8.44, 6.60 Hz, 1H), 6.42 (d, *J* = 8.44 Hz, 1H), 6.90–6.96 (m, 2H), 7.35 (d, *J* = 15.41 Hz, 1H), 7.37–7.41 (m, 2H), 7.56–7.61 (m, 2H), 7.77 (d, *J* = 15.77 Hz, 1H), 8.04–8.07 (m, 2H); ^{13}C NMR (101 MHz, $CDCl_3$): δ 24.4, 26.3, 36.7, 40.3, 44.3, 55.5, 57.5, 75.0, 82.0, 113.4, 114.5, 119.6, 126.3, 129.2, 130.4, 131.1, 135.1, 137.1, 138.4, 145.2, 161.9,

174.1, 176.3, 189.6; NSI-MS: *m/z* 564, 566; HRMS (NSI): For $C_{29}H_{26}BrNO_6$+H $(M+H)^+$ *m/z* calcd., 564.1022; found, 564.1016.

BrDPD17A (*endo-anti*): ^{1}H NMR (300 MHz, $CDCl_3$): *δ* 1.42 (s, 3H), 1.58 (s, 3H), 3.50–3.60 (m, 1H), 3.62–3.70 (m, 1H), 3.77 (d, *J* = 8.10 Hz, 1H), 3.85 (s, 3H), 4.25–4.44 (m, 2H), 6.19 (dd, *J* = 8.48, 6.59 Hz, 1H), 6.42 (d, *J*= 8.48 Hz, 1H), 6.89–6.98 (m, 2H), 7.31–7.42 (m, 3H), 7.55–7.63 (m, 2H), 7.77 (d, *J* = 15.64 Hz, 1H), 8.03–8.10 (m, 2H); ^{13}C NMR (75 MHz, $CDCl_3$): *δ* 25.1, 25.4, 35.9, 42.3, 46.8, 55.5, 57.7, 78.0, 83.7, 110.7, 114.5, 119.5, 126.2, 127.5, 129.2, 129.8, 130.4, 134.6, 134.9, 138.6, 145.5, 161.9, 172.1, 174.4, 189.6; NSI-MS: *m/z* 564, 566; HRMS (NSI): For $C_{29}H_{26}BrNO_6$+H $(M+H)^+$ *m/z* calcd., 564.1022; found, 564.1016.

(*E*)-4-bromo-6-(4-(3-(3,4-dimethoxyphenyl)acryloyl)phenyl)-2,2-dimethyl-3a,4,-4a,7a,8,8a-hexahydro-5*H*-4,8-etheno[1,3]dioxolo[4,5-*f*]isoindole-5,7(6*H*)-dione

BrDPD18A (*endo-anti*): ^{1}H NMR (300 MHz, $CDCl_3$): *δ* 1.36 (s, 3H), 1.41 (s, 3H), 3.01–3.23 (m, 2H), 3.55–3.65 (m, 1H), 3.94 (d, *J* = 4.33 Hz, 6H), 4.38–4.52 (m, 2H), 6.05–6.14 (m, 1H), 6.27–6.35 (m, 1H), 6.85–6.95 (m, 1H), 7.09–7.23 (m, 2H), 7.27–7.44 (m, 4H), 7.74 (d, *J* = 15.64 Hz, 1H), 8.01–8.10 (m, 2H); ^{13}C NMR (75 MHz, $CDCl_3$): *δ* 25.1, 25.4, 35.9, 42.3, 46.8, 56.0, 57.6, 78.0, 83.7, 110.2, 110.8, 111.2, 119.9, 123.4, 126.4, 127.7, 129.3, 129.8, 134.6, 134.9, 138.6, 145.9, 149.4, 151.7, 172.1, 174.4, 189.9; NSI-MS: *m/z* 594, 596; HRMS (NSI): For $C_{30}H_{28}BrNO_7$+H $(M+H)^+$ *m/z* calcd., 594.1127; found, 594.1122.

(*E*)-4-bromo-2,2-dimethyl-6-(4-(3-(4-(methylthio)phenyl)acryloyl)phenyl)-3a,4,4a,7a,8,8a-hexahydro-5*H*-4,8-etheno[1,3]dioxolo[4,5-*f*]isoindole-5,7(6*H*)-dione

BrDPD20S (*endo-syn*): ^{1}H NMR (400 MHz, $CDCl_3$): δ 1.35–1.45 (m, 3H), 1.54 (s, 3H), 2.48–2.53 (m, 3H), 3.55 (dt, *J* = 6.61, 3.31 Hz, 1H), 3.63–3.70 (m, 1H), 3.73–3.79 (m, 1H), 4.26–4.47 (m, 2H), 6.14–6.24 (m, 1H), 6.42 (d, *J* = 8.14 Hz, 1H), 7.20–7.30 (m, 2H), 7.36–7.48 (m, 3H), 7.54 (d, *J* = 8.65 Hz, 2H), 7.76 (d, *J* = 15.77 Hz, 1H), 8.06 (d, *J* = 8.65 Hz, 2H); ^{13}C NMR (101 MHz, $CDCl_3$): δ 15.2, 24.3, 26.3, 30.7, 40.3, 44.3, 57.5, 75.0, 82.0, 113.0, 120.0, 126.0, 126.4, 128.9, 129.2, 131.1, 135.3, 137.1, 138.2, 142.8, 145.0, 174.1, 176.3, 189.5; NSI-MS: *m/z* 580, 582; HRMS (NSI): For $C_{29}H_{26}BrNO_5S$+H $(M+H)^+$ *m/z* calcd., 580.0793; found, 580.0788.

BrDPD20A (*endo-anti*): ^{1}H NMR (400 MHz, $CDCl_3$): δ 1.36 (s, 3H), 1.41 (s, 3H), 2.51 (s, 3H), 3.09 (dd, *J* = 8.39, 2.80 Hz, 1H), 3.17–3.22 (m, 1H), 3.56–3.65 (m, 1H), 4.40–4.52 (m, 2H), 6.05–6.13 (m, 1H), 6.31 (d, *J* = 8.65 Hz, 1H), 7.21–7.29 (m, 2H), 7.36–7.46 (m, 3H), 7.54 (d, *J* = 8.14 Hz, 2H), 7.76 (d, *J* = 15.77 Hz, 1H), 8.06 (d, *J* = 8.65 Hz, 2H); ^{13}C NMR (101 MHz, $CDCl_3$): δ 15.2, 25.1, 25.4, 35.9, 42.3, 46.8, 57.6, 78.0, 83.7, 110.8, 120.7, 126.0, 126.4, 128.9, 129.3, 129.8, 113.2, 134.6, 138.4, 142.8, 145.0, 172.1, 174.3, 189.5; NSI-MS: *m/z* 580, 582; HRMS (NSI): For $C_{29}H_{26}BrNO_5S$+H $(M+H)^+$ *m/z* calcd., 580.0793; found, 580.0788.

(*E*)-4-bromo-2,2-dimethyl-6-(4-(3-(3-nitrophenyl)acryloyl)phenyl)-3a,4,4a,7a,8,-8a-hexahydro-5*H*-4,8-etheno[1,3]dioxolo[4,5-*f*]isoindole-5,7(6*H*)-dione

BrDPD21A (*endo-anti*): ^{1}H NMR (300 MHz, $CDCl_3$): δ 1.36 (s, 3H), 1.41 (s, 3H), 3.07–3.26 (m, 2H), 3.49–3.53 (m, 1H), 3.49–3.67 (m, 1H), 4.32–4.54 (m, 2H), 6.04–6.16 (m, 1H), 6.25–6.38 (m, 1H), 7.38–7.50 (m, 2H), 7.55–7.68 (m, 2H), 7.78–7.97

(m, 2H), 8.07–8.16 (m, 2H), 8.27 (dd, *J* = 9.32, 1.22 Hz, 1H), 8.50 (t, *J* = 1.88 Hz, 1H); ^{13}C NMR (75 MHz, $CDCl_3$): *δ* 25.1, 25.4, 35.9, 42.4, 46.8, 57.6, 78.0, 83.7, 110.8, 122.5, 124.3, 124.9, 126.6, 129.4, 129.7, 129.8, 130.1, 134.4, 134.6, 135.6, 136.5, 142.4, 148.8, 172.1, 174.3, 188.7; NSI-MS: *m/z* 579, 581; HRMS (NSI): For $C_{28}H_{23}BrN_2O_7$+H $(M+H)^+$ *m/z* calcd., 579.0767; found, 579.0761.

4-bromo-6-ethyl-2,2-dimethyl-3a,4,4a,7a,8,8a-hexahydro-5*H*-4,8-etheno[1,3]-dioxolo[4,5-*f*]isoindole-5,7(6*H*)-dione

BrDPD23S (*endo-syn*): ^{1}H NMR (300 MHz, $CDCl_3$): *δ* 1.09 (t, *J* = 7.25 Hz, 3H), 1.39 (s, 3H), 1.53 (s, 3H), 3.36–3.60 (m, 5H), 4.21–4.28 (m, 1H), 4.31–4.38 (m, 1H), 5.97–6.11 (m, 1H), 6.27 (d, *J* = 9.04 Hz, 1H); ^{13}C NMR (75 MHz, $CDCl_3$): *δ* 13.0, 24.4, 26.3, 34.0, 36.3, 40.1, 44.1, 57.7, 75.1, 82.1, 113.2, 130.7, 136.8, 175.3, 177.3; NSI-MS: *m/z* 356, 358; HRMS (NSI): For $C_{15}H_{18}BrNO_4$+H $(M+H)^+$ *m/z* calcd., 356.0497; found, 356.0492.

BrDPD23A (*endo-anti*): ^{1}H NMR (300 MHz, $CDCl_3$): *δ* 1.10 (t, *J* = 7.16 Hz, 3H), 1.33 (s, 3H), 1.38 (s, 3H), 2.85 (dd, *J* = 8.29, 2.64 Hz, 1H), 2.93–3.01 (m, 1H), 3.43–3.56 (m, 3H), 4.34–4.42 (m, 2H), 5.94 (dd, *J* = 8.57, 6.31 Hz, 1H), 6.17 (dd, *J* = 8.67, 0.94 Hz, 1H); ^{13}C NMR (75 MHz, $CDCl_3$): *δ* 12.9, 25.1, 25.4, 34.2, 35.6, 42.2, 46.6, 57.8, 78.1, 83.7, 110.6, 129.4, 134.2, 173.3, 175.4; NSI-MS: *m/z* 356, 358; HRMS (NSI): For $C_{15}H_{18}BrNO_4$+H $(M+H)^+$ *m/z* calcd., 356.0497; found, 356.0492.

4-bromo-2,2-dimethyl-6-(2-morpholinoethyl)-3a,4,4a,7a,8,8a-hexahydro-5*H*-4,8-etheno[1,3]dioxolo[4,5-*f*]isoindole-5,7(6*H*)-dione

BrDPD24S (*endo-syn*): ^{1}H NMR (300 MHz, $CDCl_3$): *δ* 1.39 (s, 3H), 1.54 (s, 3H), 2.35–2.53 (m, 6H), 3.38–3.49 (m, 2H), 3.51–3.71 (m, 7H), 4.22–4.29 (m, 1H), 4.31–

4.38 (m, 1H), 6.03 (dd, *J* = 8.29, 6.78 Hz, 1H), 6.26 (d, *J* = 8.48 Hz, 1H); ^{13}C NMR (75 MHz, $CDCl_3$): *δ* 24.4, 26.3, 35.8, 36.3, 40.2, 44.1, 53.4, 55.3, 57.7, 67.1 75.1, 82.1 113.3, 130.7, 136.8, 175.4, 177.5; NSI-MS: *m/z* 441, 443; HRMS (NSI): For $C_{19}H_{25}BrN_2O_5$+H $(M+H)^+$ *m/z* calcd., 441.1025; found, 441.1020.

BrDPD24A (*endo-anti*): ^{1}H NMR (400 MHz, $CDCl_3$): *δ* 1.33 (s, 3H), 1.38 (s, 3H), 2.36–2.51 (m, 6H), 2.88 (dd, *J* = 8.14, 2.54 Hz, 1H), 2.99 (d, *J* = 8.14 Hz, 1H), 3.47 (dt, *J* = 5.85, 2.67 Hz, 1H), 3.55–3.67 (m, 6H), 4.35–4.42 (m, 2H), 5.94 (dd, *J* = 8.65, 6.10 Hz, 1H), 6.16 (d, *J* = 8.65 Hz, 1H); ^{13}C NMR (101 MHz, $CDCl_3$): *δ* 25.1, 25.4, 35.6, 36.0, 42.3, 46.6, 53.4, 56.2, 57.8, 67.1, 78.1, 83.8, 110.6, 129.4, 134.2, 173.5, 175.6; NSI-MS: *m/z* 441, 443; HRMS (NSI): For $C_{19}H_{25}BrN_2O_5$+H $(M+H)^+$ *m/z* calcd., 441.1025; found, 441.1020.

4.2.1.4.8. General procedure for [4+2] cycloadditions with unprotected (*1S-cis*)-3-bromo-3,5-cyclohexadiene-1,2-diol (22)

A mixture of dienediol (22, 0.07 mmol) and a dienophile (0.08 mmol) in toluene (5 mL) was refluxed with a drying tube for 2-4 days. Reaction progress was monitored by TLC. After the reaction was completed, the solvent was removed under reduced pressure at 25 ºC and the crude compound was purified by column chromatography using ethyl acetate and petroleum ether as eluents to afford cycloadducts in 40-70% yield. The compounds were characterized by ^{1}H NMR, ^{13}C NMR and mass spectrometry.

TLC: 3:7 ethyl acetate, dichloromethane, R_f 0.4-0.6.

5-bromo-10,11-dihydroxy-2-phenyl-5,8-dihydro-1*H*-5,8-ethano[1,2,4]triazolo[1,2-a]pyridazine-1,3(2*H*)-dione

BrDUD01A (*anti*): ^{1}H NMR (300 MHz, Acetone-d_6): δ 4.26 (d, J = 7.35 Hz, 1H), 4.50 (dd, J = 7.16, 3.77 Hz, 1H), 4.98 (ddd, J = 5.60, 4.00, 1.51 Hz, 1H), 6.48 (ddd, J = 8.48, 5.65, 0.75 Hz, 1H), 6.60–6.66 (m, 1H), 7.37–7.55 (m, 5H); ^{13}C NMR (75 MHz, Acetone-d_6): δ 54.4, 67.5, 72.3, 73.6, 127.1, 129.3, 129.8, 130.3, 132.5, 136.0, 155.1, 155.6; NSI-MS: *m/z* 366, 368; HRMS (NSI): For $C_{14}H_{12}BrN_3O_4$+H $(M+H)^+$ *m/z* calcd., 366.0089; found, 366.0084.

4-bromo-2-(4-fluorophenyl)-8,9-dihydroxy-3a,4,7,7a-tetrahydro-1*H*-4,7-ethano-isoindole-1,3(2*H*)-dione

BrDUD02S (*endo-syn*): ^{1}H NMR (300 MHz, DMSO–d_6): δ 3.01 - 3.11 (m, 1H), 3.45–3.52 (m, 1H), 3.60 (d, J = 8.29 Hz, 1H), 3.64–3.74 (m, 2H), 5.41–5.60 (m, 2H), 6.19 (dd, J = 8.67, 6.40 Hz, 1H), 6.33 (d, J = 8.48 Hz, 1H), 7.15–7.25 (m, 2H), 7.27–7.37 (m, 2H); ^{13}C NMR (75 MHz, $CDCl_3$): δ 44.4, 64.3, 70.5, 115.7, 116.0, 128.0, 129.0, 129.2, 131.2, 136.0, 159.8, 163.1, 175.0, 177.1; NSI-MS: *m/z* 382, 384; HRMS (NSI): For $C_{16}H_{13}BrFNO_4$+H $(M+H)^+$ *m/z* calcd., 382.009; found, 382.0085.

4-bromo-2-(4-bromophenyl)-8,9-dihydroxy-3a,4,7,7a-tetrahydro-1*H*-4,7-ethano-isoindole-1,3(2*H*)-dione

BrDUD03S (*endo-syn*): ^{1}H NMR (300 MHz, Acetone-d_6): δ 3.20–3.35 (m, 1H), 3.58–3.68 (m, 1H), 3.70–3.80 (m, 1H), 3.83–3.96 (m, 2H), 4.83 (d, J = 3.39 Hz, 1H), 5.17 (d, J = 3.58 Hz, 1H), 6.24 (dd, J = 8.67, 6.40 Hz, 1H), 6.33–6.40 (m, 1H), 7.13–7.23 (m, 2H), 7.60–7.69 (m, 2H); ^{13}C NMR (75 MHz, Acetone-d_6): δ 40.2, 40.9, 45.3, 63.9,

65.5, 71.8, 122.2, 129.7, 132.1, 132.7, 132.9, 137.4, 175.3, 177.3; NSI-MS: *m/z* 441, 443; HRMS (NSI): For $C_{16}H_{13}Br_2NO_4$ $(M+H)^+$ *m/z* calcd., 441.9289; found, 441.9284.

2-(4-acetylphenyl)-4-bromo-8,9-dihydroxy-3a,4,7,7a-tetrahydro-1*H*-4,7-ethano-isoindole-1,3(2*H*)-dione

BrDUD04S (*endo-syn*): ^{1}H NMR (400 MHz, DMSO-d_6): δ 2.60 (s, 3H), 3.03–3.13 (m, 1H), 3.51 (dd, *J* = 8.39, 2.80 Hz, 1H), 3.59–3.76 (m, 3H), 5.46 (d, *J* = 4.07 Hz, 1H), 5.56 (d, *J* = 4.58 Hz, 1H), 6.20 (dd, *J* = 8.65, 6.61 Hz, 1H), 6.34 (d, *J* = 8.65 Hz, 1H), 7.33 (d, *J* = 8.65 Hz, 2H), 8.05 (d, *J* = 8.65 Hz, 2H); ^{13}C NMR (101 MHz, DMSO-d_6): *δ* 26.8, 39.1, 44.6, 64.2, 70.5, 127.0, 128.8, 131.3, 136.0, 136.1, 136.4, 174.8, 176.9, 197.2; NSI-MS: *m/z* 406, 408; HRMS (NSI): For $C_{18}H_{16}BrNO_5$+H $(M+H)^+$ *m/z* calcd.,406.029; found,406.024 .

4-bromo-8,9-dihydroxy-2-(4-methoxyphenyl)-3a,4,7,7a-tetrahydro-1*H*-4,7-etha-noisoindole-1,3(2*H*)-dione

BrDUD05S (*endo-syn*): ^{1}H NMR (500 MHz, Acetone-d_6): *δ* 3.26–3.33 (m, 1H), 3.53–3.60 (m, 1H), 3.64–3.69 (m, 1H), 3.75 (s, 3H), 3.86 (d, *J* = 3.20 Hz, 2H), 6.09–6.17 (m, 1H), 6.31 (s, 1H), 6.85–6.93 (m, 2H), 7.02–7.08 (m, 2H); ^{13}C NMR (126 MHz, Acetone-d_6): *δ* 39.2, 39.9, 44.1, 55.3, 62.7, 64.5, 70.8, 114.2, 124.8, 127.9, 131.0, 136.7, 160.5, 175.2, 177.2; NSI-MS: *m/z* 394, 396; HRMS (NSI): For $C_{17}H_{16}BrNO_5$+H $(M+H)^+$ *m/z* calcd., 394.029; found, 394.0285.

BrDUD05A (*endo-anti*): ^{1}H NMR (300 MHz, Acetone-d_6): *δ* 3.23–3.43 (m, 3H), 3.80–3.84 (m, 3H), 4.02–4.16 (m, 1H), 4.22–4.33 (m, 1H), 4.59 (d, *J* = 4.33 Hz, 1H), 4.77 (br. s, 1H), 6.08–6.30 (m, 2H), 6.92–7.15 (m, 4H); ^{13}C NMR (75 MHz, Acetone-d_6): *δ* 39.6, 43.4, 48.6, 55.8, 64.8, 70.1, 75.2, 114.8, 126.2, 128.9, 131.3, 135.5, 160.4,

174.1, 176.3; NSI-MS: *m/z* 394, 396; HRMS (NSI): For $C_{17}H_{16}BrNO_5$+H $(M+H)^+$ *m/z* calcd., 394.029; found, 394.0285.

4-bromo-8,9-dihydroxy-2-(3,4,5-trimethoxyphenyl)-3a,4,7,7a-tetrahydro-1*H*-4,7-ethanoisoindole-1,3(2*H*)-dione

BrDUD06S (e*ndo-syn*): ^{1}H NMR (400 MHz, Acetone-d_6): δ 3.19–3.28 (m, 1H), 3.59 (dd, *J* = 8.39, 2.80 Hz, 1H), 3.68–3.81 (m, 10H), 3.84–3.94 (m, 2H), 4.76–4.86 (m, 1H), 5.16 (d, *J* = 4.07 Hz, 1H), 6.24 (dd, *J* = 8.90, 6.36 Hz, 1H), 6.37 (d, *J* = 8.65 Hz, 1H), 6.49 (s, 2H); ^{13}C NMR (101 MHz, Acetone-d_6): δ 40.2, 40.8, 45.2, 56.6, 60.6, 64.0, 65.5, 71.8, 106.0, 129.2, 132.0, 137.4, 139.3, 154.3, 175.5, 177.5; NSI-MS: *m/z* 454, 456; HRMS (NSI): For $C_{19}H_{20}BrNO_7$+H $(M+H)^+$ *m/z* calcd., 454.0501; found, 454.0496.

BrDUD06A (*endo-anti*): ^{1}H NMR (300 MHz, Acetone-d_6): δ 3.26–3.35 (m, 2H), 3.36–3.42 (m, 1H), 3.74 (s, 3H), 3.76–3.81 (m, 6H), 4.03–4.13 (m, 1H), 4.23–4.30 (m, 1H), 4.59 (d, *J* = 4.52 Hz, 1H), 4.78 (d, *J* = 6.22 Hz, 1H), 6.10–6.19 (m, 1H), 6.23–6.30 (m, 1H), 6.46–6.49 (m, 2H); ^{13}C NMR (75 MHz, Acetone-d_6): δ 39.6, 43.4, 48.7, 56.6, 60.6, 64.8, 70.1, 75.2, 105.9, 129.1, 131.3, 134.7, 135.5, 154.3, 178.8, 176.1; NSI-MS: *m/z* 454, 456; HRMS (NSI): For $C_{19}H_{20}BrNO_7$+H $(M+H)^+$ *m/z* calcd., 454.0501; found, 454.0496.

3-(4-bromo-8,9-dihydroxy-1,3-dioxo-1,3,3a,4,7,7a-hexahydro-2*H*-4,7-ethanoiso-indol-2-yl)phenyl acetate

BrDUD07S (*endo-syn*): ^{1}H NMR (300 MHz, Acetone-d_6): δ 2.25–2.29 (m, 3H), 3.25 (dtd, *J* = 6.29, 3.03, 3.03, 1.41 Hz, 1H), 3.60–3.67 (m, 1H), 3.72–3.79 (m, 1H), 3.82–3.97 (m, 2H), 4.82–4.87 (m, 1H), 5.12–5.20 (m, 1H), 6.19–6.28 (m, 1H), 6.38 (d, *J* =

8.67 Hz, 1H), 7.03 (t, *J* = 2.17 Hz, 1H), 7.15 (dddd, *J* = 12.24, 8.10, 2.07, 0.94 Hz, 2H), 7.42–7.54 (m, 1H); ^{13}C NMR (75 MHz, Acetone-d_6): *δ* 20.9, 40.2, 40.9, 45.3, 47.4, 65.5, 71.8, 121.2, 122.6, 124.9, 130.1, 132.1, 134.4, 137.4, 151.9, 169.4, 175.3, 177.3; NSI-MS: *m/z* 422, 424; HRMS (NSI): For $C_{18}H_{16}BrNO_6$+H $(M+H)^+$ *m/z* calcd.,422.0239; found, 422.0234 .

BrDUD07A (*endo-anti*): ^{1}H NMR (300 MHz, Acetone-d_6): *δ* 2.26 (s, 3H), 3.25–3.47 (m, 3H), 4.04–4.16 (m, 1H), 4.27 (d, *J* = 4.33 Hz, 1H), 4.60 (d, *J* = 4.90 Hz, 1H), 4.73–4.82 (m, 1H), 6.10–6.20 (m, 1H), 6.22–6.31 (m, 1H), 6.98–7.05 (m, 1H), 7.08–7.23 (m, 2H), 7.42–7.55 (m, 1H); ^{13}C NMR (75 MHz, Acetone-d_6): *δ* 20.9, 39.6, 40.2, 43.5, 48.7, 70.1, 75.2, 121.2, 122.7, 124.8, 130.2, 131.4, 134.3, 135.5, 151.9, 170.4, 173.6, 175.9; NSI-MS: *m/z* 422, 424; HRMS (NSI): For $C_{18}H_{16}BrNO_6$+H $(M+H)^+$ *m/z* calcd., 422.0239; found, 422.0234 .

4-bromo-8,9-dihydroxy-2-(4-nitrophenyl)-3a,4,7,7a-tetrahydro-1*H*-4,7-ethanoiso-indole-1,3(2*H*)-dione

BrDUD08S (*endo-syn*): ^{1}H NMR (300 MHz, Acetone-d_6): *δ* 3.23–3.34 (m, 1H), 3.64–3.72 (m, 1H), 3.77–3.84 (m, 1H), 3.86–3.97 (m, 2H), 4.85 (d, *J* = 3.96 Hz, 1H), 5.17–5.22 (m, 1H), 6.27 (dd, *J* = 8.67, 6.40 Hz, 1H), 6.36–6.44 (m, 1H), 7.53–7.63 (m, 2H), 8.32–8.39 (m, 2H); ^{13}C NMR (Acetone-d_6): *δ* 40.3, 41.1, 45.5, 63.8, 65.5, 71.7, 124.8, 126.3, 128.5, 132.2, 137.5, 139.1, 175.1, 177.2; NSI-MS: *m/z* 409, 411; HRMS (NSI): For $C_{16}H_{13}BrN_2O_6$+H $(M+H)^+$ *m/z* calcd.,409.0035; found,409.0029 .

BrDUD08A (*endo-syn*): ^{1}H NMR (300 MHz, Acetone-d_6): *δ* 0.97–1.06 (m, 3H), 3.07–3.13 (m, 1H), 3.17–3.34 (m, 2H), 3.40 (q, *J* = 7.16 Hz, 2H), 4.02 (ddd, *J* = 7.39, 5.89, 1.22 Hz, 1H), 4.16–4.24 (m, 1H), 4.54 (d, *J* = 4.90 Hz, 1H), 4.69–4.75 (m, 1H), 5.99 (dd, *J* = 8.57, 6.31 Hz, 1H), 6.08–6.15 (m, 1H); ^{13}C NMR (75 MHz, Acetone-d_6): *δ*

39.1, 43.3, 48.4, 69.5, 74.6, 74.7, 124.4, 128.0, 131.0, 131.7, 135.1, 138.5, 173.0, 175.7; NSI-MS: *m/z* 409, 411; HRMS (NSI): For $C_{16}H_{13}BrN_2O_6$+H $(M+H)^+$ *m/z* calcd.,409.0035; found,409.0029 .

Methyl-(*E*)-3-(4-(4-bromo-2,2-dimethyl-5,7-dioxo-3a,4,4a,5,7,7a,8,8a-octahydro-6*H*-4,8-etheno[1,3]dioxolo[4,5-*f*]isoindol-6-yl)phenyl)acrylate

BrDUD10S (*endo-syn*): ^{1}H NMR (400 MHz, Acetone-d_6): δ 3.26 (dtd, *J* = 6.36, 2.92, 2.92, 1.53 Hz, 1H), 3.64 (dd, *J* = 8.14, 3.05 Hz, 1H), 3.71–3.79 (m, 4H), 3.85–3.95 (m, 2H), 4.83 (d, *J* = 4.07 Hz, 1H), 5.13–5.21 (m, 1H), 6.25 (dd, *J* = 8.65, 6.61 Hz, 1H), 6.39 (d, *J* = 8.65 Hz, 1H), 6.59 (d, *J* = 16.28 Hz, 1H), 7.28–7.35 (m, 2H), 7.69 (d, *J* = 16.28 Hz, 1H), 7.74–7.82 (m, 2H); ^{13}C NMR (101 MHz, Acetone-d_6): δ 40.2, 40.9, 45.4, 47.5, 51.8, 64.0, 65.5, 71.8, 119.8, 128.1, 129.3, 132.1, 135.2, 137.4, 144.2, 167.3, 175.3, 177.4; NSI-MS: *m/z* 448, 450; HRMS (NSI): For $C_{20}H_{18}BrNO_6$ +H $(M+H)^+$ *m/z* calcd., 448.0395; found, 448.0390.

BrDUD10A (*endo-anti*) : ^{1}H NMR (300 MHz, Acetone-d_6): δ 3.27–3.48 (m, 3H), 3.76 (s, 3H), 4.06–4.17 (m, 1H), 4.28 (d, *J* = 7.35 Hz, 1H), 4.52–4.67 (m, 1H), 4.79 (br. s, 1H), 6.10–6.21 (m, 1H), 6.24–6.33 (m, 1H), 6.59 (d, *J* = 16.01 Hz, 1H), 7.26–7.34 (m, 2H), 7.69 (d, *J* = 16.20 Hz, 1H), 7.74–7.82 (m, 2H); ^{13}C NMR (75 MHz, $CDCl_3$): δ 39.6, 43.6, 48.8, 51.8, 64.7, 70.1, 75.2, 119.9, 128.1, 129.3, 131.4, 135.0, 135.3, 135.5, 144.2, 167.3, 173.8, 176.0; NSI-MS: *m/z* 448, 450; HRMS (NSI): For $C_{20}H_{18}BrNO_6$ +H $(M+H)^+$ *m/z* calcd., 448.0395; found, 448.0390.

4-bromo-2-(4-cinnamoylphenyl)-8,9-dihydroxy-3a,4,7,7a-tetrahydro-1*H*-4,7-ethanoisoindole-1,3(2*H*)-dione

BrDUD12S (*endo-syn*): ^{1}H NMR (500 MHz, $CDCl_3$): *δ* 3.45–3.49 (m, 1H), 3.67–3.72 (m, 2H), 3.91–3.99 (m, 2H), 6.17–6.23 (m, 1H), 6.41 (dd, *J* = 8.70, 1.22 Hz, 1H), 7.39–7.44 (m, 5H), 7.47 (d, *J* = 15.72 Hz, 1H), 7.61–7.68 (m, 2H), 7.80 (d, *J* = 15.72 Hz, 1H), 8.03–8.11 (m, 2H); ^{13}C NMR (126 MHz, $CDCl_3$): *δ* 38.7, 40.0, 44.0, 62.7, 64.8, 71.1, 121.8, 126.4, 128.6, 129.0, 129.3, 130.8, 131.3, 134.7, 135.4, 136.3, 138.1, 145.6, 174.3, 176.3, 189.7; NSI-MS: *m/z* 494, 496; HRMS (NSI): For $C_{25}H_{20}NO_5Br$+H $(M+H)^+$ *m/z* calcd., 494.0603; found, 494.0598.

(*E*)-4-bromo-2-(4-(3-(4-fluorophenyl)acryloyl)phenyl)-8,9-dihydroxy-3a,4,7,7a-tetrahydro-1*H*-4,7-ethanoisoindole-1,3(2*H*)-dione

BrDUD13S (*endo-syn*): ^{1}H NMR (300 MHz, Acetone-d_6): *δ* 3.21–3.36 (m, 1H), 3.55–3.98 (m, 4H), 4.74–4.93 (m, 1H), 5.19 (t, *J* = 3.39 Hz, 1H), 6.19–6.52 (m, 2H), 7.11–7.54 (m, 4H), 7.77–8.01 (m, 4H), 8.17–8.29 (m, 2H); NSI-MS: *m/z* 512, 514; HRMS (NSI): For $C_{25}H_{19}BrFNO_5$ +H $(M+H)^+$ *m/z* calcd., 512.0509; found, 512.0503.

(*E*)-4-bromo-2-(4-(3-(4-chlorophenyl)acryloyl)phenyl)-8,9-dihydroxy-3a,4,7,7a-tetrahydro-1*H*-4,7-ethanoisoindole-1,3(2*H*)-dione

BrDUD14S (*endo-syn*): ^{1}H NMR (500 MHz, $CDCl_3$): 3.26–3.5 (m, 1H), 3.62–3.87 (m, 4H), 6.24–6.3 (m, 1H), 6.37–6.44 (m, 1H), 7.33–7.46 (m, 3H), 7.53–7.60 (m, 4H), 7.74 (d, *J* = 15.72 Hz, 1H), 8.05–8.11 (m, 2H); ^{13}C NMR (126 MHz, $CDCl_3$): *δ* 38.6, 40.1, 44.0, 62.7, 64.8, 71.1, 131.8, 132.6, 122.2, 125.5, 129.3, 129.4, 129.7, 133.3, 134.5, 135.4, 136.7, 136.9, 143.8, 174.5, 176.6, 189.7; HRMS (NSI): For $C_{25}H_{19}BrClNO_5$ +H $(M+H)^+$ *m/z* calcd.,528.0213; found, 528.0207.

(*E*)-4-bromo-8,9-dihydroxy-2-(4-(3-(p-tolyl)acryloyl)phenyl)-3a,4,7,7a-tetrahydro-1*H*-4,7-ethanoisoindole-1,3(2*H*)-dione

BrDUD16S (*endo-syn*): ^{1}H NMR (500 MHz, $CDCl_3$): δ 2.39 (s, 3H), 3.44–3.50 (m, 1H), 3.67–3.73 (m, 2H), 3.89–4.01 (m, 2H), 6.17–6.23 (m, 1H), 6.41 (dd, *J* = 8.62, 1.30 Hz, 1H), 7.22 (d, *J* = 7.93 Hz, 2H), 7.37–7.45 (m, 3H), 7.53 (d, *J* = 8.24 Hz, 2H), 7.79 (d, *J* = 16.02 Hz, 1H), 8.04–8.09 (m, 2H); ^{13}C NMR (126 MHz, $CDCl_3$): δ 21.6, 38.7, 40.0, 44.0, 62.7, 64.8, 71.1, 120.8, 126.4, 128.6, 129.3, 129.8, 131.2, 132.0, 135.3, 136.3, 138.2, 141.4, 145.7, 174.3, 176.3, 189.8; NSI-MS: *m/z* 508, 510; HRMS (NSI): For $C_{26}H_{22}NO_5Br$+H $(M+H)^+$ *m/z* calcd., 508.0759; found, 508.0754.

(*E*)-4-bromo-8,9-dihydroxy-2-(4-(3-(4-methoxyphenyl)acryloyl)phenyl)-3a,4,7,7a-tetrahydro-1*H*-4,7-ethanoisoindole-1,3(2*H*)-dione

BrDUD17S (*endo-syn*): ^{1}H NMR (300 MHz, $CDCl_3$): δ 3.21–3.30 (m, 2H), 3.47 (ddd, *J* = 4.76, 3.16, 1.51 Hz, 1H), 3.70 (d, *J* = 1.51 Hz, 2H), 3.85 (s, 3H), 3.88–4.01 (m, 2H), 6.20 (dd, *J* = 8.67, 6.40 Hz, 1H), 6.41 (dd, *J* = 8.67, 1.13 Hz, 1H), 6.89–6.98 (m, 2H), 7.29–7.43 (m, 3H), 7.54–7.63 (m, 2H), 7.78 (d, *J* = 15.64 Hz, 1H), 8.01–8.10 (m, 2H); ^{13}C NMR (75 MHz, $CDCl_3$): δ 38.7, 40.0, 44.0, 55.5, 62.7, 64.8, 71.1, 114.5, 119.6, 126.4, 127.5, 129.2, 130.4, 131.2, 135.2, 136.4, 138.4, 145.5, 161.9, 174.2, 176.4, 189.7; NSI-MS: *m/z* 524, 526; HRMS (NSI): For $C_{26}H_{22}BrNO_6$+H $(M+H)^+$ *m/z* calcd., 524.0709; found, 524.0703.

(*E*)-4-bromo-2-(4-(3-(3,4-dimethoxyphenyl)acryloyl)phenyl)-8,9-dihydroxy-3a,4,-7,7a-tetrahydro-1*H*-4,7-ethanoisoindole-1,3(2*H*)-dione

BrDUD18S (*endo-syn*): ^{1}H NMR (300 MHz, $CDCl_3$): δ 3.31–3.50 (m, 3H), 3.60–3.71 (m, 3H), 3.74–3.87 (m, 1H), 3.93 (d, *J* = 4.71 Hz, 6H), 6.15–6.23 (m, 1H), 6.38–6.44

(m, 1H), 6.90 (d, *J* = 8.67 Hz, 1H), 7.11–7.24 (m, 2H), 7.27–7.43 (m, 3H), 7.74 (d, *J* = 15.64 Hz, 1H), 8.01–8.08 (m, 2H); ^{13}C NMR (75 MHz, $CDCl_3$): *δ* 38.7, 40.0, 44.0, 55.8, 56.1, 62.6, 64.8, 71.1, 110.2, 111.2, 120.0, 123.4, 126.4, 127.7, 129.2, 131.2, 135.4, 136.4, 138.4, 145.9, 149.3, 151.7, 174.3, 176.4, 189.9; NSI-MS: *m/z* 554, 556; HRMS (NSI): For $C_{27}H_{24}BrNO_7$+H $(M+H)^+$ *m/z* calcd., 554.0814; found, 554.0809.

(*E*)-4-bromo-8,9-dihydroxy-2-(4-(3-(3,4,5-trimethoxyphenyl)acryloyl)phenyl)-3a,4,7,7a-tetrahydro-1*H*-4,7-ethanoisoindole-1,3(2*H*)-dione

BrDUD19S (*endo-syn*): ^{1}H NMR (300 MHz, $CDCl_3$): *δ* 3.29–3.37 (m, 2H), 3.47 (td, *J* = 3.16, 1.22 Hz, 1H), 3.66–3.72 (m, 2H), 3.82–4.03 (m, 11H), 6.11–6.28 (m, 1H), 6.41 (dd, *J* = 8.67, 1.13 Hz, 1H), 6.85 (s, 2H), 7.27–7.45 (m, 3H), 7.69 (d, *J* = 15.64 Hz, 1H), 8.00–8.09 (m, 2H); ^{13}C NMR (75 MHz, $CDCl_3$): *δ* 38.7. 40.0. 44.0. 56.3. 61.1. 62.6. 64.8. 71.1. 105.8. 107.4. 121.5. 126.4. 129.3. 130.2. 131.2. 135.3. 136.4. 138.2. 145.9. 153.6. 174.3. 176.4. 190.0; NSI-MS: *m/z* 584, 586; HRMS (NSI): For $C_{28}H_{26}NO_8Br$+H $(M+H)^+$ *m/z* calcd., 584.092; found, 584.0915.

(*E*)-4-bromo-8,9-dihydroxy-2-(4-(3-(4-(methylthio)phenyl)acryloyl)phenyl)-3a,4,-7,7a-tetrahydro-1*H*-4,7-ethanoisoindole-1,3(2*H*)-dione

BrDUD20S (*endo-syn*): ^{1}H NMR (500 MHz, $CDCl_3$): *δ* 2.49–2.53 (m, 3H), 3.43–3.48 (m, 1H), 3.66–3.72 (m, 2H), 3.89–3.99 (m, 2H), 6.16–6.22 (m, 1H), 6.41 (dd, *J* = 8.70, 1.07 Hz, 1H), 7.23–7.28 (m, 2 H) 7.37–7.45 (m, 3H), 7.51–7.57 (m, 2H), 7.75 (d, *J* = 15.72 Hz, 1H), 8.03–8.08 (m, 2H); ^{13}C NMR (126 MHz, $CDCl_3$): *δ* 15.1, 38.7, 40.0, 44.0, 62.6, 64.8, 71.0, 120.7, 126.0, 126.4, 129.0, 129.2, 131.1, 131.2, 135.3, 136.4, 138.2, 142.8, 145.2, 174.3, 176.4, 189.7; NSI-MS: *m/z* 540, 542; HRMS (NSI): For $C_{26}H_{22}BrNO_5S$+H $(M+H)^+$ *m/z* calcd., 540.048; found, 540.0475.

(*E*)-4-bromo-8,9-dihydroxy-2-(4-(3-(3-nitrophenyl)acryloyl)phenyl)-3a,4,7,7a-tetrahydro-1*H*-4,7-ethanoisoindole-1,3(2*H*)-dione

BrDUD21S (*endo-syn*): ^{1}H NMR (500 MHz, $CDCl_3$): δ 3.46–3.51 (m, 1H), 3.68–3.72 (m, 2H), 3.89–4.02 (m, 2H), 6.17–6.24 (m, 1H), 6.39–6.44 (m, 1H), 7.41–7.48 (m, 2H), 7.56–7.66 (m, 2H), 7.83 (d, *J* = 15.72 Hz, 1H), 7.92 (d, *J* = 7.78 Hz, 1H), 8.07–8.13 (m, 2H), 8.26 (ddd, *J* = 8.20, 2.25, 0.99 Hz, 1H), 8.50 (t, *J* = 1.91 Hz, 1H); ^{13}C NMR (126 MHz, $CDCl_3$): δ 38.7, 40.1, 44.0, 62.6, 64.8, 71.1, 122.5, 124.3, 124.9, 126.6, 129.4, 130.2, 131.2, 134.4, 135.8, 136.4, 136.5, 137.4, 142.4, 148.8, 174.2, 176.3, 188.7; NSI-MS: *m/z* 539, 541; HRMS (NSI): For $C_{25}H_{19}N_2O_7Br$+H $(M+H)^+$ *m/z* calcd., 539.0454; found, 539.0448.

4-bromo-8,9-dihydroxy-2-(2-methyl-4-oxo-4*H*-chromen-7-yl)-3a,4,7,7a-tetrahydro-1*H*-4,7-ethanoisoindole-1,3(2*H*)-dione

BrDUD22S (*endo-syn*): ^{1}H NMR (300 MHz, Acetone-d_6): δ 2.42 (s, 3H), 3.29 (dtd, *J* = 6.22, 3.01, 3.01, 1.32 Hz, 1H), 3.64–3.73 (m, 1H), 3.76–3.83 (m, 1H), 3.85–3.97 (m, 2H), 4.86 (d, *J* = 4.14 Hz, 1H), 5.17–5.23 (m, 1H), 6.18 (d, *J* = 0.75 Hz, 1H), 6.29 (dd, *J* = 8.67, 6.40 Hz, 1H), 6.38–6.46 (m, 1H), 7.33 (dd, *J* = 8.48, 1.88 Hz, 1H), 7.44 (d, *J* = 1.70 Hz, 1H), 8.12 (d, *J* = 8.48 Hz, 1H); ^{13}C NMR (75 MHz, $CDCl_3$): δ 20.3, 40.3, 41.1, 45.5, 63.9, 65.5, 71.8, 111.1, 117, 123.8, 124.2, 126.4, 132.2, 137.5, 137.8, 157, 167.8, 175.1, 177, 177.2; NSI-MS: *m/z* 446, 448; HRMS (NSI): For $C_{20}H_{16}BrNO_6$ $(M+H)^+$ *m/z* calcd.,446.0239; found, 446.0235.

4-bromo-2-ethyl-8,9-dihydroxy-3a,4,7,7a-tetrahydro-1*H*-4,7-ethanoisoindole-1,3(2*H*)-dione

BrDUD23S (*endo-syn*): ^{1}H NMR (400 MHz, Acetone-d_6): δ 1.02 (t, J = 7.12 Hz, 3H), 3.08–3.19 (m, 1H), 3.33–3.45 (m, 3H), 3.49–3.58 (m, 1H), 3.77–3.92 (m, 2H), 4.75 (br. s, 1H), 5.09 (br. s, 1H), 6.08 (dd, J = 8.65, 6.10 Hz, 1H), 6.23 (d, J = 8.65 Hz, 1H); ^{13}C NMR (101 MHz, Acetone-d_6): δ 13.1, 33.9, 39.9, 40.5, 44.9, 64.0, 65.5, 71.8, 131.8, 137.1, 176.0, 178.0; NSI-MS: *m/z* 356,358; HRMS (NSI): For $C_{15}H_{18}BrNO_4$+H $(M+H)^+$ *m/z* calcd.,356.0497; found,356.0491.

1-bromo-9,10-dihydroxy-1,4,4a,8a-tetrahydro-1,4-ethanonaphthalene-5,8-dione

BrDUD25S (*endo-syn*): ^{1}H NMR (300 MHz, Acetone-d_6): δ 3.22 (dtd, J = 6.33, 3.10, 3.10, 1.41 Hz, 1H), 3.51–3.68 (m, 2H), 3.73–3.87 (m, 2H), 4.75 (br. s., 1H), 5.13 (br. s., 1H), 6.15 (dd, J = 8.67, 6.59 Hz, 1H), 6.33 (dd, J = 8.57, 1.22 Hz, 1H), 6.61–6.83 (m, 2H); ^{13}C NMR (75 MHz, Acetone-d_6): δ 43.3, 45.7, 49.0, 65.0, 71.0, 72.4, 132.7, 138.6, 142.6, 143.8, 196.0, 199.0; NSI-MS: *m/z* 298, 300; HRMS (NSI): For $C_{12}H_{11}BrO_4$+H $(M+H)^+$ *m/z* calcd., 298.9919; found, 298.9913.

1-bromo-11,12-dihydroxy-1,4,4a,9a-tetrahydro-1,4-ethanoanthracene-9,10-dione

BrDUD26S (*endo-syn*): ^{1}H NMR (300 MHz, Acetone-d_6): δ 3.21–3.39 (m, 1H), 3.69–3.92 (m, 4H), 4.73–4.90 (m, 1H), 5.11–5.27 (m, 1H), 5.90–6.15 (m, 2H), 7.67–7.91 (m, 4H); ^{13}C NMR (75 MHz, Acetone-d_6): δ 43.8, 46.8, 49.8, 65.0, 66.6, 72.4, 126.5, 127.1, 132.7, 134.4, 135.0, 137.6, 138.6, 195.5, 197.6; NSI-MS: *m/z* 349, 351; HRMS (NSI): For $C_{16}H_{13}BrO_4$+H $(M+H)^+$ *m/z* calcd., 349.0048; found, 349.0070.

4.2.1.4.9. General procedure for [4+2] cycloadditions with protected hetero-aryl dienediols

The appropriate dienophile (0.04 mmol) was added to a solution of a dienediol (0.03 mmol) in methanol (0.2 mL) and chloroform (3 mL). This mixture was heated to 100-110 °C in a sealed vessel and stirred for 3-4 days until the dienediols had reacted completely (monitored by TLC). Subsequently, the solvent was evaporated under reduced pressure at 25 ºC and the crude compound was purified by flash column column chromatography using methanol and dichloromethane as eluents to obtain pure compounds in 22-45% yields. Compounds were characterized by ^{1}H NMR, ^{13}C NMR and high resolution mass spectroscopy.

TLC: 1:9 methanol, dichloromethane, R_f 0.4-0.6.

10,11-dihydroxy-2-phenyl-5-(pyridin-2-yl)-5,8-dihydro-1*H*-5,8-ethano[1,2,4]-triazolo[1,2-a]pyridazine-1,3(2*H*)-dione

Py2DUD01A (*endo-anti*): ^{1}H NMR (500 MHz, $CDCl_3$): δ 4.09–4.14 (m, 1H), 4.44 (d, J = 8.39 Hz, 1H), 5.12 (ddd, J = 6.22, 2.71, 1.45 Hz, 1H), 6.65–6.69 (m, 1H), 6.72–6.76 (m, 1H), 7.26–7.45 (m, 6H), 7.69–7.75 (m, 1H), 7.84–7.91 (m, 1H), 8.55–8.62 (m, 1H); ^{13}C NMR (126 MHz, Methanol-d_4): δ 58.6, 64.3, 68.6, 70.4, 124.6, 127.2, 129.1, 130.2, 131.0, 132.3, 135.1, 126.5, 155.0, 160.1, 156.3, 157.2; NSI-MS: *m/z* 365; HRMS (NSI): For $C_{19}H_{16}N_4O_4$+H $(M+H)^+$ *m/z* calcd., 365.125; found, 365.1244.

10,11-dihydroxy-2-phenyl-5-(pyridin-3-yl)-5,8-dihydro-1*H*-5,8-ethano-[1,2,4]triazo-lo-[1,2-a]pyridazine-1,3(2*H*)-dione

Py3DUD01A (a*nti)*: ^{1}H NMR (500 MHz, Methanol-d_4) δ ppm 4.10 (s, 2H), 5.02–5.13 (m, 1H), 6.72–6.81 (m, 2H), 7.32–7.60 (m, 6H), 8.15–8.28 (m, 1H), 8.51–8.65, (m, 1H), 8.94 (s, 1H); ^{13}C NMR (126 MHz, Methanol-d_4): δ 58.4, 64.2, 68.1, 68.4, 124.4,

127.5, 129.6, 130.1, 131.1, 132.8, 134.3, 135.9, 138.0, 149.2, 149.9, 156.2, 156.8; NSI-MS: *m/z* 365; HRMS (NSI): For $C_{19}H_{16}N_4O_4$+H $(M+H)^+$ *m/z* calcd., 365.125; found, 365.1244.

8,9-dihydroxy-4-(pyridin-3-yl)-2-(3,4,5-trimethoxyphenyl)-3a,4,7,7a-tetrahydro-1*H*-4,7-ethanoisoindole-1,3(2*H*)-dione

Py3DUD06S (*endo-syn)*: ^{1}H NMR (500 MHz, $CDCl_3$): *δ* 3.27 (dd, *J* = 8.32, 2.52 Hz, 1H), 3.75–3.89 (m, 11H), 3.92–4.00 (m, 2H), 5.06–5.14 (m, 2H), 6.27–6.33 (m, 2H), 6.60 (dd, *J* = 8.70, 6.26 Hz, 1H), 6.74 (d, *J* = 8.70 Hz, 1H), 7.50–7.56 (m, 1H), 8.03 (d, *J* = 7.78 Hz, 1H), 8.59–8.66 (m, 1H), 9.15 (br. s, 1H); NSI-MS: *m/z* 453; HRMS (NSI): For $C_{24}H_{24}N_2O_7$+H $(M+H)^+$ *m/z* calcd., 453.1662; found, 453.1656.

Methyl-(*E*)-3-(4-(8,9-dihydroxy-1,3-dioxo-4-(pyridin-3-yl)-1,3,3a,4,7,7a-hexahydro-2*H*-4,7-ethanoisoindol-2-yl)phenyl)acrylate

Py3DUD10S (*endo-syn)*: ^{1}H NMR (500 MHz, $CDCl_3$): *δ* 3.44–3.55 (m, 2H), 3.67–3.77 (m, 5H), 3.82–3.88 (m, 1H), 4.07–4.16 (m, 1H), 6.30–6.52 (m, 3H), 7.09–7.19 (m, 2H), 7.45–7.65 (m, 3H), 7.75 (dd, *J* = 8.24, 5.34 Hz, 1H), 8.42 (d, *J* = 8.24 Hz, 1H), 8.58 (d, *J* = 5.03 Hz, 1H), 8.95 (s, 1H); ^{13}C NMR (126 MHz, $CDCl_3$): *δ* 38.7, 39.3, 40.3, 50.3, 51.8, 63.7, 70.4, 119.1, 122.1, 125.1, 126.6, 128.6, 132.5, 132.9, 133.4, 134.7, 140.7, 141.2, 143.0, 143.5, 167.3, 176.8, 177.6; NSI-MS: *m/z* 447; HRMS (NSI): For $C_{25}H_{22}N_2O_6$+H $(M+H)^+$ *m/z* calcd., 447.1556; found, 447.1551.

(*E*)-2-(4-(3-(4-fluorophenyl)acryloyl)phenyl)-8,9-dihydroxy-4-(pyridin-3-yl)-3a,4,-7,7a-tetrahydro-1*H*-4,7-ethanoisoindole-1,3(2*H*)-dione

Py3DUD13S (*endo-syn)*: ^{1}H NMR (500 MHz, $CDCl_3$): *δ* 2.95–3.09 (m, 1H), 3.34–3.47 (m, 2H), 3.79 (dd, *J* = 8.54, 3.36 Hz, 1H), 4.10 (d, *J* = 8.39 Hz, 1H), 6.43 (s,

2H), 7.01 (s, 2H), 7.22 (d, *J* = 8.70 Hz, 2H), 7.30 (d, *J* = 15.72 Hz, 1H), 7.53 (dd, *J* = 8.70, 5.34 Hz, 2H), 7.64 (d, *J* = 15.87 Hz, 2H), 7.93 (d, *J* = 8.70 Hz, 2H), 8.31–8.41 (m, 1H), 8.49–8.59 (m, 1 H) 8.85–8.93 (m, 1H); ^{13}C NMR (126 MHz, $CDCl_3$): *δ* 38.6, 39.3, 40.3, 46.0, 63.5, 70.4, 116.0, 116.1, 121.2, 125.0, 126.3, 129.1, 130.4, 131.4, 132.7, 133.0, 135.3, 137.7, 139.6, 142.4, 144.5, 163.1, 165.2, 176.7, 177.7, 190.0; NSI-MS: *m/z* 511; HRMS (NSI): For $C_{30}H_{23}N_2O_5F$+H $(M+H)^+$ *m/z* calcd., 511.1669; found, 511.1664.

(*E*)-8,9-dihydroxy-2-(4-(3-(4-methoxyphenyl)acryloyl)phenyl)-4-(pyridin-3-yl)-3a,4,7,7a-tetrahydro-1*H*-4,7-ethanoisoindole-1,3(2*H*)-dione

Py3DUD17S (*endo-syn)*: ^{1}H NMR (500 MHz, $CDCl_3$): *δ* 3.34–3.39 (m, 2H), 3.61–3.65 (m, 1H), 3.72 (s, 3H), 3.74–3.79 (m, 1H), 4.05–4.09 (m, 1H), 6.35–6.43 (m, 2H), 6.78–6.83 (m, 2H), 7.15–7.24 (m, 3H), 7.44–7.48 (m, 2H), 7.57–7.64 (m, 1H), 7.86–7.91 (m, 2H), 8.29 (d, *J* = 8.24 Hz, 1H), 8.48 (d, *J* = 5.04 Hz, 1H), 8.84 (s, 1H); ^{13}C NMR (126 MHz, $CDCl_3$): *δ* 38.6, 39.3, 40.3, 46.0, 50.0, 63.4, 70.4, 114.3, 119.1, 124.8, 126.2, 127.1, 129.0, 130.3, 131.5, 132.8, 132.9, 135.0, 138.1, 140.0, 142.1, 144.2, 145.9, 161.9, 176.7, 177.7, 190.2; NSI-MS: *m/z* 523; HRMS (NSI): For $C_{31}H_{26}N_2O_6$+H $(M+H)^+$ *m/z* calcd., 523.1869; found, 523.1864.

(*E*)-8,9-dihydroxy-4-(pyridin-3-yl)-2-(4-(3-(3,4,5-trimethoxyphenyl)acryloyl)phenyl)-3a,4,7,7a-tetrahydro-1*H*-4,7-ethanoisoindole-1,3(2*H*)-dione

Py3DUD19S (*endo-syn)*: ^{1}H NMR (500 MHz, $CDCl_3$): *δ* 3.53–3.66 (m, 2H), 3.76 (dd, *J* = 8.16, 2.82 Hz, 1H), 3.85–3.94 (m, 9H), 3.97 (dd, *J* = 8.32, 3.28 Hz, 1H), 4.23 (d, *J* = 8.39 Hz, 1H), 6.42–6.59 (m, 3H), 6.78–6.86 (m, 2H), 7.26–7.32 (m, 4H), 7.65 (d, *J* = 15.56 Hz, 1H), 7.72–7.83 (m, 1H), 7.94–8.05 (m, 2H), 8.40 (d, *J* = 8.24 Hz, 1H), 8.51 (d, *J* = 4.58 Hz, 1H), 9.08–9.18 (m, 1H); ^{13}C NMR (126 MHz, $CDCl_3$): *δ* 38.9,

39.2, 40.2, 50.5, 56.3, 61.1, 63.9, 71.0, 105.8, 121.4, 125.5, 126.4, 129.3, 130.1, 132.5, 133.7, 135.1, 138.3, 140.7, 142.6, 144.0, 144.4, 145.9, 153.6, 176.6, 177.0, 189.8; NSI-MS: *m/z* 583; HRMS (NSI): For $C_{33}H_{30}N_2O_8$+H $(M+H)^+$ *m/z* calcd., 583.208; found, 583.2075.

(*E*)-8,9-dihydroxy-2-(4-(3-(4-(methylthio)phenyl)acryloyl)phenyl)-4-(pyridin-3-yl)-3a,4,7,7a-tetrahydro-1*H*-4,7-ethanoisoindole-1,3(2*H*)-dione

Py3DUD20S (*endo-syn)*: ^{1}H NMR (500 MHz, $CDCl_3$): *δ* 2.58 (s, 3H), 3.48–3.57 (m, 2H), 3.72–3.79 (m, 1H), 3.86 (dd, *J* = 8.47, 3.43 Hz, 1H), 4.11–4.16 (m, 1H), 6.42–6.54 (m, 2H), 7.18–7.31 (m, 3H), 7.36 (d, *J* = 15.56 Hz, 1H), 7.45–7.53 (m, 2H), 7.63–7.79 (m, 3H), 7.95–8.03 (m, 2H), 8.60–8.68 (m, 2H), 9.05 (m, 1H); ^{13}C NMR (126 MHz, $CDCl_3$): *δ* 15.0, 38.7, 39.4, 40.3, 50.4, 63.5, 70.3, 120.5, 123.5, 124.2, 125.9, 126.3, 128.9, 129.2, 131.0, 131.7, 133.9, 135.0, 138.6, 141.4, 142.9, 143.7, 145.4, 145.6, 176.7, 177.3, 185.7; NSI-MS: *m/z* 539; HRMS (NSI): For $C_{31}H_{26}N_2O_5S$+H $(M+H)^+$ *m/z* calcd., 539.164; found, 539.1635.

(*E*)-8,9-dihydroxy-2-(4-(3-(3-nitrophenyl)acryloyl)phenyl)-4-(pyridin-3-yl)-3a,4,-7,7a-tetrahydro-1*H*-4,7-ethanoisoindole-1,3(2*H*)-dione

Py3DUD21S (*endo-syn)*: ^{1}H NMR (500 MHz, $CDCl_3$): *δ* 3.54–3.65 (m, 2H), 3.76–3.82 (m, 1H), 3.94–3.99 (m, 1H), 4.23–4.27 (m, 1H), 6.47–6.52 (m, 2H), 7.34–7.39 (m, 2H), 7.56 (d, *J* = 15.72 Hz, 1H), 7.58–7.63 (m, 1H), 7.79 (d, *J* = 15.8 Hz, 1H), 7.89 (d, *J* = 7.63 Hz, 1H), 7.92–7.99 (m, 2H), 8.02–8.07 (m, 2H), 8.10–8.14 (m, 1H), 8.22–8.27 (m, 1H), 8.48 (t, *J* = 1.91 Hz, 1H), 8.75 (d, *J* = 2.14 Hz, 1H); ^{13}C NMR (126 MHz, $CDCl_3$): *δ* 38.8, 39.4, 40.4, 50.7, 63.8, 70.6, 122.5, 124.2, 124.9, 126.5, 128.4, 129.3, 129.6, 130.1, 132.4, 134.4, 133.6, 135.0, 135.7, 135.9, 137.3, 138.2, 142.4,

143.5, 148.7, 176.6, 176.7, 188.8; NSI-MS: *m/z* 538; HRMS (NSI): For $C_{30}H_{23}N_3O_7$+H $(M+H)^+$ *m/z* calcd., 538.1614; found, 538.1609.

10,11-dihydroxy-2-phenyl-5-(pyridin-4-yl)-5,8-dihydro-1*H*-5,8-ethano[1,2,4]-triazolo-[1,2-a]pyridazine-1,3(2*H*)-dione

Py4DUD01A (a*nti)*: ^{1}H NMR (500 MHz, Methanol-d_4): δ 3.78–3.84 (m, 1H), 4.08 (s, 1H), 4.98–5.04 (m, 1H), 6.77–6.86 (m, 1H), 6.98–7.04 (m, 1H), 7.23–7.64 (m, 5H), 7.80–7.87 (m, 2 H), 8.63 (d, *J* = 5.95 Hz, 2H); ^{13}C NMR (126 MHz, Methanol-d_4): δ 59.8, 68.2, 76.2, 78.9, 124.9, 127.3, 129.7, 130.0, 130.2, 130.3, 132.1, 149.8, 158.2, 156.4; NSI-MS: *m/z* 365; HRMS (NSI): For $C_{19}H_{16}N_4O_4$+H $(M+H)^+$ *m/z* calcd., 365.125; found, 365.1244.

(*E*)-8,9-dihydroxy-2-(4-(3-(4-methoxyphenyl)acryloyl)phenyl)-4-(pyridin-4-yl)-3a,4,7,7a-tetrahydro-1*H*-4,7-ethanoisoindole-1,3(2*H*)-dione

Py4DUD17S *(endo-syn):* ^{1}H NMR (500 MHz, $CDCl_3$): δ 3.46– 3.52 (m, 1H), 3.75–3.90 (m, 7H), 4.26 (s, 1H) ,6.51–6.58 (m, 1 H), 6.73 (d, *J* = 8.70 Hz, 1H), 6.93 (d, *J* = 8.70 Hz, 2H), 7.28–7.36 (m, 4 H) 7.55–7.61 (m, 3H), 7.75 (d, *J* = 15.7 Hz, 1H), 7.99–8.06 (m, 2H), 8.78 (d, *J* = 5.34 Hz, 1H), 9.25–9.33 (m, 1H); ^{13}C NMR (126 MHz, $CDCl_3$): δ 38.3, 41.4, 46.5, 53.1, 55.5, 65.1, 79.9, 114.5, 119.5, 121.0, 126.3, 127.5, 129.2, 130.1, 130.4, 131.1, 135.0, 138.4, 145.5, 157.2, 158.8, 161.9, 174.6, 176.9, 189.6; NSI-MS: *m/z* 523; HRMS (NSI): For $C_{31}H_{26}N_2O_6$+H $(M+H)^+$ *m/z* calcd., 523.1869; found, 523.1864.

PmDUD06S (*endo-syn*): ^{1}H NMR (500 MHz, $CDCl_3$): δ 3.55 (dt, *J* = 6.33, 2.56 Hz, 1H), 3.67–3.72 (m, 1H), 3.77–3.83 (m, 9H), 3.86–3.92 (m, 3H), 6.31 (s, 2H), 6.48–6.55 (m, 1H), 6.60 (d, *J* = 8.54 Hz, 1H), 7.57–7.64 (m, 1H), 8.75–8.82 (m, 1H), 9.23

(d, *J* = 1.37 Hz, 1H); ^{13}C NMR (126 MHz, $CDCl_3$): *δ* 38.1, 40.5, 43.0, 49.6, 56.3, 60.9, 65.1, 67.7, 104.1, 120.9, 127.1, 130.4, 133.0, 138.4, 153.6, 157.1, 157.5, 176.9, 177.6; NSI-MS: *m/z* 454; HRMS (NSI): For $C_{23}H_{23}N_3O_7$+H $(M+H)^+$ *m/z* calcd., 454.1614; found, 454.1609.

Methyl-(E)-3-(4-(8,9-dihydroxy-1,3-dioxo-4-(pyrimidin-4-yl)-1,3,3a,4,7,7a-hexa-hydro-2*H*-4,7-ethanoisoindol-2-yl)phenyl)acrylate

PmDUD10S (*endo-syn)*: ^{1}H NMR (500 MHz, $CDCl_3$): *δ* 3.51–3.57 (m, 1H), 3.68–3.73 (m, 1H), 3.75–3.81 (m, 3H), 3.86–3.96 (m, 3H), 6.41 (d, *J* = 16.02 Hz, 1H), 6.45–6.51 (m, 1H), 6.55–6.61 (m, 1H), 7.15–7.23 (m, 2H), 7.51–7.60 (m, 3H), 7.64 (d, *J* = 16.02 Hz, 1H), 8.73–8.81 (m, 1H), 9.20 (s, 1H); ^{13}C NMR (126 MHz, $CDCl_3$): *δ* 38.2, 40.5, 42.9, 49.7, 51.9, 64.9, 67.7, 119.2, 120.9, 126.7, 128.6, 130.4, 133.0, 134.7, 143.4, 157.3, 157.6, 167.1, 168.8, 176.3, 177.3; NSI-MS: *m/z* 448; HRMS (NSI): For $C_{24}H_{21}N_3O_6$+H $(M+H)^+$ *m/z* calcd., 448.1508; found, 448.1503.

(*E*)-2-(4-(3-(4-fluorophenyl)acryloyl)phenyl)-8,9-dihydroxy-4-(pyrimidin-4-yl)-3a,4,7,7a-tetrahydro-1*H*-4,7-ethanoisoindole-1,3(2*H*)-dione

PmDUD13S (*endo-syn)*: ^{1}H NMR (500 MHz, $CDCl_3$): *δ* 3.55–3.59 (m, 1H), 3.74 (dd, *J* = 8.54, 2.90 Hz, 1H), 3.88–3.94 (m, 3H), 6.49–6.54 (m, 1H), 6.60 (d, *J* = 8.54 Hz, 1H), 7.08–7.14 (m, 2H), 7.31–7.40 (m, 3H), 7.56–7.64 (m, 3H), 7.75 (d, *J* = 15.72 Hz, 1H), 8.01–8.06 (m, 2H), 8.81 (d, *J* = 5.34 Hz, 1H), 9.24 (d, *J* = 1.22 Hz, 1H); ^{13}C NMR (126 MHz, $CDCl_3$): *δ* 38.3, 40.6, 43.2, 49.6, 65.0, 67.6, 116.3, 120.8, 121.5, 120.4, 129.3, 130.4, 131.1, 133.1, 135.4, 138.0, 144.3, 157.4, 157.7, 163.2, 165.3, 168.7, 176.2, 177.1, 189.3; NSI-MS: *m/z* 512; HRMS (NSI): For $C_{29}H_{22}N_3O_5F$+H $(M+H)^+$ *m/z* calcd., 512.1621; found, 512.1616.

(*E*)-8,9-dihydroxy-2-(4-(3-(4-methoxyphenyl)acryloyl)phenyl)-4-(pyrimidin-4-yl)-3a,4,7,7a-tetrahydro-1*H*-4,7-ethanoisoindole-1,3(2*H*)-dione

PmDUD17S (*endo-syn)*: ^{1}H NMR (500 MHz, $CDCl_3$): *δ* 3.54–3.59 (m, 1H), 3.73 (dd, *J* = 8.54, 2.90 Hz, 1H), 3.85 (s, 3H), 3.89–3.94 (m, 3H), 6.51 (dd, *J* = 8.62, 6.49 Hz, 1H), 6.60 (d, *J* = 8.24 Hz, 1H), 6.90–6.96 (m, 2H), 7.29–7.36 (m, 3H), 7.55–7.61 (m, 3H), 7.76 (d, *J* = 15.56 Hz, 1H), 7.99–8.05 (m, 2H), 8.80 (d, *J* = 5.34 Hz, 1H), 9.23 (d, *J* = 1.22 Hz, 1H); ^{13}C NMR (126 MHz, $CDCl_3$): *δ* 38.3, 40.6, 43.1, 49.6, 55.5, 65.0, 67.7, 114.5, 119.5, 120.8, 126.3, 127.4, 129.2, 130.3, 130.4, 133.1, 135.1, 138.4, 145.5, 157.4, 157.7, 161.9, 168.8, 176.2, 177.2, 189.6; NSI-MS: *m/z* 524; HRMS (NSI): For $C_{30}H_{25}N_3O_6$+H $(M+H)^+$ *m/z* calcd., 524.1821; found, 524.1816.

(*E*)-2-(4-(3-(3,4-dimethoxyphenyl)acryloyl)phenyl)-8,9-dihydroxy-4-(pyrimidin-4-yl)-3a,4,7,7a-tetrahydro-1*H*-4,7-ethanoisoindole-1,3(2*H*)-dione

PmDUD18S (*endo-syn)*: ^{1}H NMR (500 MHz, $CDCl_3$): *δ* 3.54–3.59 (m, 1H), 3.71–3.76 (m, 1H), 3.88–3.95 (m, 9H), 6.51 (dd, *J* = 8.62, 6.49 Hz, 1H), 6.60 (d, *J* = 8.54 Hz, 1H), 6.87–6.91 (m, 1H), 7.13 (d, *J* = 1.98 Hz, 1H), 7.21 (dd, *J* = 8.39, 1.98 Hz, 1H), 7.26–7.35 (m, 3H), 7.57–7.61 (m, 1H), 7.72 (d, *J* = 15.72 Hz, 1H), 8.00–8.04 (m, 2H), 8.81 (d, *J* = 5.49 Hz, 1H), 9.24 (d, *J* = 1.22 Hz, 1H); ^{13}C NMR (126 MHz, $CDCl_3$): *δ* 38.3, 40.6, 43.2, 49.6, 56.0, 65.0, 67.6, 110.2, 111.2, 119.9, 120.8, 123.3, 126.3, 127.7, 129.2, 130.3, 133.1, 135.1, 138.4, 145.8, 149.4, 151.7, 157.4, 157.7, 176.2, 177.2, 189.7; NSI-MS: *m/z* 554; HRMS (NSI): For $C_{31}H_{27}N_3O_7$+H $(M+H)^+$ *m/z* calcd., 554.1927; found, 554.1922.

(*E*)-8,9-dihydroxy-4-(pyrimidin-4-yl)-2-(4-(3-(3,4,5-trimethoxyphenyl)acryloyl)-phenyl)-3a,4,7,7a-tetrahydro-1*H*-4,7-ethanoisoindole-1,3(2*H*)-dione

PmDUD19S (*endo-syn)*: ^{1}H NMR (500 MHz, $CDCl_3$): δ 3.56 (dd, *J* = 3.81, 2.59 Hz, 1H), 3.72–3.76 (m, 1H), 3.87–3.94 (m, 12H), 6.48–6.53 (m, 1H), 6.61 (d, *J* = 8.54 Hz, 1H), 6.83 (s, 2H), 7.26–7.36 (m, 3H), 7.58 (dd, *J* = 5.42, 1.30 Hz, 1H), 7.67 (d, *J* = 15.72 Hz, 1H), 7.99–8.04 (m, 2H), 8.78–8.82 (m, 1H), 9.23 (d, *J* = 1.22 Hz, 1H); ^{13}C NMR (126 MHz, $CDCl_3$): δ 38.3, 40.6, 48.0, 49.7, 56.3, 61.1, 64.9, 67.7, 105.8, 120.8, 121.4, 126.3, 129.3, 130.1, 130.4, 133.0, 135.2, 138.2, 140.7, 145.8, 153.5, 157.4, 157.7, 168.8, 176.2, 177.2, 189.8; NSI-MS: *m/z* 584; HRMS (NSI): For $C_{32}H_{29}N_3O_8$+H $(M+H)^+$ *m/z* calcd., 584.2033; found, 584.2027.

(*E*)-8,9-dihydroxy-2-(4-(3-(4-(methylthio)phenyl)acryloyl)phenyl)-4-(pyrimidin-4-yl)-3a,4,7,7a-tetrahydro-1*H*-4,7-ethanoisoindole-1,3(2H)-dione

PmDUD20S (*endo-syn)*: ^{1}H NMR (500 MHz, $CDCl_3$): δ 2.49–2.53 (m, 3H), 3.54–3.59 (m, 1H), 3.70–3.76 (m, 1H), 3.87–3.95 (m, 3H), 6.51 (dd, *J* = 8.62, 6.48 Hz, 1H), 6.60 (d, *J* = 8.54 Hz, 1H), 7.22–7.28 (m, 2H), 7.30–7.35 (m, 2H), 7.39 (d, *J* = 15.41 Hz, 1H), 7.49–7.60 (m, 3H), 7.74 (d, *J* = 15.41 Hz, 1H), 8.00–8.05 (m, 2H); ^{13}C NMR (126 MHz, $CDCl_3$): δ 15.1, 38.3, 40.6, 43.1, 49.6, 65.0, 67.7, 120.7, 120.8, 126.0, 126.3, 128.9, 129.2, 130.3, 131.2, 133.1, 135.2, 138.2, 142.8, 145.1, 157.4, 157.7, 168.7, 176.2, 177.1, 189.5; NSI-MS: *m/z* 540; HRMS (NSI): For $C_{30}H_{25}N_3O_5S$ $(M+H)^+$ *m/z* calcd., 540.1593; found, 540.1588.

(*E*)-8,9-dihydroxy-2-(4-(3-(3-nitrophenyl)acryloyl)phenyl)-4-(pyrimidin-4-yl)-3a,4,7,7a-tetrahydro-1*H*-4,7-ethanoisoindole-1,3(2*H*)-dione

PmDUD21S (*endo-syn)*: ^{1}H NMR (500 MHz, $CDCl_3$): δ 3.54–3.60 (m, 1H), 3.71–3.77 (m, 1H), 3.88–3.96 (m, 3H), 6.48–6.55 (m, 1H), 6.58–6.64 (m, 1H), 7.35–7.41 (m, 2H), 7.51–7.66 (m, 3H), 7.78–7.85 (m, 1H), 7.90 (d, *J*=7.78 Hz, 1H), 8.04–8.10 (m, 2H), 8.20–8.30 (m, 1H), 8.49 (t, *J* = 1.91 Hz, 1H), 8.75–8.85 (m, 1H), 9.21–9.26 (m, 1H); ^{13}C NMR (126 MHz, $CDCl_3$): δ 38.3, 40.6, 43.2, 49.6, 65.0, 67.6, 120.8, 122.5, 124.3, 124.9, 126.5, 129.4, 130.2, 130.3, 133.1, 134.4, 135.8, 136.5, 137.3, 142.4, 148.8, 157.5, 157.8, 168.7, 176.1, 177.1, 188.6; NSI-MS: *m/z* 539; HRMS (NSI): For $C_{29}H_{22}N_4O_7$+H $(M+H)^+$ *m/z* calcd., 539.1566; found, 539.1561.

Methyl-(*E*)-3-(4-(8,9-dihydroxy-4-(1*H*-imidazol-1-yl)-1,3-dioxo-1,3,3a,4,7,7a-hexahydro-2*H*-4,7-ethanoisoindol-2-yl)phenyl)acrylate

ImDUD10S (*endo-syn*): ^{1}H NMR (500 MHz, Acetone-d_6): δ 3.36 (dtd, *J* = 6.37, 3.07, 3.07, 1.22 Hz, 1H), 3.69**–**3.77 (m, 5H), 3.96 (dd, *J* = 8.62, 3.13 Hz, 1H), 4.24 (d, *J* = 8.39 Hz, 1H), 6.49 (dd, *J* = 8.77, 6.48 Hz, 1H), 6.58 (d, *J* = 15.87 Hz, 1H), 6.72 (d, *J* = 8.85 Hz, 1H), 6.90–6.97 (m, 1H), 7.25–7.29 (m, 2H), 7.41 (t, *J* = 1.30 Hz, 1H), 7.67 (d, *J* = 16.02 Hz, 1H), 7.72–7.77 (m, 2H), 7.98 (t, *J* = 1.07 Hz, 1H); ^{13}C NMR (126 MHz, Acetone-d_6): δ 30.7, 39.6, 41.3, 41.9, 51.8, 64.6, 65.6, 118.9, 119.8, 128.0, 129.0, 129.3, 132.3, 133.4, 137.6, 144.1, 167.3, 175.7, 177.7; NSI-MS: *m/z* 436; HRMS (NSI): For $C_{26}H_{22}NO_5Br$+H $(M+H)^+$ *m/z* calcd., 436.1508; found, 436.1503.

4.2.1.4.10. Modifications of bridged bicycles

4.2.1.4.10.1. Debromination to obtain BzDPD01A and BzDPD10A

Tributyltin hydride (0.019 mmol) and AIBN (0.006 mmol) were added to a solution of compound BrDPD01A or BrDPD10A (0.013 mmol) (Fig. 7) in dry benzene (3 mL). The resultant reaction mixture was refluxed in a flask with a drying tube. After 16h, the reaction was cooled to RT, an aqueous saturated KF solution (5 mL) was added and the mixture was stirred for 1h. Resultant tin fluoride salts were removed by filtration and the aqueous layer was extracted with ethyl acetate (2 x 5 mL). Organic layers were combined, dried over Na_2SO_4 and filtered. Solvent was evaporated under reduced pressure at 30 ºC, and the obtained crude product was purified by column chromatography using ethyl acetate and petroleum ether as eluents to obtain the compounds in 60-70% yield. Purified compounds were characterized by ^{1}H NMR, ^{13}C NMR and mass spectrometry.

TLC: 1:1 ethyl acetate, petroleum ether, R_f 0.4 and 0.6.

2,2-dimethyl-7-phenyl-3a,4,10,10a-tetrahydro-6*H*-4,10-etheno[1,3]dioxolo[4,5-*d*][1,2,4]triazolo[1,2-*a*]pyridazine-6,8(7*H*)-dione

BzDPD01A (*anti*): ^{1}H NMR (600 MHz, $CDCl_3$): δ 1.35 (s, 6H), 4.63–4.68 (m, 2H), 5.06–5.21 (m, 2H), 6.39–6.43 (m, 2H), 7.33–7.38 (m, 1H), 7.39–7.46 (m, 4H); ^{13}C NMR (75 MHz, $CDCl_3$): δ 25.4, 25.5, 52.4, 74.0, 112.2, 125.6, 128.5, 128.9, 129.2, 131.3, 155.7; NSI-MS: *m/z* 328; HRMS (NSI): For $C_{17}H_{17}N_3O_4$+H $(M+H)^+$ *m/z* calcd., 328.1297; found, 328.1292.

Methyl-(*E*)-3-(4-(2,2-dimethyl-5,7-dioxo-3a,4,4a,5,7,7a,8,8a-octahydro-6*H*-4,8-ethe-no[1,3]dioxolo[4,5-*f*]isoindol-6-yl)phenyl)acrylate

BzDPD10A (*endo-anti*): ^{1}H NMR (300 MHz, $CDCl_3$): δ 1.36 (s, 3H), 1.51 (s, 3H), 3.50 (s, 4H), 3.80 (s, 3H), 4.18 (s, 2H), 6.23 (dd, *J* = 4.05, 2.73 Hz, 2H), 6.42 (d, *J* = 16.01 Hz, 1H), 7.20–7.29 (m, 2H), 7.57 (d, *J* = 8.48 Hz, 2H), 7.67 (d, *J* = 16.01 Hz, 1H); ^{13}C NMR (75 MHz, $CDCl_3$): δ 24.3, 26.4, 37.1, 37.9, 51.8, 74.0, 112.7, 119.1, 126.8, 128.6, 131.8, 133.5, 134.6, 143.6, 167.2, 178.2; NSI-MS: *m/z* 410; HRMS (NSI): For $C_{23}H_{23}NO_6$+H $(M+H)^+$ *m/z* calcd.410.1603,; found, 410.1608.

4.2.1.4.10.2. Synthesis of BrDUD01AR and BrDUD02SR by reduction

Activated palladium on charcoal (10 mg) was added to a solution of compounds BrDUD01A or BrDUD02S (0.025 mmol) in methanol (5 mL). The mixture was stirred at RT under hydrogen gas pressure with balloons. After 16 h, the reaction mixture was filtered through a celite bed and the filtrate was evaporated under reduced pressure at RT. Pure compounds were obtained without any further purification in 75-85% yield. These were analyzed by ^{1}H NMR, ^{13}C NMR and mass spectrometry.

TLC: 1:1 ethyl acetate, petroleum ether, R_f 0.3 and 0.6.

5-bromo-6,7-dihydroxy-2-phenyltetrahydro-1*H*-5,8-ethano[1,2,4]triazolo[1,2-a]pyridazine-1,3(2*H*)-dione

BrDUD01AR (a*nti*) :^{1}H NMR (500 MHz, $CDCl_3$): δ 1.80–1.92 (m, 1H), 2.35 (dddd, *J* = 13.81, 11.22, 5.04, 2.90 Hz, 1H), 2.47 (ddd, *J* = 14.11, 11.22, 2.90 Hz, 1H), 2.81 (ddd, *J* = 14.15, 11.33, 6.41 Hz, 1H), 3.27–3.35 (m, 1H), 3.44 (s, 1H), 4.14 (d, *J* = 7.78 Hz, 1H), 4.23 (dd, *J* = 7.63, 3.20 Hz, 1H), 4.52 (ddd, *J* = 4.81, 3.13, 1.53 Hz, 1H), 7.32–7.39 (m, 1H), 7.41–7.51 (m, 4H); ^{13}C NMR (126 MHz, $CDCl_3$): δ 22.1,

35.8, 54.7, 69.5, 72.0, 73.2, 126.1, 126.6, 128.4, 129.4, 155.1, 155.3; NSI-MS: *m/z* 368, 370; HRMS (NSI): For $C_{14}H_{14}BrN_3O_4$ $(M+H)^+$ *m/z* calcd.,368.0246; found, 368.0241 .

4-bromo-2-(4-fluorophenyl)-5,6-dihydroxyhexahydro-1*H*-4,7-ethanoisoindole-1,3(2*H*)-dione

BrDUD02SR (*endo-syn*): ^{1}H NMR (500 MHz, Acetone–d_6): δ 1.70–1.80 (m, 2H), 2.09–2.36 (m, 3H), 3.57 (dd, *J* = 9.84, 2.98 Hz, 1H), 3.71–3.80 (m, 1H), 4.11–4.30 (m, 2H), 4.82 (d, *J* = 3.66 Hz, 1H), 5.14 (br. s, 1H), 7.21–7.31 (m, 2H), 7.36–7.44 (m, 2H); ^{13}C NMR (126 MHz, Acetone–d_6): δ 21.4, 31.1, 34.8, 41.5, 44.8, 69.3, 75.3, 116.4, 116.6, 130.0, 161.9, 163.9, 176.3, 178.3; NSI-MS: *m/z* 468, 470; HRMS (NSI): For $C_{20}H_{19}BrFNO_6$+H $(M+H)^+$ *m/z* calcd., 468.0458; found, 468.0453.

4.2.1.4.10.3. Synthesis of BrDUD01ARAc and BrDUD02SRAc by O-acetylation

Acetic anhydride (0.03 mmol) and a catalytic amount of 4-dimethylamino pyridine were added to a solution of BrDUD10AR or BrDUD02SR (0.014 mmol) in THF (3 mL), pre-cooled to 0°C. The resultant reaction mixture was stirred at RT until the starting material completely reacted (monitored by TLC). After completion of the reaction, ice-cold water (3 mL) was added. The organic layer was separated and saturated brine solution (10 mL) was added to the aqueous layer which subsequently was extracted with ethyl acetate (2 x 5 mL). Organic layers were combined, dried over Na_2SO_4 and concentrated under vacuum at RT. The crude compounds were purified by column chromatography using ethyl acetate and petroleum ether as eluents to afford pure compounds in 75-85% yield. The compounds were characterized by ^{1}H NMR, ^{13}C NMR and mass spectrometry.

TLC: 1:1 ethyl acetate, petroleum ether, R_f 0.4-0.6.

5-bromo-1,3-dioxo-2-phenylhexahydro-1*H*-5,8-ethano[1,2,4]triazolo[1,2-a]pyridazine-6,7-diyl diacetate

BrDUD01ARAc (*anti*): ^{1}H NMR (500 MHz, $CDCl_3$): δ 1.96–2.06 (m, 4H), 2.14 (s, 3H), 2.39 (ddt, *J* = 13.83, 11.65, 4.20, 4.20 Hz, 1H), 2.52 (ddd, *J* = 14.53, 11.18, 3.74 Hz, 1H), 2.84 (ddd, *J* = 14.34, 11.52, 5.57 Hz, 1H), 4.59 (dt, *J* = 4.65, 2.10 Hz, 1H), 5.24 (dd, *J* = 8.24, 2.44 Hz, 1H), 5.38 (d, *J* = 8.24 Hz, 1H), 7.36–7.41 (m, 1H), 7.44–7.52 (m, 4H); ^{13}C NMR (126 MHz, $CDCl_3$): δ 20.3, 20.4, 22.7, 35.5, 51.7, 66.9, 69.2, 72.3, 125.5, 128.4, 129.3, 131.4, 152.3, 153.7, 168.9, 169.0; NSI-MS: *m/z* 452, 454; HRMS (NSI): For $C_{18}H_{18}BrN_3O_6$ $(M+H)^+$ *m/z* calcd.,452.0457; found, 452.0452.

4-bromo-2-(4-fluorophenyl)-1,3-dioxooctahydro-1*H*-4,7-ethanoisoindole-5,6-diyl diacetate

BrDUD02SRAc (*endo-syn*): ^{1}H NMR (400 MHz, $CDCl_3$): δ 1.73–1.83 (m, 2H), 2.08 (s, 3H), 2.11–2.21 (m, 4H), 2.31–2.42 (m, 1H), 2.47–2.53 (m, 1H), 3.55 (dt, *J* = 9.92, 1.40 Hz, 1H), 3.74 (dd, *J* = 9.92, 2.29 Hz, 1H), 5.28 (dd, *J* = 8.39, 2.80 Hz, 1H), 5.39 (d, *J* = 8.65 Hz, 1H), 7.14–7.22 (m, 2H), 7.26–7.32 (m, 2H); ^{13}C NMR (101 MHz, $CDCl_3$): δ 20.4, 20.6, 20.8, 30.0, 31.3, 40.1, 44.2, 56.9, 69.1, 73.7, 116.3, 116.6, 128.1, 160.8, 164.1, 169.1, 174.3, 176.3; NSI-MS: *m/z* 468, 470; HRMS (NSI): For $C_{20}H_{19}BrFNO_6$+H $(M+H)^+$ *m/z* calcd., 468.0458; found, 468.0453.

4.2.2. Biology

4.2.2.1. Work with microorganisms

4.2.2.1.1. Cultivation of microorganisms

All assays with microorganisms were carried out under sterile conditions. The bacterial and yeast cells were revived from frozen cultures (at -20 ºC), whenever necessary. To start a new culture, fresh medium (20 mL) was added to a frozen culture (1 mL) and shaken over night at 30 ºC. Subsequently, the OD of the new culture was determined at 600 nm, using a photometer.

4.2.2.1.2. Agar diffusion assay

Complete media were used for the agar diffusion assay, EBS medium for bacteria and M90 medium for yeasts media with agar were heated in a microwave oven until the agar had melted. Then they were cooled in a water bath, pre-heated to 50 ºC. The microorganisms were added to these media to obtain a final OD of 0.01 for bacteria and 0.1 for yeasts. The inoculated media (15 mL) were poured onto petri dishes and the agar was allowed to solidify. Paper discs (6 mm diameter) were placed on the agar surface and the test compounds, dissolved in DMSO, were added to the paper discs (20 µl). Thereafter, the petri dishes were incubated for 1 day in an incubator at 30 ºC. After 24 hours of incubation time, the diameter of the inhibition zone (halo) was measured, if present.

4.2.2.2. Work with mammalian cell cultures

4.2.2.2.1. Cultivation and trypsinisation of cells

The whole work with mammalian cell cultures was carried out under sterile conditions. Cells were grown in cell culture flasks at 37 ºC under 10% CO_2 in appropriate media, with periodical passaging. The required media for the cultivation were pre-warmed to 37 ºC prior to use. For harvesting, cultivated cells were trypsinised to split them for seeding the required number per well in a MTP. For trypsinisation the cell medium (10 mL) was removed from the culture flask, and the cell surface was rinsed once with EBSS (10 mL), followed by the addition of 1mL of trypsin. The flask was incubated at 37 ºC for 5-10 min, and the trypsination was terminated by adding 10 mL of fresh medium.

4.2.2.2.2. Cell viability assay (MTT assay)

The Assay was carried out in 96 well plates. L929 cells (mouse fibroblast) were suspended (50,000 cells/mL) in culture medium and 120 µl of cell suspension was added into each well. The peripheral rows were omitted. The test compounds, dissolved in either DMSO or DMSO/Methanol (1/1, v/v), were serially diluted with the same culture medium in a separate 96 well plate. The final compound dilution (60 µl) was transferred to the cells in two replicates to reach final concentrations in the range 37 µg/mL to 0.2 ng/mL. After 5 days of incubation at 37 ºC, the metabolic activity of the cells was determined by using 3-(4,5-dimethylthiazol-2-yl)-2,5-diphenyltetrazolium bromide (MTT). Twenty µl of MTT (0.5 mg/mL) in PBS was added to the cells. After 2h of incubation the micro-titre plates were centrifuged (1744 rcf/min) and the medium was removed by tapping. The precipitate was washed with 100 µl of PBS and the formazan crystals were dissolved by adding 100

µl of acidic isopropanol (0.4% hydrochloric acid). The absorbance of the colored solution was measured in a plate reader at 595 nm.

4.2.2.2.3. Impedance measurement assay

A. Experimental procedure: The impedance assay was performed with L929 cells. These cells were grown in medium (DMEM, 10% FBS) at 37 ºC for 3 weeks. Two days before starting the assay, the cells were trypsinised and were split into equal volumes and growth was continued to confluency. Medium (60 µl) was added to each well of a 96 well plate equipped with gold electrodes for impedance measurement (E-96 plate, Roche/Acea Biosciences) and of a normal micro-titre plate (MTP). Both plates were kept under a sterile bench for 30 minutes with the lids closed. Thereafter, the cells were trypsinized (see 4.2.2.1.1) and suspended in 30 mL of medium, pre-warmed to 37 ºC, to reach a density of 100000 cells/mL (calculated with a cell counter). A background impedance measurement (step 1) was carried out approximately over one minute in the incubator of the impedance reader at 37 ºC. After step 1, the E-plate was removed and 120 µL of cell suspension was added into each well of the E- and MT plate. Both plates were left for 30 minutes under the laminar-flow hood to reach a homogenous distribution of the cells. After 30 minutes, the E-plate was clamped back into the incubator of the impedance reader and step 2 of the schedule (2-1 to 2-3) with parameters as given in the Table 7 was initiated to start the second impedance measurement.

After termination of step 2, both E-plate and MTP were placed under the sterile bench and test compounds dissolved in DMSO/MeOH (1/1, v/v) were added to the cells in triplicates, in volumes of 1-3 µl to reach the IC_{90} of the MTT assay. The test compounds were added rapidly to start the measurement as soon as possible

after the compound addition in order to record the early effects of the compounds on the cellular processes. Subsequently, the E-plate was immediately placed back in the incubator of the impedance reader, and step 3 of the measurement schedule was started (Table 7). The measurement was terminated after 5 days. The recorded impedance data was analyzed. The MTP was used to observe the morphological changes of the cells under the microscope.

Table 7. Parameters for the impedance monitoring for steps 2 and 3 of the measurement schedule

Step	Measurement interval (min)	Duration (h)
2-1	05	01
2-2	15	03
2-3	30	20
3-1	05	01
3-2	15	03
3-3	30	20
3-4	30	300

B. Data analysis

The so-called time-dependent cellular response profiles (TCRP) were recorded by Roche RTCA software. The statistical programming language R, Version 2.12.2 (R Development Core Team, 2011) was used for the execution of data mining and processing. The raw cell index (CI) data provided by RTCA software was normalized by dividing the cell indices for each time point after the compound addition, by the cell index at the reference point as suggested by Abassi and co-workers.[82] The last measurement recorded before the addition of compounds was used as the reference point. Only the readings after compound addition were considered for subsequent

analysis. The outliers out of triplicates were detected and removed by the median polish method. Cubic smoothing splines fitting was used to reduce the dimensionality of the data set and to approximate the TCRPs. Spline basis coefficients were used as descriptors to construct the distance matrix which was used for hierarchical cluster analysis to construct dendrograms. The distance matrix provided numerical values (Euclidean distance) to assess similarities between reference compounds with known biological activity and test compounds. These numerical values were used to select the compounds for further biological activity assays. A heat map was generated which displays the Z-transformed values of the 22 descriptors which correspond to the basis spline coefficients. Hierarchical cluster analysis was done for the reference compounds together with the test compounds.

4.2.2.2.4. High content analysis with automated microscope

A. Instrument and equipment

ImageXpress Micro (IXM)

High-Speed Laser Autofocus

Digital CCD-Camera

300 Watt Xenon-arc lamp

Filter Sets:
- DAPI
- FITC
- TRITC
- Texas Red

Nikon Objective:
- 4X Plan Apo, NA (Numerical Aperture) 0,20
- 10X S Fluor, NA 0,50
- 20X S Fluor, NA 0,75
- 40X Plan Apo, NA 0,95
- 60X Plan Fluor, NA 0,85

B. Experimental procedure

Confluent KB 3–1 cells were harvested according to the procedure mentioned in 4.2.2.2.1. Cells (60 µl) were seeded into six 384 well MTPs with 2500 cells/well and were incubated for 1h at RT, followed by 3h at 37 ºC. Compounds (100 µl), dissolved in DMSO/MeOH in a 1/1 ratio (v/v) were added to the MTPs to reach the IC_{50} of MTT assay, with the help of a robotic pin-tool. Cells were incubated for overnight at 37 ºC followed by washing and staining steps with appropriate reagents or antibodies described in 4.2.2.2.5. All washing steps were done with PBS (50 µl). Additional details of the staining of the six plates are given in Table 8. After the staining step, cells were stored at 4 ºC, sealed with parafilm and wrapped in aluminum foil prior to image acquisition.

Table 8. Details of targeted proteins and their visualization

Plate number	Staining reagent or antibody		Fixation reagents	Dilution of stains or antibodies	Incubation time (h)
	Primary	Secondary			
I	Alexa fluor phalloidin 488	Not required	F[a]	1:400	1
	Monoclonal anti-α-tubulin; Clone B-5-1-2	Anti-mouse IgG Atto 594	F	1:6000	1
II	GRP 94	Labeled rabbit anti-rat IgG	M/A[b]	1:4000	1
	monoclonal anti-pan cytokeratin; clone C-11	Anti-mouse IgG Atto 594	M/A	1:2000	1
III	Anillin	Atto 488 goat anti-rabbit IgG	F	1:1000	1
	Monoclonal anti-splicing factor SC-35	Anti-mouse IgG Atto 594	F	1:4000	1
IV	Phospho-p38, MAP kinase (Thr180/Tyr182)	Atto 488 goat anti-rabbit IgG	F	1:400	O.N.[c]
	Phospho-44/42, MAP kinase (Erk 1/2) (Thr202/Tyr204)	Anti-mouse IgG Atto 594	F	1:400	O.N.
V	Anti-c-Fos	Atto 488 goat anti-rabbit IgG	F	1:3000	1
	Monoclonal Anti-p53	Anti-mouse IgG Atto 594	F	1:1600	1
VI	Anti-phospho-CREB (pSer133)	Atto 488 goat anti-rabbit IgG	F	1:1000	O.N.
	Mouse anti-calmodulin	Anti-mouse IgG Atto 594	F	1:400	O.N.

F-Formalin, M/A-MeoH/Acetone, O.N.-Overnight

C. Image analysis, software and application modules

MetaXpress (2.0.0.13, Molecular Device) is the software used for the image acquisition with automated microscope. The important settings used for recording the images were mentioned below.

Objective and camera: 10X was used with binning of 2 and gain of 1

Plate: Corning 384-well plastic 3683 and parameters for the plate type were already set and were not changed

Wells to visit: Four sites were chosen for each well according to the cells distribution

Time-lapse: only one time point

Acquisition loop: 3 wavelengths selected and laser-based focusing enabled

Autofocus: focus on well bottom for all sites

Setting for each wavelength: W1for DAPI, W2 for FITC and W3 for Texas Red. Exposure time was adjusted according to the staining intensity.

Acquired images were analyzed in two ways, i) cell based and ii) image based with two application modules i) Transfluor for SC-35 staining ii) Multi wavelength cell scoring for all other staining.

Cell and image-based analysis: Cell-based analysis takes individual cells into consideration whereas image-based analysis takes an average of all the sites in one well. In this work both kinds of analyses were performed, but from the previous experiences, output from image-based analysis was considered for the final evaluation.

Multi wavelength cell scoring (MWCS): This module is used to analyze cells with more than one staining. Size of the object (minimum and maximum width) and stain intensities for each wavelength were altered manually. In this experiment the three used wavelengths were W1: DAPI, W2: FITC and W3: Texas Red. Descriptors used for the image analysis in both ways were shown in Table 9.

Table 9. Descriptors used in Multi wavelength scoring for both image and cell-based analysis

Image-based analysis
Total cells: Total number of cells based on DAPI.
(%) Positive W2/W3: Number of cells stained for each wavelength (both absolute and relative)
Scoring profile 1--/12-/1-3/123: absolute number of cells which are stained for different wavelength, For example: 1-3 shows the number of cells stained only for 1(W1) and 3 (W3) but not 2 (W2) and so on.
Cell-based analysis
Total area: Nuclear surface
Stained area W1/W2/W3: Coloured surface of respective staining
Positive W2/W3: absolute number of cells stained for each wavelength
Average/integrated intensity W1/W2/W3: average/integrated intensity of each stain

Transfluor: This module was used for counting objects like pits and vesicles which were stained with SC-35. Parameters such as the nucleus size, vesicle and pit count were altered. Descriptors used in the Transfluor module for the analysis are show in Table 10.

Table 10. Descriptors used in the Transfluor application module for image analysis

Image-based analysis
Pit count per cell: Total number of pits per cell
Pit average intensity: average intensity of all the pits in each well
Vesicle count per cell: absolute number of vesicles per cell
Vesicle average/integrated intensity: average or integrated intensity of all the vesicles in each well
Nuclear count: Total number of cells based on W1 wavelength
Nuclear average intensity: average intensity of all the cells in a well
Same descriptors were used for Cell-based analysis

D. Data analysis, software and methodology

Data obtained from application modules are analyzed using AcuityXpress™. The flow of the analysis is shown below.

Annotation: All micro-titre plates were annotated with compound labels in respective wells in an *excel* file. This file was imported to AcuityXpress™ in *csv* file format.

Normalization: The data was normalized against the negative control (DMSO:MeOH, 1/1, v/v) with a linear scaling method, Control Mean Scaling. Each of the six plates was normalized separately based on cell- or image-based analysis. For this assay min-max scaling was used, which is independent of controls. All cell-based parameters have a prefix of cell and image-based parameters have no prefix.

Dataset creation: All the six plates used for HCIA experiment were combined into one dataset. Two kinds of dataset are possible and were created namely, cell-based and image-based. For each kind of dataset, their respective descriptors were used.

Centering and scaling of the data: For better comparison the data was centered and scaled, i.e., subtracting the mean from each data point and dividing each data point by the variance (average of squared difference from the mean), which gave Z-values.

Analysis method: After the data transformation, it was analysed using two different analysis methods, hierarchical and non-hierarchical clustering, with AcuityXpress™.

In Hierarchical cluster, the number of clusters is derived from the analysis. Similarity metrics defined by the Euclidean squared metric was used to convert descriptor rows into clusters. These clusters are linked together with the degree of similarity to produce the dendrogram which determines the grouping of these descriptor rows in heat maps. This method was employed to construct the dendrograms associated with a heat map with all of the test compounds and reference compounds.

Match to mean profile: The data set can be sorted, based on similarity profiles of compounds of interest. This method was followed to obtain numerical correlation coefficient values, in addition to the two-dimensional visual representation. The profile of a test compounds was selected in the AcuityXpress interface, by clicking its row in the Data tab and the “Match to Mean Profile” command was executed. The output gave the distance values between the selected compound and the remaining compounds in the data set. This procedure was repeated for all test compounds and the generated file was exported each time to an *excel* data sheet.

4.2.2.2.5. Immuno-fluorescence assays for the inhibition of actin and tubulin polymerization

Cells were cultivated on cover slips for fluorescence staining. Sterile cover slips (13 mm diameter) were placed in each well of a 4-well MTP. PtK2 cells were harvested by trypsinising a confluent cell culture (see 4.2.2.2.1) and were diluted to 10-fold with medium. To each MTP well, 750 µl of the cell suspension was added and the cells were incubated for overnight at 37 ºC. Thereafter, the test compounds (1 µl), dissolved in DMSO, appropriate positive controls (1 µl in DMSO) or blank (DMSO, 1 µl) were added. The total concentration of DMSO in a well did not exceed 1%. Cells were incubated with the test compounds for overnight at 37 ºC.

A. Fixation: After the incubation, medium was carefully aspirated under vacuum suction. The cells were incubated with 750 µl of formalin (3.7% (v/v) of formaldehyde in PBS) for 10 minutes. The cells were washed once with PBS (750 µl) and incubated with 750 µl Triton X-100 (0.1% (v/v) in PBS) for 5 minutes to make the cells permeable. Triton X-100 was aspirated and cells were washed with PBS (750 µl).

B. Staining: Appropriate antibodies were used for specific proteins staining. The cells were incubated with 240 µl of primary antibody dilution for one hour at 37 ºC and were subsequently washed twice with PBS (750 µl). Thereafter, the primary antibodies were labeled with 240 µl of a dilution of the secondary antibody (containing a fluorescent reporter) by incubation for 1h at 37 ºC. Cells were washed twice with PBS (750 µl). Then, for the nucleolus staining, the cells were incubated with 20 µl DAPI (1 µg/mL in PBS) for 10 minutes at RT followed by a PBS (750 µl) washing. The cover slips were taken out of the wells, towel-dried and embedded onto a microscopic glass slide with a drop of embedding medium (ProLong Antifade). The pri-

mary and secondary antibodies used for staining of actin and tubulin protein structures are given in Table 11.

Table 11. List of the antibodies used for the staining of actin and tublin structures in PtK2 cells

Stained structure	Primary antibody	Secondary antibody
Actin	Alexa Fluor Phalloidin 488	No secondary antibody needed
α-Tubulin	Anti- α-Tubulin	Alexa Fluor 488

C. Generation of images: The images of stained protein structures in the cells were captured with the CCD camera mounted on the Axioplan fluorescence microscope. Neofluor objectives with 63x and 100x magnification were used to view the images. All images were taken with 63x magnification.

4.2.2.2.6. Histone deacetylase inhibition assay

Substrates provided in the commercial kit were thawed at room temperature and mixed to homogenize. Dilutions were made according to the assay protocol supplied with the kit. Reagents in the kit were added to the wells of 96 well MTPs according to Table 12.

Table 12. Reagent addition scheme for HDAC activity or inhibitor test

Type of reaction	Assay Buffer (µl)	HDAC Inhibitor Solution (µl)	HeLa Lysate or Test Sample (µl)	HDAC Substrate Solution (µl)
100 % HDAC Sample	35	0	15	50
Test-compound	30	5	15	50
No HDAC	50	0	0	50

The MTP was incubated for 30 minutes at 30 ºC. Thereafter, 10 µl of developer solution was added to each well and the plate was incubated for 10 more minutes at RT. After the incubation time fluorescence at 460 nm was measured with the fluorimeter plate reader.

4.2.2.2.7. Proteasome inhibition assay

All contents supplied in the commercial kit were thawed at RT and used in the assay according to the instructions provided. All solid substrates or reagents supplied were dissolved in the appropriate buffer solution. The Proteasome reagent was prepared with a peptide substrate Suc-LLVY-Glo^{TM}, containing a luminescent reporter, and a luciferin detection reagent. The prepared reagent was kept at RT for 60 minutes before use to remove any contamination of free aminoluciferin.

Each reaction was done in duplicate. KB 3–1 cells were harvested as described in 4.2.2.2.1 and seeded (50 µl) into a 96 well white walled MTP with 15,000 cells/well. Cells were incubated for 2 h at 37 ºC. Test compounds (1-2 µl), dissolved in DMSO/MeOH (1/1, v/v) were added to the cells, and the cells were incubated for another 2h at 37 ºC. The MTP was allowed to equilibrate to RT. The proteasome reagent (50 µl) was added to the cells and the contents of the wells were mixed using

a plate shaker for 2 minutes. Thereafter, the MTP was incubated for 20 minutes at RT with the lid closed. Subsequently, the luminescence of each well was measured with a plate reader.

5. Abbreviations

AIBN	Azoisobutyronitrile
ARHDO	Aryl hydroxy dioxygenase
CI	Cell index
DAPI	4',6-diamidino-2-phenylindole
DMEM	Dulbecco’s modified eagle’s medium
DMSO	Dimethyl sulfoxide
EBSS	Earle's balanced salt solution
FBS	Fetal bovine serum
FDA	Food and drug administration
FITC	Fluorescein isothiocyanate
HCIA	High content image analysis
HDAC	Histone deacetylase
HOMO	Highest occupied molecular orbital
HPLC	High pressure liquid chromatography
HRMS	High-resolution mass spectrum
LC-MS	Liquid chromatography-mass spectrum
LUMO	Lowest unoccupied molecular orbital
MEM	Minimum essential media
MTP	Microtitre plate
MTT	3-(4,5-Dimethylthiazol-2-yl)-2,5-diphenyltetrazoliumbromid
MWCS	Multi wavelength cell scoring
NME	New molecular entity
NMR	Nuclear magnetic resonance
NOE	Nuclear overhauser effect

NSI	Nanospray Ionization
OD	Optical density
O.N	Over night
PBS	Phosphate buffered saline
rcf	Relative centrifugal force
RT	Room temperature
TCRP	Time-dependent cellular response profile
TLC	Thin layer chromatography

6. References

1. Sasaki *et al*. *Cancer Res.*, *71*, 6051−6060, **2011**.
2. Shah *et al*. *Cancer Cell*, 2, 117−125, **2002**.
3. Shah *et al*. *Science*, *305*, 399−401, **2004**.
4. Yun *et al*. *Proc. Natl. Acad. Sci. U.S.A*., *105*, 2070−2075, **2008**.
5. Walsh, C. *Nature*, *406*, 775−777, **2000**.
6. Gilbert, C.; Bestman-Smith, J. and Boivin, G. *Drug Resist. Updates*, *5*, 88−114, **2002**.
7. White, T. C.; Marr, K. A. and Bowden, R. A. *Clin. Microbiol. Rev.*, *11*, 382−402, **1998**.
8. Bloland *et al*. *J. Infect. Dis.*, *167*, 932−937, **1993**.
9. Lashley, F. R. *Expert Rev. Anti Infect. Ther.*, *2*, 299–316, **2004**.
10. Munos, B. *Nat. Rev.*, 959-968, **2009**.
11. Mullard, A. *Nature*, *13*, 85-89, **2014**.
12. Danishefsky, S. *Nat. Prod. Rep.*, *27*, 1114–1116, **2010**.
13. Butler, M. S. *Nat. Prod. Rep.*, *22*, 162-195, **2008**.
14. Lam, K. S. *Trends Microbiol.*, *15*, 279-289, **2007**.
15. Corey, E. J. and Cheng, X. M. *The Logic of Chemical Synthesis,* Wiley, **1989**.
16. Leznoff, C. C. and Wond, J. Y. *Can. J. Chem.*, *50*, 2892, **1972**.
17. Camps *et al. Tetrahedron Lett., 12*, 1713–1714, **1971**.
18. Patchornik, A. and Kraus, M. A. *J. Am. Chem. Soc.*, *92*, 7857, **1970**.
19. Crowley, J. I. and Rapoport, H. *J. Am. Chem. Soc.*, *92*, 6363, **1970**.
20. Yedida, V. and Leznoff, C. C. *Can. J. Chem.*, *58*, 1140, **1980**.
21. Schreiber, S. L. *Science*, *287*, 1964–1969, **2000**.
22. Wilk *et al*. *Biol. Chem.*, *391*, 491–497, **2010**.

23. Christopher, W. *Trends in Pharmacological Sciences*, *33*, 224–232, **2012**.
24. Hertzberg, R. P. and Pope, A. J. *Curr. Opin. Chem. Biol.*, *4*, 445–451, **2000**.
25. Mander, T. *Drug Discov. Today*, *5*, 223–225, **2000**.
26. Davis *et al. Curr. Top. Med. Chem.*, *5*, 421–439, **2005**.
27. Payne *et al. Nat. Rev. Drug Discov.*, *6*, 29–40, **2007**.
28. (a) Muegge, I. *Med. Res. Rev.*, *23*, 302–321, **2003**; (b) Egan, W. J.; Walters, W. P. and Murcko, M. A. *Curr. Opin. Drug Discov. Dev.*, *5*, 540-549, **2002**.
29. Lipinski *et al. Adv. Drug Deliv. Rev.*, *23*, 3–25, **1997**.
30. Feher, M. and Schmidt, J. M. *J. Chem. Inf. Comput. Sci*., *43*, 218–226, **2003**.
31. Axerio-Cilies *et al. Eur. J. Med. Chem.*, *44*, 1128–1134, **2009**.
32. Bade *et al. Eur. J. Med. Chem.*, *45*, 5646–5652, **2010**.
33. Medina-Franco, J. L. *Drug Dev. Res.*, *73,* 430–438, **2012**.
34. Dandapani, S. and Marcaurelle, L. A. *Nat. Chem. Biol. 6*, 861–863, **2010**.
35. Ruddigkeit *et al. J. Chem. Inf. model. 52*, 2864–2875, **2012**.
36. Sauer, W. H. and Schwarz, M. K. *J. Chem. Inf. Comput. Sci.*, *43*, 987–1003, **2003**.
37. Bemis, G. W. and Murcko, M. A. *J. Med. Chem.*, *39,* 2887–2893, **1996**.
38. (a) Lovering, F.; Bikker, J. and Humblet, C. *J. Med. Chem.*, *52*, 6752–6756, **2009**; (b) Ritchie *et al. Drug Discov. Today*, *16*, 164–171, **2011**.
39. Klebe, G. and Boehm, H. J. *J. Recept. Signal Transduct. Res.*, *17*, 459–473, **1997**.
40. Huggins *et al. J. Med. Chem.*, *55*, 1424–1444, **2012**.
41. DeSimone R. W., *Comb. Chem. High Throughput Screen*, *7*, 473–493, **2004**.
42. Boyd D. R. and Sheldrake, G. N. *Nat. Prod. Rep.*, 309–324, **1998**.
43. Kobal *et al*. *J. Am. Chem. Soc.*, *95*, 4420, **1973**.

44. Hudlicky, T.; Gonzalez, D. and Gibson, D. T. *Aldrichimica Acta*, *32*, 33–62, **1999**.
45. Budke *et al. J. Med. Chem.*, 56, 254–263, **2013**.
46. Dimmock, *et al*. *Curr. Med. Chem.*, *6*, 1125–1149, **1999**.
47. Kumar *et al*. *J. Med. Chem.*, *54*, 4147–4159, **2011**.
48. Jha *et al. Bioorg. Med. Chem. Lett.*, *17*, 4545–4550, **2007**.
49. (a) Sova, M. *Mini Rev. Med. Chem.*, *12*, 749–767, **2012**; (b) De, P.; Baltas, M. and Bedos-Belval, F. *Curr. Med. Chem.*, *18*, 1672–703, **2011**.
50. Sharma *et al. Curr. Med. Chem.*, *18*, 3825–3852, **2011**.
51. Hong *et al*. *Org. Biomol. Chem.*, *7*, 3400–3406, **2009**.
52. Davison et al. *Int. Pat. Appl.*, WO 9530646 A1 19951116, **1995**.
53. Salewska *et al. J. Enzyme Inhib. Med. Chem., 27,* 117–124, **2012**.
54. Matuszak *et al*. *J. Med. Chem.*, *52*, 7410–7420, **2009**.
55. Hudlicky *et al*. *J. Org. Chem.*, *57*, 1026–1028, **1992**.
56. Ley *et al*. *Synlett*, 741–742, **1991**.
57. Pittol *et al. J. Chem. Soc. Perkin Trans. I*, 1160–1162, **1989**.
58. Gillard, J. R. and Burnell, D. J. *J. Chem. Soc. Chem. Commun.*, 1439–1440, **1989**.
59. Feher, M. and Schmidt, J. M. *J. Chem. Inf. Comput. Sci.*, *43*, 218–227, **2003**.
60. (a) Cotterill, I. C.; Roberts, S. M. and Williams, J. O. *J. Chem. Soc. Chem. Commun.*, 1628–1629, **1988**; (b) Hudlicky, T and Olivo, H. F. *J. Am. Chem. Soc.*, *114*, 9694–9699, **1992**.
61. (a) Engberts, J. B. F. N. *Pure. Appl. Chem.*, *67*, 823–828, **1995**. (b) Wijnen, J. W. Ph.D. Thesis, University of Groningen, 1997; (c) Otto, S., Blokzijl, W. and Engberts, J. B. F. N. *J. Org. Chem.*, *59*, 5372–5376, **1994**.
62. Zielinski *et al*. *Appl. Environ. Microbiol.*, *72*, 2191–2199, **2006**.

63. (a) Appukkuttan, P.; Mehtaa, V. P. and Van der Eycken, E. V. *Chem. Soc. Rev.*, *39*, 1467–1477, **2010**; (b) de la Hoz *et al. Eur. J. Org. Chem.,* 3659–3673, **2000**.

64. Jenkins *et al*. *J. Chem. Soc. Perkin Trans. I*, 2467–2656, **1995**.

65. Mahon *et al J. Chem. Soc. Perkin Trans. I*, 1255–1263, **1991**.

66. Dobbs, A. *J. Org. Chem.*, *66*, 638–641, **2001**.

67. Vollhardt, K.; Peter, C. and Schore, N. E. *Organic Chemistry: Structure and Function*. New York: W.H. Freeman and Company, **2007**.

68. Bauer, A. W.; Perry, D. M. and Kirby, W. M. M. *A. M. A. Arch. Intern. Med.*, *104,* 208–216, **1959**.

69. Mosmann, T., *J. lmmunol. Methods*, *65,* 55–63, **1983**.

70. Solly *et al.*, *ASSAY Drug Dev. Technol.*, *2*, 363–372, **2004**.

71. (a) Perlman *et al*., *Science*, *306*, 1194–1198, **2004**. (b) Price *et al*., *J. Cell. Biochem. Suppl.*, *39*, 194–210, **2002**.

72. Diestel, R. Ph.D. Thesis, Technical University Carolo-Wilhelmina, Braunschweig, **2010**.

73. Roberts *et al.*, Molecular Biology of the Cell, 4th Edition, Routledge, 2002.

74. Spector, *et al*., *Cell Motil. Cytoskeleton*, *13*, 127–144, **1989**.

75. (a) Downing, K. H. and Nogales, E. *Curr. Opin. Cell Biol.*, *10*, 16–22, **1998**; (b) Jordan *et al*. *Med. Res. Rev.*, *16*, 259–296, **1996**.

76. Grozinger, C. M. and Schreiber, S. L. *Chem. Biol.*, *9*, 3–16, **2002**.

77. Wegener *et al.*, *Chem. Biolo*., *10*, 61–68, **2003**.

78. (a) Chauhan, D., Hideshima, T. and Anderson, K. C. *Annu. Rev. Pharmacol. Toxicol.*, *45,* 465–476, **2005**. (b) Voorhees *et al*. *Clin. Cancer Res.*, *9*, 6316–6325, **2003**.

79. Arora, M. *Mater.Methods*, *3*, 175, **2013**.

80. Law et al., *J. Med. Mircrobiol*., *37*, 15–21, **1992**.

81. Still, W. C., Kahn, M. and Mitra, A., *J. Org. Chem.*, *43*, 2923–2925, **1978**.

82. Abassi et al., *Chem. Biolo.*, *16*, 712–723, **2009.**

Appendix

Table 3 Numerical distance values obtained from the impedance measurement performed with bridged bicyclic compounds derived from dienediols 22 and 23 (1st experiment)

	Bridged bicyclic compound															
Reference compound	**BrDPD17A**	**BrDPD20A**	**BrDPD13A**	**BrDPD10S**	**BrDPD10A**	**BzDPD01A**	**BzDPD10A**	**BrDUD17S**	**BrDUD19S**	**BrDUD01A**	**BrDUD21S**	**BrDUD20S**	**BrDUD18S**	**BrDUD26S**	**BrDUD12S**	**BrDUD16S**
Epothilon	5,488	4,489	2,491	1,387	1,332	3,769	4,674	2,394	3,019	1,084	5,638	3,572	3,733	5,520	5,914	6,051
Mevastatin	2,223	1,157	2,544	4,677	3,945	7,429	4,642	4,735	4,880	4,149	2,281	2,495	3,269	1,770	2,620	2,550
Simvastatin	2,224	1,194	2,626	4,725	4,003	7,481	4,628	4,797	4,897	4,200	2,283	2,489	3,260	1,794	2,621	2,540
Myxothiazol	3,339	1,903	2,129	3,763	3,089	6,558	3,561	3,672	3,613	3,265	3,414	1,532	2,195	2,732	3,750	3,770
Neopeltolid	3,172	1,756	2,157	3,907	3,222	6,701	3,716	3,841	3,836	3,406	3,244	1,685	2,365	2,549	3,582	3,582
Oligomycin	2,972	1,552	2,360	4,206	3,509	6,997	3,801	4,118	4,062	3,699	3,027	1,747	2,467	2,320	3,365	3,350
CruentarenA	3,194	1,750	2,244	4,005	3,319	6,798	3,622	3,907	3,846	3,507	3,254	1,652	2,352	2,532	3,587	3,580
GephyronicAcidA	5,492	4,195	2,543	1,940	1,713	4,490	3,311	2,044	2,011	1,666	5,610	2,642	2,703	5,090	5,920	6,019
Cycloheximid	5,181	3,983	2,302	1,913	1,532	4,541	3,501	2,051	2,172	1,511	5,311	2,505	2,676	4,890	5,619	5,733
Anisomycin	5,217	3,965	2,140	1,685	1,421	4,354	3,787	2,195	2,537	1,367	5,338	2,844	3,025	4,900	5,643	5,735
MG132	4,714	3,458	1,238	1,909	1,247	4,654	4,011	2,112	3,059	1,471	4,824	2,741	3,175	4,169	5,145	5,227
Velcade	4,507	3,245	1,628	2,477	1,858	5,217	3,522	2,228	2,697	2,019	4,624	2,152	2,521	4,126	4,931	5,011
SB202190	3,615	2,486	1,307	2,895	2,234	5,670	4,108	3,203	3,648	2,393	3,735	2,327	2,921	3,354	4,051	4,079
SB203580	3,683	2,631	1,274	2,683	2,010	5,439	4,257	3,085	3,571	2,148	3,817	2,412	2,991	3,549	4,127	4,194
Vioprolid	5,413	4,261	2,325	1,492	1,238	4,070	3,932	2,020	2,452	1,121	5,545	3,035	3,191	5,228	5,839	5,957
CytochalasinD	9,711	8,678	6,293	3,922	4,598	2,092	7,501	4,425	5,270	4,340	9,857	7,416	7,284	9,632	10,117	10,313
RhizopodinA	11,02	10,371	7,850	5,685	6,368	3,192	10,160	6,885	8,055	6,116	11,19	9,685	9,761	11,225	11,401	11,59
LatrunculinB	8,939	8,475	6,053	4,465	4,841	2,852	9,262	5,595	7,170	4,671	9,098	8,229	8,464	9,308	9,288	9,508
Nocodazol	5,239	4,184	1,998	1,252	0,950	3,851	4,571	2,280	3,089	0,822	5,373	3,438	3,703	5,173	5,650	5,778
Griseofulvin	5,156	4,080	1,810	1,191	0,786	3,914	4,478	2,179	3,069	0,722	5,291	3,317	3,617	4,993	5,581	5,696
TubulysinB	5,199	4,135	1,929	1,192	0,846	3,881	4,509	2,195	3,040	0,721	5,339	3,336	3,618	5,060	5,630	5,749
Etoposid	6,641	5,506	3,241	1,068	1,599	2,816	4,810	2,079	2,907	1,310	6,776	4,293	4,338	6,408	7,066	7,208
Camptothecin	7,530	6,554	4,026	1,608	2,353	1,530	6,093	2,880	4,092	2,065	7,678	5,581	5,662	7,437	7,946	8,098
Saframycin	6,574	5,597	3,116	0,814	1,457	2,386	5,491	2,383	3,612	1,136	6,722	4,722	4,878	6,490	6,995	7,139
Oxamflatin	5,576	4,485	2,079	0,834	0,689	3,492	4,686	2,025	3,146	0,563	5,709	3,671	3,939	5,311	6,006	6,129
Scriptaid	5,720	4,585	2,225	0,877	0,927	3,478	4,613	2,090	3,112	0,795	5,849	3,717	3,960	5,387	6,150	6,263
DMSO	6,307	5,307	2,834	0,619	1,187	2,657	5,273	2,224	3,463	0,857	6,452	4,448	4,623	6,195	6,729	6,868
Taxol	5,646	4,606	2,460	1,090	1,158	3,594	4,584	2,337	3,025	0,880	5,793	3,649	3,837	5,544	6,077	6,188

Table 2. Numerical distance values obtained from the impedance measurement performed with bridged bicyclic compounds derived from dienediols 22 and 23 (repetition experiment)

	Bridged bicyclic compound																
Reference compound	**BrDPD17A**	**BrDPD20A**	**BrDPD13A**	**BrDPD10S**	**BrDPD10A**	**BzDPD01A**	**BzDPD10A**	**BrDUD17S**	**BrDUD19S**	**BrDUD01A**	**BrDUD21S**	**BrDUD20S**	**BrDUD18S**	**BrDUD26S**	**BrDUD12S**	**BrDUD16S**	**BrDUD14S**
EpothilonB	3.590	5.436	1.768	1.536	1.247	4.968	3.829	2.242	3.217	1.399	3.384	2.405	4.021	2.539	3.418	2.173	2.590
Mevastatin	0.987	2.169	4.100	4.863	4.427	8.712	3.922	4.880	3.131	4.638	2.146	3.523	1.987	5.974	1.843	5.549	6.081
Simvastatin	1.076	2.176	4.168	4.916	4.482	8.765	3.923	4.937	3.142	4.690	2.159	3.548	1.985	6.033	1.880	5.604	6.137
MyxothiazolA	1.429	3.262	3.365	3.978	3.506	7.841	2.750	3.803	1.926	3.760	1.219	2.252	1.395	5.088	1.105	4.621	5.197
Neopeltolid	1.310	3.098	3.479	4.121	3.656	7.988	2.922	3.976	2.127	3.899	1.356	2.473	1.450	5.235	1.189	4.773	5.345
Oligomycin	1.282	2.899	3.745	4.415	3.949	8.283	3.063	4.260	2.291	4.195	1.441	2.717	1.397	5.523	1.236	5.065	5.637
CruentarenA	1.387	3.114	3.574	4.219	3.752	8.086	2.863	4.038	2.116	4.001	1.381	2.504	1.414	5.323	1.218	4.859	5.438
GephyronicAcidA	3.411	5.418	2.253	2.171	1.772	5.723	2.475	1.980	2.100	2.021	2.649	1.258	3.221	3.135	2.766	2.639	3.220
Cycloheximid	3.111	5.120	2.074	2.100	1.659	5.781	2.630	2.005	2.142	1.940	2.486	1.295	3.075	3.110	2.553	2.628	3.206
Anisomycin	3.154	5.144	1.897	1.954	1.557	5.612	2.928	2.123	2.372	1.767	2.719	1.645	3.290	3.010	2.754	2.546	3.086
MG132	2.499	4.642	1.522	2.091	1.700	5.948	3.051	2.219	2.424	1.886	2.548	1.874	2.989	3.150	2.308	2.690	3.269
Velcade	2.342	4.446	2.103	2.659	2.199	6.489	2.570	2.264	2.079	2.488	2.047	1.547	2.555	3.625	2.002	3.201	3.785
SB202190	1.543	3.565	2.467	3.109	2.695	6.958	3.216	3.265	2.489	2.884	2.024	2.322	2.403	4.229	1.801	3.799	4.335
SB203580	1.635	3.637	2.260	2.873	2.455	6.714	3.351	3.143	2.538	2.650	2.093	2.275	2.531	4.004	1.886	3.585	4.101
Vioprolid	3.377	5.349	1.810	1.680	1.271	5.308	3.093	1.899	2.620	1.532	2.949	1.759	3.555	2.705	2.988	2.244	2.797
CytochalasinD	7.784	9.651	4.688	3.736	4.069	1.983	6.911	4.148	6.717	3.954	7.357	5.759	7.981	2.908	7.408	3.216	2.821
RhizopodinA	9.394	10.982	6.318	5.486	5.962	2.222	9.479	6.652	9.113	5.665	9.509	8.176	10.136	4.715	9.429	5.114	4.518
LatrunculinB	7.487	8.912	4.705	4.153	4.551	2.747	8.434	5.495	7.829	4.319	7.939	6.946	8.533	3.621	7.751	4.000	3.530
Nocodazol	3.257	5.163	1.366	1.422	1.051	5.102	3.698	2.159	3.071	1.239	3.218	2.308	3.826	2.511	3.193	2.120	2.586
Griseofulvin	3.114	5.086	1.240	1.394	1.019	5.188	3.577	2.095	2.956	1.179	3.109	2.200	3.688	2.528	3.037	2.104	2.602
TubulysinB	3.176	5.136	1.320	1.382	1.018	5.146	3.613	2.099	2.974	1.177	3.138	2.211	3.716	2.516	3.080	2.096	2.581
Etoposid	4.608	6.572	1.976	1.124	1.176	4.008	4.041	1.854	3.669	1.156	4.208	2.734	4.814	1.713	4.224	1.326	1.721
Camptothecin	5.582	7.470	2.467	1.437	1.886	2.706	5.338	2.633	4.989	1.626	5.452	4.029	6.066	1.076	5.409	1.170	0.935
Saframycin	4.615	6.515	1.669	0.693	1.042	3.624	4.668	2.171	4.207	0.792	4.560	3.284	5.165	1.280	4.501	1.037	1.259
Oxamflatin	3.515	5.509	1.103	1.010	0.770	4.765	3.789	1.958	3.206	0.803	3.481	2.396	4.045	2.124	3.356	1.684	2.181
Scriptaid	3.651	5.649	1.294	1.115	0.950	4.752	3.738	2.017	3.191	0.919	3.547	2.393	4.098	2.171	3.436	1.717	2.204
DMSO	4.326	6.247	1.452	0.569	0.815	3.907	4.430	2.035	3.949	0.588	4.278	3.043	4.879	1.448	4.209	1.115	1.467
Taxol	3.674	5.584	1.664	1.321	1.097	4.840	3.746	2.171	3.228	1.149	3.501	2.401	4.099	2.379	3.517	1.965	2.402

Table 3. Numerical distance values obtained from the impedance measurement performed with bridged bicyclic compounds derived from hetero-aryl dienediols (1st experiment).

	Bridged bicyclic compound													
Reference Compound	**PmDUD06S**	**PmDUD19S**	**PmDUD20S**	**PmDUD13S**	**PmDUD21S**	**Py3DUD01A**	**Py3DUD17S**	**Py3DUD19S**	**Py3DUD20S**	**Py3DUD13S**	**Py3DUD21S**	**Py3DUD10S**	**Py4DUD01A**	**ImDUD10S**
Epothilon	1,257	2,334	1,727	2,195	1,761	1,238	1,946	1,713	1,909	2,633	2,149	1,776	1,012	1,305
Mevastatin	3,404	3,694	3,335	2,943	3,466	3,412	3,000	5,202	2,922	2,309	2,747	2,635	3,638	3,206
Simvastatin	3,454	3,728	3,381	2,988	3,515	3,462	3,049	5,249	2,971	2,345	2,795	2,684	3,681	3,253
MyxothiazolA	2,434	2,449	2,212	1,773	2,354	2,437	1,927	4,171	1,876	1,130	1,659	1,671	2,693	2,212
Neopeltolid	2,588	2,654	2,399	1,962	2,537	2,594	2,090	4,343	2,037	1,302	1,827	1,816	2,842	2,372
Oligomycin	2,877	2,911	2,681	2,230	2,812	2,884	2,367	4,641	2,309	1,545	2,088	2,090	3,135	2,659
CruentarenA	2,673	2,681	2,458	2,011	2,589	2,684	2,140	4,426	2,087	1,341	1,876	1,888	2,929	2,456
GephyronicAcid A	1,180	1,211	1,012	1,367	1,075	1,184	1,243	2,002	1,297	1,852	1,470	1,411	1,217	1,124
Cycloheximid	0,942	1,318	0,876	1,266	1,004	0,929	1,063	2,028	1,075	1,700	1,237	1,150	1,023	0,852
Anisomycin	0,887	1,567	1,044	1,431	1,085	0,900	1,225	1,998	1,230	1,890	1,488	1,148	0,894	0,827
MG132	0,791	1,765	1,007	1,245	1,024	0,791	0,862	2,368	0,880	1,677	1,219	0,703	1,142	0,716
Velcade	1,204	1,488	0,978	0,926	1,163	1,206	0,644	2,748	0,544	1,056	0,494	0,919	1,465	1,107
SB202190	1,663	2,375	1,781	1,632	1,916	1,685	1,448	3,430	1,359	1,328	1,351	0,993	1,857	1,487
SB203580	1,467	2,348	1,673	1,624	1,810	1,473	1,428	3,220	1,320	1,462	1,361	0,869	1,650	1,283
CytochalasinD	5,056	5,522	5,320	5,876	5,213	5,034	5,675	3,384	5,714	6,604	5,999	5,811	4,840	5,225
RhizopodinA	6,978	7,973	7,506	8,101	7,410	6,974	7,779	5,547	7,789	8,739	8,133	7,705	6,709	7,163
LatrunculinB	5,521	6,758	6,122	6,667	6,035	5,498	6,331	4,536	6,312	7,235	6,629	6,142	5,313	5,674
Nocodazol	0,823	2,183	1,434	1,925	1,444	0,849	1,591	1,730	1,544	2,390	1,868	1,361	0,594	0,915
Griseofulvin	0,598	2,078	1,284	1,783	1,301	0,625	1,409	1,726	1,377	2,259	1,727	1,185	0,452	0,713
TubulysinB	0,694	2,104	1,333	1,833	1,354	0,691	1,491	1,702	1,461	2,323	1,798	1,269	0,529	0,777
Etoposid	1,835	2,547	2,164	2,745	2,084	1,824	2,495	0,824	2,534	3,411	2,853	2,554	1,639	1,979
Camptothecin	2,877	3,800	3,342	3,952	3,249	2,872	3,627	1,407	3,651	4,620	4,002	3,647	2,627	3,070
Saframycin	1,958	3,082	2,500	3,102	2,431	1,951	2,757	1,000	2,767	3,729	3,122	2,709	1,703	2,143
Oxamflatin	0,907	2,250	1,526	2,074	1,470	0,903	1,724	1,381	1,733	2,656	2,102	1,587	0,843	1,058
Scriptaid	1,061	2,243	1,595	2,137	1,524	1,066	1,812	1,392	1,836	2,730	2,209	1,704	0,998	1,200
DMSO	1,664	2,842	2,229	2,821	2,163	1,657	2,469	0,976	2,480	3,434	2,835	2,410	1,419	1,846
Taxol2	1,149	2,284	1,666	2,197	1,686	1,163	1,873	1,508	1,864	2,686	2,182	1,745	0,831	1,257

Table 4. Numerical distance values obtained from the impedance measurement performed with bridged bicyclic compounds derived from hetero-aryl dienediols (repetition experiment).

	Bridged bicyclic compound													
Reference compound	**PmDUD06S**	**PmDUD19S**	**PmDUD20S**	**PmDUD13S**	**PmDUD21S**	**Py3DUD01A**	**Py3DUD17S**	**Py3DUD19S**	**Py3DUD20S**	**Py3DUD13S**	**Py3DUD21S**	**Py3DUD10S**	**Py4DUD01A**	**ImDUD10S**
Epothilon	1,928	2,950	2,520	2,567	2,423	2,160	2,598	1,957	2,567	3,079	2,643	2,491	1,671	2,121
Mevastatin	2,658	2,733	2,739	2,681	2,749	2,310	2,504	3,305	2,249	1,992	2,176	2,094	2,904	2,324
Simvastatin	2,717	2,758	2,787	2,726	2,800	2,359	2,548	3,334	2,307	2,027	2,230	2,150	2,954	2,374
MyxothiazolA	1,768	1,540	1,626	1,538	1,683	1,340	1,362	2,047	1,306	0,909	1,245	1,197	1,974	1,370
Neopeltolid	1,896	1,731	1,806	1,722	1,854	1,481	1,534	2,262	1,443	1,048	1,367	1,324	2,114	1,505
Oligomycin	2,159	1,926	2,046	1,969	2,095	1,738	1,779	2,529	1,669	1,230	1,581	1,534	2,384	1,768
CruentarenA	1,961	1,730	1,841	1,768	1,886	1,531	1,559	2,300	1,483	1,060	1,393	1,350	2,174	1,562
GephyronicAcid A	1,601	1,932	1,678	1,721	1,639	1,657	1,734	0,837	1,978	2,296	2,046	1,987	1,375	1,643
Cycloheximid	1,348	1,868	1,511	1,582	1,498	1,418	1,594	0,845	1,746	2,145	1,809	1,734	1,128	1,404
Anisomycin	1,343	2,137	1,774	1,811	1,637	1,464	1,796	1,136	1,890	2,320	1,987	1,845	1,094	1,429
MG132	0,653	2,034	1,370	1,454	1,116	0,948	1,404	1,439	1,305	1,984	1,508	1,315	0,696	0,863
Velcade	0,826	1,473	0,989	1,131	1,035	0,841	0,939	1,231	0,880	1,420	0,842	0,961	0,810	0,851
SB202190	1,067	1,971	1,648	1,660	1,566	0,837	1,439	1,900	1,192	1,480	1,159	0,971	1,205	0,800
SB203580	0,985	2,055	1,661	1,681	1,565	0,849	1,538	1,840	1,249	1,660	1,279	1,030	1,091	0,802
CytochalasinD	5,858	6,656	6,208	6,277	6,100	6,205	6,409	5,574	6,482	7,073	6,615	6,523	5,611	6,169
RhizopodinA	7,745	8,970	8,409	8,489	8,228	8,123	8,573	7,856	8,516	9,190	8,656	8,475	7,515	8,069
LatrunculinB	6,150	7,563	6,912	6,991	6,730	6,548	7,083	6,577	6,898	7,635	7,039	6,822	5,996	6,485
Nocodazol	1,471	2,747	2,229	2,299	2,065	1,752	2,293	1,792	2,210	2,815	2,308	2,115	1,207	1,707
Griseofulvin	1,280	2,622	2,062	2,136	1,881	1,586	2,126	1,690	2,043	2,672	2,166	1,976	1,031	1,530
TubulysinB	1,382	2,663	2,117	2,181	1,948	1,674	2,194	1,715	2,117	2,734	2,247	2,059	1,141	1,619
Etoposid	2,651	3,544	3,079	3,146	2,938	2,948	3,228	2,403	3,311	3,867	3,448	3,316	2,389	2,907
Camptothecin	3,686	4,812	4,269	4,355	4,100	4,058	4,426	3,697	4,427	5,076	4,564	4,418	3,429	4,005
Saframycin	2,759	3,977	3,411	3,493	3,236	3,125	3,551	2,893	3,515	4,174	3,653	3,491	2,509	3,070
Oxamflatin	1,648	2,951	2,347	2,422	2,138	1,993	2,460	1,944	2,410	3,063	2,581	2,384	1,447	1,933
Scriptaid	1,774	2,986	2,419	2,488	2,195	2,093	2,526	1,957	2,514	3,131	2,693	2,497	1,566	2,034
DMSO	2,463	3,703	3,131	3,210	2,956	2,827	3,259	2,631	3,224	3,878	3,360	3,197	2,218	2,771
Taxol2	1,886	2,969	2,515	2,573	2,370	2,137	2,583	1,936	2,586	3,125	2,682	2,526	1,599	2,087

Table 5. Numerical correlation values of 30 bridged bicyclic compounds obtained from the high content analysis (1st experiment). The similarity values with first 30 reference compounds are shown.

BrDPD17A	1.000	BrDPD20A	1.000	BrDPD110S	1.000	ImDUD10S	1.000	Py3DUD10S	1.000	PmDUD06S	1.000	BrDPD10A	1.000	Py3DUD01A	1.000
Amanitin	0.857	Anisomycin	0.913	Chivosazol A	0.928	Mevastatin	0.884	H89	0.927	Staurosporine	0.917	Tunicamycin	0.895	Myxothiazol A	0.900
Anisomycin	0.795	Griseofulvin	0.835	DMSO:MeOH	0.896	SB203580	0.877	SB203580	0.925	Simvastatin	0.906	Oligomycin	0.880	LY294002	0.885
SB202190	0.787	Amanitin	0.833	SB202190	0.878	DMSO:MeOH	0.864	Saframycin	0.911	Saframycin	0.877	Myxothiazol A	0.879	SB203580	0.878
Actinomycin D	0.766	SB202190	0.787	Griseofulvin	0.874	Saframycin	0.850	Oligomycin	0.876	Soraphen A	0.876	Soraphen A	0.876	Mevastatin	0.868
Apicidin	0.763	Gephyronsäure A	0.766	Mevastatin	0.854	Chivosazol A	0.845	Mevastatin	0.865	DMSO:MeOH	0.875	Mevastatin	0.872	PD169316	0.857
Griseofulvin	0.750	Mevastatin	0.761	Colchicine	0.851	LY294002	0.845	DMSO:MeOH	0.864	H89	0.868	SB203580	0.867	Tunicamycin	0.857
Alsterpaullone	0.742	Podophyllotoxin	0.749	Saframycin	0.849	Amanitin	0.822	Staurosporine	0.819	Tunicamycin	0.859	Cruentaren A	0.864	Oligomycin	0.846
Chelerythrine	0.720	Chivosazol A	0.744	Archazolid B	0.848	SB202190	0.813	PD169316	0.817	Rapamycin	0.858	Podophyllotoxin	0.861	Velcade	0.846
Chivosazol A	0.682	DMSO:MeOH	0.742	Anisomycin	0.844	Oligomycin	0.812	Methotrexate	0.817	Oligomycin	0.850	Staurosporine	0.860	Podophyllotoxin	0.823
Mevastatin	0.673	LY294002	0.738	Podophyllotoxin	0.834	Podophyllotoxin	0.803	Rapamycin	0.813	Nocodazole	0.848	Simvastatin	0.855	DMSO:MeOH	0.811
DMSO:MeOH	0.662	Indirubin monoxime	0.737	Amanitin	0.814	H89	0.795	Tunicamycin	0.807	SB203580	0.848	DMSO:MeOH	0.845	Dexamethasone	0.804
LY294002	0.661	Alsterpaullone	0.717	SB203580	0.807	Archazolid B	0.794	Chivosazol A	0.800	Mevastatin	0.833	Dexamethasone	0.843	Soraphen A	0.800
Saframycin	0.650	Actinomycin D	0.710	Staurosporine	0.805	Tunicamycin	0.793	Soraphen A	0.799	Podophyllotoxin	0.832	Velcade	0.841	Rapamycin	0.793
SB203580	0.648	Purvalanol A	0.699	Soraphen A	0.803	PD169316	0.784	Simvastatin	0.798	Archazolid B	0.828	PD169316	0.840	Cruentaren A	0.790
A23187 free acid	0.625	Tunicamycin	0.696	Apicularen	0.803	Anisomycin	0.783	LY294002	0.798	Emetine	0.823	Rapamycin	0.840	Saframycin	0.780
Methotrexate	0.623	Colchicine	0.696	Actinomycin D	0.803	Velcade	0.778	Nocodazole	0.793	PD169316	0.819	LY294002	0.833	Staurosporine	0.774
H89	0.619	SB203580	0.695	LY294002	0.797	Griseofulvin	0.775	Archazolid B	0.789	Chivosazol A	0.796	Saframycin	0.812	Simvastatin	0.770
Emetine	0.615	Staurosporine	0.691	Purvalanol A	0.794	Soraphen A	0.774	Podophyllotoxin	0.787	Methotrexate	0.795	H89	0.811	H89	0.769
Podophyllotoxin	0.614	Saframycin	0.689	Tunicamycin	0.794	Colchicine	0.774	SB202190	0.786	Dexamethasone	0.789	Archazolid B	0.786	Archazolid B	0.746
PD169316	0.612	Apicidin	0.688	Chelerythrine	0.792	Actinomycin D	0.768	Dexamethasone	0.774	Cruentaren A	0.787	Camptothecin	0.776	Purvalanol A	0.736
Apicularen	0.612	Velcade	0.684	Gephyronsäure A	0.784	Staurosporine	0.764	Myxothiazol A	0.769	Colchicine	0.778	Myriaporon	0.768	Chivosazol A	0.734
Colchicine	0.609	Soraphen A	0.679	Nocodazole	0.783	Apicidin	0.764	Emetine	0.751	Myxothiazol A	0.770	Nocodazole	0.759	Camptothecin	0.733
Velcade	0.598	Chelerythrine	0.676	Apicidin	0.780	Methotrexate	0.754	Velcade	0.749	LY294002	0.768	Trichostatin	0.757	Myriaporon	0.732
Purvalanol A	0.591	Archazolid B	0.674	Simvastatin	0.776	Chelerythrine	0.752	Colchicine	0.742	Apicularen	0.764	Cycloheximide	0.747	Indirubin monoxime	0.731
Tunicamycin	0.590	PD169316	0.672	Emetine	0.773	Nocodazole	0.748	Apicularen	0.738	SB202190	0.758	MG132	0.746	Doxorubicin	0.730
Archazolid B	0.590	Emetine	0.665	Methotrexate	0.771	Myxothiazol A	0.746	Amanitin	0.733	Vinblastine	0.757	Chivosazol A	0.746	Nocodazole	0.716
Staurosporine	0.586	Apicularen	0.657	H89	0.759	Purvalanol A	0.745	Cruentaren A	0.721	Purvalanol A	0.755	MeOH	0.734	Colchicine	0.708
Gephyronsäure A	0.583	Argyrin A	0.646	Oligomycin	0.756	Simvastatin	0.743	Anisomycin	0.716	Camptothecin	0.752	Doxorubicin	0.733	Amanitin	0.704
Soraphen A	0.580	Simvastatin	0.643	Velcade	0.742	Rapamycin	0.741	Apicidin	0.714	Velcade	0.742	Purvalanol A	0.730	Gephyronsäure A	0.704

Continued on next page

PmDUD21S	1.000	BrDUD14S	1.000	BrDUD12S	1.000	Py3DUD19S	1.000	PmDUD13S	1.000	Py4DUD01A	1.000	BrDUD26S	1.000	BrDPD13A	1.000
Tunicamycin	0.900	Cycloheximide	0.901	MG132	0.932	Camptothecin	0.909	Soraphen A	0.863	Simvastatin	0.876	Simvastatin	0.856	Gephyronsäure A	0.870
Myxothiazol A	0.880	MG132	0.900	Cycloheximide	0.895	Tunicamycin	0.864	Podophyllotoxin	0.850	Staurosporine	0.876	Staurosporine	0.849	Podophyllotoxin	0.820
Cruentaren A	0.871	Camptothecin	0.882	Myriaporon	0.867	Soraphen A	0.858	Simvastatin	0.849	Soraphen A	0.848	Archazolid B	0.847	Brefeldin A	0.810
Soraphen A	0.854	Cruentaren A	0.879	Cruentaren A	0.860	Simvastatin	0.856	Chondramid C	0.843	Tunicamycin	0.836	Gephyronsäure A	0.837	Chondramid C	0.806
Velcade	0.852	Myriaporon	0.877	Camptothecin	0.841	Ratjadon C	0.856	Purvalanol A	0.838	Podophyllotoxin	0.833	Podophyllotoxin	0.826	Archazolid B	0.805
Camptothecin	0.848	Ratjadon C	0.847	MeOH	0.822	Cruentaren A	0.850	Tunicamycin	0.837	Brefeldin A	0.812	Nocodazole	0.823	Colchicine	0.799
PD169316	0.845	MeOH	0.836	Ratjadon C	0.820	MeOH	0.838	Staurosporine	0.837	Cruentaren A	0.801	DMSO:MeOH	0.814	Staurosporine	0.796
Podophyllotoxin	0.836	Tunicamycin	0.835	Tunicamycin	0.820	Doxorubicin	0.822	Brefeldin A	0.834	MG132	0.800	Colchicine	0.810	Simvastatin	0.791
LY294002	0.831	Soraphen A	0.826	Trichostatin	0.814	Dexamethasone	0.816	Tubulysin B	0.825	Cycloheximide	0.798	Brefeldin A	0.805	Soraphen A	0.786
MG132	0.826	Trichostatin	0.820	Soraphen A	0.808	Purvalanol A	0.813	Camptothecin	0.819	Myriaporon	0.795	Soraphen A	0.800	Cytochalasin D	0.785
Rapamycin	0.819	Myxothiazol A	0.802	Brefeldin A	0.785	MG132	0.812	Gephyronsäure A	0.818	Trichostatin	0.793	Cytochalasin D	0.793	DMSO:MeOH	0.779
Myriaporon	0.819	Podophyllotoxin	0.796	Podophyllotoxin	0.784	Myriaporon	0.812	Colchicine	0.802	Puromycin	0.791	Wortmannin	0.791	Chivosazol A	0.769
Dexamethasone	0.814	Simvastatin	0.793	Myxothiazol A	0.783	Staurosporine	0.812	Archazolid B	0.802	MeOH	0.789	Vinblastine	0.790	Puromycin	0.759
Cycloheximide	0.809	Brefeldin A	0.786	Simvastatin	0.777	Rapamycin	0.812	Ratjadon C	0.800	DMSO:MeOH	0.785	Chivosazol A	0.787	Purvalanol A	0.758
Simvastatin	0.800	Velcade	0.780	Indirubin monoxime	0.772	Podophyllotoxin	0.809	Cycloheximide	0.795	Rapamycin	0.782	Apicularen	0.779	Tunicamycin	0.754
Oligomycin	0.799	Dexamethasone	0.778	Velcade	0.762	Cycloheximide	0.803	DMSO:MeOH	0.789	Camptothecin	0.782	Tunicamycin	0.776	Wortmannin	0.749
Doxorubicin	0.797	Chondramid C	0.767	Rapamycin	0.760	PD169316	0.794	Indirubin monoxime	0.788	Gephyronsäure A	0.779	Saframycin	0.775	Nocodazole	0.742
Purvalanol A	0.795	Staurosporine	0.765	Staurosporine	0.758	Myxothiazol A	0.792	MG132	0.782	Archazolid B	0.761	Puromycin	0.774	Tubulysin B	0.740
Mevastatin	0.794	Rapamycin	0.761	Chondramid C	0.756	Oligomycin	0.789	Myriaporon	0.776	Nocodazole	0.758	Mevastatin	0.756	Indirubin monoxime	0.731
Indirubin monoxime	0.791	Indirubin monoxime	0.759	PD169316	0.748	Nocodazole	0.788	Puromycin	0.772	Ratjadon C	0.756	Chondramid C	0.748	Griseofulvin	0.730
Ratjadon C	0.788	PMA	0.758	PMA	0.744	Trichostatin	0.787	MeOH	0.770	Mevastatin	0.755	Purvalanol A	0.746	Cycloheximide	0.726
Staurosporine	0.785	PD169316	0.754	Tubulysin B	0.738	Archazolid B	0.786	Nocodazole	0.764	Emetine	0.755	Myriaporon	0.739	Mevastatin	0.726
SB203580	0.775	Doxorubicin	0.750	Dexamethasone	0.737	DMSO:MeOH	0.778	Cruentaren A	0.763	Indirubin monoxime	0.755	Camptothecin	0.739	Apicularen	0.726
DMSO:MeOH	0.773	Purvalanol A	0.749	Purvalanol A	0.731	Colchicine	0.764	Emetine	0.762	PMA	0.754	Emetine	0.738	Vinblastine	0.722
MeOH	0.767	LY294002	0.740	Doxorubicin	0.721	Brefeldin A	0.763	Trichostatin	0.757	PD169316	0.752	Cycloheximide	0.730	Camptothecin	0.716
Trichostatin	0.746	Oligomycin	0.735	LY294002	0.720	Chondramid C	0.758	Chivosazol A	0.754	Purvalanol A	0.747	MeOH	0.724	Myriaporon	0.711
Chondramid C	0.744	Tubulysin B	0.725	Puromycin	0.714	PMA	0.754	Rapamycin	0.747	Myxothiazol A	0.739	PMA	0.720	Saframycin	0.709
Archazolid B	0.742	DMSO:MeOH	0.723	Gephyronsäure A	0.707	Aphidicolin	0.752	Mevastatin	0.747	Tubulysin B	0.736	SB203580	0.719	Emetine	0.702
Gephyronsäure A	0.721	Mevastatin	0.723	Oligomycin	0.706	Mevastatin	0.751	Wortmannin	0.734	Saframycin	0.736	Ratjadon C	0.719	Ratjadon C	0.702

Continued on next page…

PmDUD20S	1.000	Py3DUD20S	1.000	Py3DUD13S	1.000	BrDUD19S	1.000	Py3DUD17S	1.000	PmDUD19S	1.000	BrDUD21S	1.000	BrDUD16S	1.000
Puromycin	0.859	Brefeldin A	0.838	Vioprolid A	0.909	Brefeldin A	0.899	MeOH	0.870	Rhizopodin A	0.803	Taxol	0.806	Scriptaid	0.807
Brefeldin A	0.839	Puromycin	0.824	Brefeldin A	0.811	Vioprolid A	0.843	Cycloheximide	0.849	Vioprolid A	0.786	Rhizopodin A	0.788	Vioprolid A	0.784
Taxol	0.776	Vioprolid A	0.814	Puromycin	0.793	Puromycin	0.833	Trichostatin	0.838	Brefeldin A	0.742	Okadaic acid	0.727	Brefeldin A	0.756
Vioprolid A	0.759	Scriptaid	0.789	Scriptaid	0.767	Wortmannin	0.808	Brefeldin A	0.833	Cycloheximide	0.735	Tubulysin B	0.725	Puromycin	0.752
Chondramid C	0.743	Ratjadon C	0.758	Oxamflatin	0.731	Scriptaid	0.803	Ratjadon C	0.833	Puromycin	0.717	Brefeldin A	0.712	Tubulysin B	0.709
Cycloheximide	0.743	Cycloheximide	0.748	Rhizopodin A	0.728	Ratjadon C	0.801	MG132	0.833	MeOH	0.707	Epothilon B	0.712	Taxol	0.691
Tubulysin B	0.740	Tubulysin B	0.747	PMA	0.726	MeOH	0.789	PMA	0.814	Ratjadon C	0.699	Puromycin	0.699	Wortmannin	0.686
Rhizopodin A	0.733	MeOH	0.736	MeOH	0.721	Cycloheximide	0.773	Myriaporon	0.805	MG132	0.697	Cycloheximide	0.690	Ratjadon C	0.672
Gephyronsäure A	0.720	Chondramid C	0.731	Cycloheximide	0.719	PMA	0.769	Oxamflatin	0.801	Myriaporon	0.695	Chondramid C	0.688	Rhizopodin A	0.666
Myriaporon	0.712	Wortmannin	0.721	Ratjadon C	0.711	Chondramid C	0.764	Camptothecin	0.786	PMA	0.689	Vioprolid A	0.671	Chondramid C	0.662
Scriptaid	0.702	Taxol	0.713	Wortmannin	0.696	Camptothecin	0.758	Puromycin	0.774	Oxamflatin	0.686	Ratjadon C	0.659	MeOH	0.646
MG132	0.693	Myriaporon	0.712	Trichostatin	0.696	Oxamflatin	0.757	Vioprolid A	0.768	Trichostatin	0.682	MG132	0.659	Cycloheximide	0.640
Epothilon B	0.692	PMA	0.707	Myriaporon	0.691	Trichostatin	0.753	Cruentaren A	0.745	Scriptaid	0.658	Myriaporon	0.636	Oxamflatin	0.638
Ratjadon C	0.685	Oxamflatin	0.706	MG132	0.661	Myriaporon	0.753	Neopeltolid	0.721	Taxol	0.638	Scriptaid	0.620	Trichostatin	0.618
MeOH	0.678	Rhizopodin A	0.695	Chondramid C	0.657	Tubulysin B	0.742	Tubulysin B	0.715	Camptothecin	0.634	MeOH	0.616	PMA	0.617
Wortmannin	0.673	Trichostatin	0.695	Tubulysin B	0.654	Simvastatin	0.731	Scriptaid	0.709	Tubulysin B	0.631	Camptothecin	0.595	Camptothecin	0.607
Trichostatin	0.670	Camptothecin	0.694	Camptothecin	0.651	MG132	0.716	Aphidicolin	0.701	Okadaic acid	0.625	Trichostatin	0.589	MG132	0.600
PMA	0.661	MG132	0.694	Taxol	0.640	Cytochalasin D	0.714	Simvastatin	0.698	Chondramid C	0.618	Indirubin monoxime	0.584	Myriaporon	0.598
Okadaic acid	0.659	Simvastatin	0.651	Neopeltolid	0.612	Archazolid B	0.702	Chondramid C	0.694	Neopeltolid	0.598	Gephyronsäure A	0.564	Okadaic acid	0.587
Podophyllotoxin	0.655	Gephyronsäure A	0.638	Simvastatin	0.608	Gephyronsäure A	0.694	Soraphen A	0.681	Cruentaren A	0.586	PMA	0.563	Cytochalasin D	0.575
Simvastatin	0.653	Epothilon B	0.634	Okadaic acid	0.597	Nocodazole	0.692	Tunicamycin	0.666	Simvastatin	0.548	Oxamflatin	0.551	Epothilon B	0.574
Indirubin monoxime	0.650	Cytochalasin D	0.629	Cruentaren A	0.585	Staurosporine	0.692	Rhizopodin A	0.664	Aphidicolin	0.540	Wortmannin	0.535	Simvastatin	0.560
Camptothecin	0.646	Soraphen A	0.620	Gephyronsäure A	0.582	Soraphen A	0.690	Wortmannin	0.663	Epothilon B	0.573	Argyrin A	0.534	Gephyronsäure A	0.551
Staurosporine	0.644	Staurosporine	0.615	Cytochalasin D	0.578	Colchicine	0.684	Staurosporine	0.657	Wortmannin	0.570	Purvalanol A	0.531	Vinblastine	0.544
Oxamflatin	0.637	Podophyllotoxin	0.612	Aphidicolin	0.575	Podophyllotoxin	0.681	Podophyllotoxin	0.644	Soraphen A	0.528	Podophyllotoxin	0.527	Purvalanol A	0.534
Soraphen A	0.632	Cruentaren A	0.610	Staurosporine	0.571	Vinblastine	0.674	Dexamethasone	0.642	Gephyronsäure A	0.518	Soraphen A	0.526	Soraphen A	0.533
Cytochalasin D	0.625	Archazolid B	0.607	Soraphen A	0.568	Taxol	0.674	Taxol	0.637	Tunicamycin	0.516	Cruentaren A	0.526	Colchicine	0.531
Tunicamycin	0.614	Purvalanol A	0.607	Epothilon B	0.563	Cruentaren A	0.670	Doxorubicin	0.623	Podophyllotoxin	0.515	Simvastatin	0.520	Archazolid B	0.527
Archazolid B	0.609	Colchicine	0.602	Podophyllotoxin	0.561	Purvalanol A	0.666	Myxothiazol A	0.622	Indirubin monoxime	0.513	Tunicamycin	0.513	Staurosporine	0.526

BrDUD17S	1.000	BzDPD10A	1.000	Py3DUD21S	1.000	BrDUD01A	1.000	BzDPD01A	1.000	BrDUD18S	1.000	BrDUD20S	1.000
Apicularen	0.912	Actinomycin D	0.924	Griseofulvin	0.884	Podophyllotoxin	0.846	Velcade	0.862	Wortmannin	0.801	Okadaic acid	-0.493
Chivosazol A	0.883	Chelerythrine	0.901	Anisomycin	0.872	LY294002	0.840	Indirubin monoxime	0.851	Puromycin	0.798	Rhizopodin A	-0.500
Colchicine	0.857	Apicidin	0.885	Purvalanol A	0.850	Mevastatin	0.830	LY294002	0.842	Scriptaid	0.797	Vioprolid A	-0.573
Archazolid B	0.841	Alsterpaullone	0.849	SB202190	0.830	Chivosazol A	0.825	Tunicamycin	0.797	Brefeldin A	0.771	Puromycin	-0.592
Griseofulvin	0.831	SB202190	0.833	Colchicine	0.805	DMSO:MeOH	0.822	PD169316	0.795	Cytochalasin D	0.722	Taxol	-0.609
Cytochalasin D	0.825	Griseofulvin	0.825	Chivosazol A	0.801	Purvalanol A	0.821	Podophyllotoxin	0.783	Vinblastine	0.719	Scriptaid	-0.609
SB202190	0.819	Chivosazol A	0.803	Amanitin	0.782	Anisomycin	0.811	Myxothiazol A	0.767	Tubulysin B	0.714	Cycloheximide	-0.613
Vinblastine	0.812	Apicularen	0.769	Emetine	0.768	Griseofulvin	0.809	Mevastatin	0.764	Vioprolid A	0.710	Epothilon B	-0.616
DMSO:MeOH	0.811	Anisomycin	0.752	DMSO:MeOH	0.762	Gephyronsäure A	0.807	Soraphen A	0.760	Chondramid C	0.693	Brefeldin A	-0.618
Nocodazole	0.807	Amanitin	0.752	Podophyllotoxin	0.760	Colchicine	0.807	Anisomycin	0.750	Gephyronsäure A	0.687	Oxamflatin	-0.636
Chelerythrine	0.805	Colchicine	0.744	Indirubin monoxime	0.748	Tunicamycin	0.803	Purvalanol A	0.747	Taxol	0.665	Myriaporon	-0.637
Saframycin	0.802	Methotrexate	0.727	Alsterpaullone	0.747	Velcade	0.800	Rapamycin	0.736	Colchicine	0.664	PMA	-0.638
Methotrexate	0.783	A23187 free acid	0.721	Argyrin A	0.747	Archazolid B	0.793	Amanitin	0.729	Simvastatin	0.659	Ratjadon C	-0.640
Actinomycin D	0.778	DMSO:MeOH	0.717	Gephyronsäure A	0.744	Soraphen A	0.785	DMSO:MeOH	0.718	Archazolid B	0.654	Tubulysin B	-0.650
Emetine	0.772	Saframycin	0.714	LY294002	0.743	Indirubin monoxime	0.783	Gephyronsäure A	0.710	Apicularen	0.651	MeOH	-0.652
Apicidin	0.768	Archazolid B	0.709	Tunicamycin	0.742	Amanitin	0.782	SB203580	0.708	Staurosporine	0.646	Chondramid C	-0.658
Gephyronsäure A	0.767	Cytochalasin D	0.683	Soraphen A	0.742	SB203580	0.761	Cruentaren A	0.702	Nocodazole	0.645	MG132	-0.661
Staurosporine	0.763	Emetine	0.677	Archazolid B	0.741	Chondramid C	0.753	Staurosporine	0.701	Ratjadon C	0.632	Wortmannin	-0.662
Podophyllotoxin	0.754	Etoposide	0.671	Mevastatin	0.736	SB202190	0.747	MG132	0.693	Emetine	0.632	Trichostatin	-0.678
Anisomycin	0.747	Mevastatin	0.671	Actinomycin D	0.720	Staurosporine	0.746	Chondramid C	0.688	Podophyllotoxin	0.621	Camptothecin	-0.686
Simvastatin	0.747	Nocodazole	0.670	Chondramid C	0.718	Saframycin	0.744	Oligomycin	0.686	MeOH	0.621	Indirubin monoxime	-0.688
Mevastatin	0.740	Purvalanol A	0.656	Apicularen	0.715	PD169316	0.736	Simvastatin	0.678	Soraphen A	0.617	Neopeltolid	-0.689
Purvalanol A	0.734	Vinblastine	0.653	Staurosporine	0.712	Simvastatin	0.732	Griseofulvin	0.675	Purvalanol A	0.616	Gephyronsäure A	-0.693
Soraphen A	0.725	Cyclosporin A	0.649	PD169316	0.709	Myxothiazol A	0.724	Cycloheximide	0.673	Oxamflatin	0.615	Simvastatin	-0.711
SB203580	0.709	SB203580	0.647	Saframycin	0.705	Oligomycin	0.722	Camptothecin	0.672	Cycloheximide	0.615	Cytochalasin D	-0.713
Alsterpaullone	0.708	Podophyllotoxin	0.643	Etoposide	0.703	Cytochalasin D	0.716	Doxorubicin	0.668	Trichostatin	0.611	Cruentaren A	-0.719
Wortmannin	0.706	Gephyronsäure A	0.633	Cytochalasin D	0.697	Argyrin A	0.715	Myriaporon	0.667	PMA	0.610	Argyrin A	-0.720
Tunicamycin	0.701	LY294002	0.629	Velcade	0.694	Actinomycin D	0.709	Chivosazol A	0.664	Camptothecin	0.606	Podophyllotoxin	-0.728
H89	0.686	H89	0.627	Simvastatin	0.693	Nocodazole	0.705	Dexamethasone	0.655	Chivosazol A	0.605	Vinblastine	-0.730

Table 6. Numerical correlation values of 30 bridged bicyclic compounds obtained from the high content analysis (repetition experiment). The similarity values with first 30 reference compounds are shown.

BzDPD10A	1	BrDPD17A	1	BrDPD20A	1	BrDUD01A	1	BrDPD10S	1	BrDPD10A	1	BzDPD01A	1	Py3DUD01A	1
Chelerythrine	0.863	A23187 free acid	0.831	Amanitin	0.792	DMSO:MeOH	0.799	Amanitin	0.874	Amanitin	0.837	Amanitin	0.837	Apicularen	0.860
Amanitin	0.782	Chelerythrine	0.813	DMSO:MeOH	0.778	Chivosazol A	0.779	Chivosazol A	0.739	Anisomycin	0.783	Anisomycin	0.795	PD169316	0.837
Chivosazol A	0.774	Amanitin	0.792	Chivosazol A	0.743	Apicularen	0.776	Anisomycin	0.731	Alsterpaullone	0.737	Chivosazol A	0.749	Archazolid B	0.812
A23187 free acid	0.759	Apicidin	0.751	Mevastatin	0.732	Mevastatin	0.758	Colchicine	0.724	Chivosazol A	0.718	Archazolid B	0.741	SB202190	0.804
Mevastatin	0.737	Chivosazol A	0.687	Cyclosporin A	0.725	PD169316	0.755	DMSO:MeOH	0.712	Colchicine	0.716	Colchicine	0.737	SB203580	0.795
DMSO:MeOH	0.736	Colchicine	0.680	Colchicine	0.724	Colchicine	0.748	Apicularen	0.704	Apicularen	0.700	Apicularen	0.733	H89	0.777
Apicidin	0.736	DMSO:MeOH	0.630	Chelerythrine	0.713	Archazolid B	0.747	PD169316	0.700	DMSO:MeOH	0.699	Alsterpaullone	0.723	Oligomycin	0.777
Colchicine	0.734	Mevastatin	0.629	Apicularen	0.702	Emetine	0.734	Chelerythrine	0.694	Archazolid B	0.688	Emetine	0.709	DMSO:MeOH	0.762
PD169316	0.697	PD169316	0.625	Brefeldin A	0.692	Chelerythrine	0.724	Archazolid B	0.690	Mevastatin	0.677	Mevastatin	0.707	Chivosazol A	0.756
Cyclosporin A	0.689	Cyclosporin A	0.605	Alsterpaullone	0.687	Simvastatin	0.721	Mevastatin	0.687	Cyclosporin A	0.663	DMSO:MeOH	0.703	Amanitin	0.744
Apicularen	0.663	Apicularen	0.581	Simvastatin	0.680	Cyclosporin A	0.720	Alsterpaullone	0.681	Chelerythrine	0.652	PD169316	0.681	Soraphen A	0.735
Oligomycin	0.639	Anisomycin	0.564	Podophyllotoxin	0.675	Oligomycin	0.703	Emetine	0.664	Emetine	0.652	Cyclosporin A	0.665	Simvastatin	0.716
Simvastatin	0.630	Actinomycin D	0.559	Anisomycin	0.672	H89	0.687	Cyclosporin A	0.656	SB203580	0.650	SB203580	0.663	Emetine	0.709
Emetine	0.627	Archazolid B	0.557	PD169316	0.670	SB202190	0.687	A23187 free acid	0.654	PD169316	0.647	H89	0.660	Mevastatin	0.707
Archazolid B	0.624	Emetine	0.544	Emetine	0.664	SB203580	0.680	SB203580	0.647	Brefeldin A	0.625	SB202190	0.655	Colchicine	0.657
SB202190	0.617	Alsterpaullone	0.541	Archazolid B	0.660	Podophyllotoxin	0.670	SB202190	0.643	SB202190	0.624	Oligomycin	0.643	LY294002	0.652
Brefeldin A	0.615	Brefeldin A	0.541	A23187 free acid	0.659	Brefeldin A	0.663	H89	0.638	H89	0.621	Chelerythrine	0.635	Cyclosporin A	0.651
Podophyllotoxin	0.610	Simvastatin	0.538	Oligomycin	0.659	Anisomycin	0.661	Oligomycin	0.637	A23187 free acid	0.617	Simvastatin	0.629	Methotrexate	0.651
H89	0.596	Oligomycin	0.532	H89	0.651	Soraphen A	0.660	Simvastatin	0.635	Simvastatin	0.610	Brefeldin A	0.604	Chelerythrine	0.637
SB203580	0.594	SB202190	0.530	SB203580	0.647	Alsterpaullone	0.649	Apicidin	0.616	Oligomycin	0.605	Soraphen A	0.582	Anisomycin	0.633
Soraphen A	0.583	SB203580	0.522	Apicidin	0.645	Apicidin	0.632	Brefeldin A	0.615	Apicidin	0.558	A23187 free acid	0.572	Podophyllotoxin	0.621
Actinomycin D	0.573	Podophyllotoxin	0.509	SB202190	0.637	A23187 free acid	0.626	Soraphen A	0.583	Soraphen A	0.557	Cytochalasin D	0.565	Saframycin	0.617
Anisomycin	0.569	H89	0.500	Soraphen A	0.609	LY294002	0.615	Podophyllotoxin	0.560	Podophyllotoxin	0.546	Podophyllotoxin	0.538	Neopeltolid	0.607
Alsterpaullone	0.564	Soraphen A	0.484	Nocodazole	0.606	Nocodazole	0.579	LY294002	0.537	Cytochalasin D	0.525	Purvalanol A	0.538	Brefeldin A	0.598
LY294002	0.561	LY294002	0.467	LY294002	0.581	Methotrexate	0.573	Methotrexate	0.518	Nocodazole	0.525	Apicidin	0.532	Alsterpaullone	0.590
Methotrexate	0.550	Methotrexate	0.452	Saframycin	0.561	PMA	0.565	Saframycin	0.510	Saframycin	0.513	Methotrexate	0.522	PMA	0.565
Nocodazole	0.547	Nocodazole	0.439	Methotrexate	0.553	Saframycin Mx1	0.560	Nocodazole	0.505	Methotrexate	0.510	Saframycin	0.517	Cycloheximide	0.549
Saframycin	0.520	Saframycin	0.421	Actinomycin D	0.540	Griseofulvin	0.542	Cytochalasin D	0.500	LY294002	0.504	Nocodazole	0.517	Griseofulvin	0.543

Continued from previous page…

PmDUD06S	1	ImDUD10S	1	Py4DUD01A	1	BrDUD12S	1	Py3DUD19S	1	PmDUD21S	1	BrDUD14S	1	BrDUD26S	1
Apicularen	0.795	SB203580	0.881	Soraphen A	0.834	H89	0.799	H89	0.799	H89	0.780	Purvalanol A	0.786	Purvalanol A	0.679
H89	0.775	Apicularen	0.847	H89	0.813	Oligomycin	0.734	SB203580	0.774	Purvalanol A	0.778	Archazolid B	0.699	MG132	0.661
Archazolid B	0.759	SB202190	0.824	Simvastatin	0.812	Saframycin	0.730	SB202190	0.769	SB203580	0.774	Apicularen	0.696	Myriaporon	0.643
Oligomycin	0.754	H89	0.814	SB203580	0.799	Purvalanol A	0.729	Saframycin	0.754	Apicularen	0.737	Cycloheximide	0.681	Cycloheximide	0.618
SB202190	0.751	Oligomycin	0.794	Oligomycin	0.787	SB203580	0.729	Oligomycin	0.749	SB202190	0.734	SB203580	0.670	Griseofulvin	0.533
Emetine	0.737	DMSO:MeOH	0.784	Apicularen	0.781	SB202190	0.725	Methotrexate	0.744	Oligomycin	0.726	H89	0.669	Saframycin	0.526
DMSO:MeOH	0.734	Archazolid B	0.766	SB202190	0.769	Soraphen A	0.712	Soraphen A	0.734	Griseofulvin	0.722	Anisomycin	0.662	H89	0.521
PD169316	0.732	Methotrexate	0.765	Saframycin	0.766	Apicularen	0.707	Apicularen	0.725	Saframycin	0.704	Myriaporon	0.638	Indirubin monoxime	0.512
SB203580	0.723	Soraphen A	0.761	LY294002	0.765	Methotrexate	0.691	Purvalanol A	0.702	Cycloheximide	0.703	Alsterpaullone	0.637	Chondramid C	0.509
Soraphen A	0.701	Saframycin	0.751	DMSO:MeOH	0.761	Cruentaren A	0.669	Dexamethasone	0.669	DMSO:MeOH	0.699	SB202190	0.636	SB203580	0.508
Chivosazol A	0.699	PD169316	0.744	Neopeltolid	0.748	Archazolid B	0.669	Neopeltolid	0.668	Soraphen A	0.683	Cytochalasin D	0.630	Apicularen	0.502
Simvastatin	0.688	Chivosazol A	0.729	Cruentaren A	0.735	Cycloheximide	0.666	Archazolid B	0.662	Methotrexate	0.676	Emetine	0.627	Cytochalasin D	0.500
Mevastatin	0.677	Simvastatin	0.727	Methotrexate	0.731	Myxothiazol A	0.665	DMSO:MeOH	0.645	Archazolid B	0.675	Griseofulvin	0.606	SB202190	0.499
Amanitin	0.660	Mevastatin	0.713	Archazolid B	0.730	Simvastatin	0.656	Cycloheximide	0.639	Cytochalasin D	0.673	DMSO:MeOH	0.599	Methotrexate	0.475
Cyclosporin A	0.635	Amanitin	0.677	PD169316	0.720	Neopeltolid	0.651	Myxothiazol A	0.639	Nocodazole	0.663	Oligomycin	0.599	Soraphen A	0.463
Podophyllotoxin	0.625	Cyclosporin A	0.673	Podophyllotoxin	0.702	DMSO:MeOH	0.648	Simvastatin	0.627	Mevastatin	0.660	Mevastatin	0.576	DMSO:MeOH	0.461
LY294002	0.620	LY294002	0.673	PMA	0.702	LY294002	0.616	LY294002	0.626	Myriaporon	0.647	Chivosazol A	0.574	Archazolid B	0.458
Anisomycin	0.613	Podophyllotoxin	0.672	Brefeldin A	0.701	Chondramid C	0.614	Cruentaren A	0.620	Emetine	0.647	Soraphen A	0.568	Oligomycin	0.455
Colchicine	0.610	Brefeldin A	0.668	Myxothiazol A	0.654	Nocodazole	0.614	PD169316	0.614	Chivosazol A	0.632	Cyclosporin A	0.561	Epothilon B	0.453
Cycloheximide	0.609	Nocodazole	0.648	Mevastatin	0.628	MG132	0.608	Griseofulvin	0.599	Simvastatin	0.625	Saframycin	0.556	Nocodazole	0.452
Neopeltolid	0.605	Emetine	0.644	Nocodazole	0.624	Myriaporon	0.601	Nocodazole	0.597	Cyclosporin A	0.621	Simvastatin	0.553	Neopeltolid	0.445
Alsterpaullone	0.595	Cruentaren A	0.643	Cycloheximide	0.621	Mevastatin	0.598	MG132	0.595	Podophyllotoxin	0.616	Methotrexate	0.536	Myxothiazol A	0.445
Purvalanol A	0.594	Neopeltolid	0.640	Emetine	0.618	Griseofulvin	0.598	Mevastatin	0.587	Myxothiazol A	0.611	Amanitin	0.533	Gephyronsäure A	0.434
Griseofulvin	0.590	Anisomycin	0.633	Chivosazol A	0.615	Dexamethasone	0.591	Chondramid C	0.584	MG132	0.605	PD169316	0.532	Cruentaren A	0.431
Methotrexate	0.588	Colchicine	0.625	Cyclosporin A	0.613	PD169316	0.590	Chivosazol A	0.580	Neopeltolid	0.604	Cruentaren A	0.531	Dexamethasone	0.426
Saframycin	0.580	Myxothiazol A	0.621	Amanitin	0.598	Emetine	0.589	Podophyllotoxin	0.573	Cruentaren A	0.601	MG132	0.527	Cyclosporin A	0.424
Cytochalasin D	0.570	Alsterpaullone	0.616	Anisomycin	0.578	Aphidicolin	0.588	Aphidicolin	0.573	Chondramid C	0.599	Nocodazole	0.524	Emetine	0.417
Brefeldin A	0.562	Chelerythrine	0.606	Chondramid C	0.565	Cytochalasin D	0.587	Emetine	0.568	PD169316	0.586	Colchicine	0.516	Alsterpaullone	0.396

Continued on next page…

PmDUD13S	1	BrDUD20S	1	BrDUD17S	1	Py3DUD13S	1	BrDPD13A	1	Py3DUD10S	1	BrDUD21S	1	BrDUD16S	1
Chondramid C	0.784	Indirubin monoxime	0.049	Colchicine	0.803	Rhizopodin A	0.514	Brefeldin A	0.833	Chivosazol A	0.869	Chondramid C	0.673	Indirubin monoxime	0.642
MG132	0.736	Rhizopodin A	-0.058	Mevastatin	0.795	Okadaic acid	0.326	Cyclosporin A	0.687	Mevastatin	0.808	Cruentaren A	0.636	Purvalanol A	0.528
Myxothiazol A	0.694	Okadaic acid	-0.138	Cyclosporin A	0.790	Vioprolid A	0.324	Alsterpaullone	0.681	Colchicine	0.797	Brefeldin A	0.626	MG132	0.512
Myriaporon	0.691	Oxamflatin	-0.225	DMSO:MeOH	0.765	Epothilon B	0.230	Colchicine	0.679	Amanitin	0.792	Ratjadon C	0.625	Myriaporon	0.440
Cycloheximide	0.684	Vioprolid A	-0.256	Chivosazol A	0.744	Indirubin monoxime	0.213	DMSO:MeOH	0.679	Apicularen	0.775	Nocodazole	0.609	Epothilon B	0.406
Cruentaren A	0.682	Vinblastine	-0.256	Amanitin	0.738	Ratjadon C	0.209	Nocodazole	0.669	Archazolid B	0.770	Myxothiazol A	0.572	Chondramid C	0.363
Saframycin	0.676	Scriptaid	-0.260	Emetine	0.726	Chondramid C	0.209	Simvastatin	0.666	Emetine	0.757	Argyrin A	0.548	Cycloheximide	0.349
Nocodazole	0.665	Epothilon B	-0.282	Chelerythrine	0.724	Tubulysin B	0.206	Mevastatin	0.658	Cyclosporin A	0.745	Wortmannin	0.538	Tubulysin B	0.336
Purvalanol A	0.659	Chondramid C	-0.287	Brefeldin A	0.716	MG132	0.174	Podophyllotoxin	0.656	Chelerythrine	0.732	Myriaporon	0.530	Myxothiazol A	0.324
H89	0.644	MG132	-0.308	Podophyllotoxin	0.689	Puromycin	0.146	Anisomycin	0.636	DMSO:MeOH	0.719	Podophyllotoxin	0.523	Saframycin	0.300
Griseofulvin	0.606	Tubulysin B	-0.328	Simvastatin	0.678	Oxamflatin	0.129	Actinomycin D	0.632	PD169316	0.694	Cycloheximide	0.513	H89	0.292
Oligomycin	0.591	Neopeltolid	-0.389	Apicularen	0.673	Wortmannin	0.044	Amanitin	0.623	SB203580	0.653	Simvastatin	0.509	Gephyronsäure A	0.286
Soraphen A	0.587	Saframycin	-0.396	Archazolid B	0.659	Myriaporon	0.032	Emetine	0.608	Anisomycin	0.644	PMA	0.499	Cytochalasin D	0.285
Cytochalasin D	0.580	Myriaporon	-0.417	Nocodazole	0.655	Trichostatin	0.028	Cruentaren A	0.585	SB202190	0.637	Staurosporine	0.478	Etoposide	0.283
Neopeltolid	0.573	Myxothiazol A	-0.417	Alsterpaullone	0.654	Taxol	0.022	Chivosazol A	0.580	Oligomycin	0.621	Alsterpaullone	0.466	Doxorubicin	0.279
Methotrexate	0.571	Cruentaren A	-0.447	Apicidin	0.649	Myxothiazol A	0.012	Apicidin	0.580	Alsterpaullone	0.620	Saframycin	0.464	Cruentaren A	0.276
Simvastatin	0.568	Taxol	-0.448	A23187 free acid	0.640	Cruentaren A	0.009	Chelerythrine	0.564	H89	0.605	DMSO:MeOH	0.461	Camptothecin	0.254
Podophyllotoxin	0.566	Trichostatin	-0.451	Actinomycin D	0.634	Scriptaid	0.006	Apicularen	0.561	Simvastatin	0.605	Velcade	0.458	SB203580	0.250
DMSO:MeOH	0.564	Cycloheximide	-0.462	Anisomycin	0.624	Cycloheximide	-0.009	Archazolid B	0.560	Cytochalasin D	0.601	Cytochalasin D	0.455	SB202190	0.244
SB203580	0.557	Etoposide	-0.472	PD169316	0.618	Neopeltolid	-0.029	A23187 free acid	0.546	A23187 free acid	0.585	MG132	0.443	Griseofulvin	0.242
Brefeldin A	0.555	Ratjadon C	-0.477	Oligomycin	0.601	Saframycin	-0.036	PMA	0.545	Griseofulvin	0.585	Griseofulvin	0.435	Methotrexate	0.236
SB202190	0.545	Methotrexate	-0.487	Cytochalasin D	0.581	Gephyronsäure A	-0.051	Cytochalasin D	0.541	Podophyllotoxin	0.572	Cyclosporin A	0.429	Aphidicolin	0.221
PMA	0.545	H89	-0.496	H89	0.578	Tunicamycin	-0.052	Staurosporine	0.533	Brefeldin A	0.565	H89	0.428	Oligomycin	0.221
Apicularen	0.543	Soraphen A	-0.498	SB203580	0.573	PMA	-0.069	Oligomycin	0.531	Soraphen A	0.565	Epothilon B	0.425	Dexamethasone	0.218
LY294002	0.531	Purvalanol A	-0.500	Griseofulvin	0.570	Nocodazole	-0.098	H89	0.529	Nocodazole	0.557	LY294002	0.409	Apicularen	0.214
Staurosporine	0.517	Puromycin	-0.502	Soraphen A	0.561	Velcade	-0.099	Myxothiazol A	0.516	Methotrexate	0.538	Soraphen A	0.402	Soraphen A	0.209
Epothilon B	0.511	LY294002	-0.505	SB202190	0.557	LY294002	-0.118	Soraphen A	0.511	Apicidin	0.534	Emetine	0.400	Nocodazole	0.206
Archazolid B	0.503	Dexamethasone	-0.528	Staurosporine	0.554	Soraphen A	-0.127	Saframycin	0.509	Purvalanol A	0.503	Mevastatin	0.399	Anisomycin	0.206

Continued on next page…

BrDUD18S	1	Py3DUD17S	1	PmDUD19S	1	BrDUD19S	1	Py3DUD21S	1	Py3DUD20S	1	PmDUD20S	1
Rhizopodin A	0.524	Oxamflatin	0.524	Chondramid C	0.639	Epothilon B	0.616	PmDUD19	0.820	Ratjadon C	0.565	Rhizopodin A	0.667
Indirubin monoxime	0.517	Chondramid C	0.512	MG132	0.578	Chondramid C	0.596	Apicularen	0.782	Trichostatin	0.536	Chondramid C	0.516
Chondramid C	0.445	MG132	0.487	Indirubin monoxime	0.556	Tubulysin B	0.572	SB203580	0.762	Oxamflatin	0.515	Oxamflatin	0.501
Epothilon B	0.361	Rhizopodin A	0.483	Rhizopodin A	0.530	Myriaporon	0.555	Chivosazol A	0.753	Chondramid C	0.469	Ratjadon C	0.431
Oxamflatin	0.350	Indirubin monoxime	0.459	Cruentaren A	0.490	MG132	0.531	SB202190	0.752	Rhizopodin A	0.465	Cruentaren A	0.338
MG132	0.299	Neopeltolid	0.403	Oxamflatin	0.484	Argyrin A	0.468	Mevastatin	0.750	PMA	0.457	Myxothiazol A	0.335
Myxothiazol A	0.293	Scriptaid	0.400	Epothilon B	0.476	Myxothiazol A	0.446	H89	0.737	Neopeltolid	0.436	MG132	0.334
Cruentaren A	0.280	Cruentaren A	0.388	Myxothiazol A	0.475	Indirubin monoxime	0.436	Oligomycin	0.731	MG132	0.409	Scriptaid	0.330
Tubulysin B	0.279	Myxothiazol A	0.370	Myriaporon	0.465	Purvalanol A	0.435	Methotrexate	0.713	Scriptaid	0.392	Neopeltolid	0.317
Myriaporon	0.276	Saframycin	0.356	Saframycin	0.438	Nocodazole	0.414	DMSO:MeOH	0.711	Vioprolid A	0.392	Vioprolid A	0.311
Saframycin	0.251	Ratjadon C	0.335	Cycloheximide	0.437	Cycloheximide	0.414	Archazolid B	0.709	Cruentaren A	0.384	Epothilon B	0.308
Okadaic acid	0.240	Trichostatin	0.331	Neopeltolid	0.431	Cruentaren A	0.413	Griseofulvin	0.705	LY294002	0.360	Trichostatin	0.302
Ratjadon C	0.205	Epothilon B	0.323	Ratjadon C	0.425	Wortmannin	0.396	Purvalanol A	0.699	Velcade	0.337	Saframycin	0.298
Neopeltolid	0.201	Cycloheximide	0.319	H89	0.375	Ratjadon C	0.379	Cyclosporin A	0.675	Cycloheximide	0.332	Indirubin monoxime	0.297
Cycloheximide	0.200	Myriaporon	0.312	Tubulysin B	0.368	Cytochalasin D	0.373	Saframycin	0.672	Tunicamycin	0.326	PMA	0.272
Scriptaid	0.197	Vioprolid A	0.301	Purvalanol A	0.361	Griseofulvin	0.355	Cytochalasin D	0.668	Soraphen A	0.325	LY294002	0.240
Vioprolid A	0.183	PMA	0.294	Vioprolid A	0.358	Saframycin	0.354	Nocodazole	0.664	Wortmannin	0.323	Cycloheximide	0.221
H89	0.169	Soraphen A	0.292	Soraphen A	0.350	Gephyronsäure A	0.350	Emetine	0.658	Myxothiazol A	0.320	Myriaporon	0.220
Purvalanol A	0.161	H89	0.290	PMA	0.346	Taxol	0.347	Soraphen A	0.655	Saframycin	0.315	Wortmannin	0.218
Nocodazole	0.150	LY294002	0.288	Wortmannin	0.337	Rhizopodin A	0.347	PD169316	0.643	Simvastatin	0.304	Soraphen A	0.209
Wortmannin	0.125	Methotrexate	0.249	Nocodazole	0.337	Brefeldin A	0.305	Podophyllotoxin	0.609	Podophyllotoxin	0.300	Tubulysin B	0.193
Soraphen A	0.124	Oligomycin	0.241	LY294002	0.335	Alsterpaullone	0.304	Colchicine	0.605	Puromycin	0.287	Nocodazole	0.193
Argyrin A	0.123	Wortmannin	0.234	Scriptaid	0.323	Staurosporine	0.301	Simvastatin	0.604	Epothilon B	0.259	Podophyllotoxin	0.179
LY294002	0.122	Tubulysin B	0.230	Trichostatin	0.320	H89	0.299	Dexamethasone	0.597	H89	0.249	H89	0.176
Methotrexate	0.117	Purvalanol A	0.226	Oligomycin	0.316	Vioprolid A	0.288	Cycloheximide	0.589	Nocodazole	0.248	Puromycin	0.165
Oligomycin	0.109	Simvastatin	0.217	Methotrexate	0.310	Okadaic acid	0.268	Amanitin	0.577	Myriaporon	0.246	Methotrexate	0.165
Trichostatin	0.104	Podophyllotoxin	0.213	Simvastatin	0.303	DMSO:MeOH	0.256	LY294002	0.554	PmDUD19	0.240	Okadaic acid	0.161
PMA	0.104	Nocodazole	0.209	Podophyllotoxin	0.298	Podophyllotoxin	0.255	Chelerythrine	0.553	Oligomycin	0.233	Simvastatin	0.161

Table 7. Reference compounds used in the high content analysis and impedance measurement

Compound	Mode of action in eukaryotic cells	Concentration (µM)	Compound	Mode of action in eukaryotic cells	Concentration (µM)
A23187	Calcium regulation	110	Mevastatin	inhibits cholesterol-biosynthesis	1200
Actinomycin	Inhibition of transcription	4,4	MG132	Proteasome inhibitor	400
Alsterpaullone	Inhibition of CD Kinase	1100	Myriaporon	Inhibits protein synthesis	70
Amanitin	Blocking of mRNA synthesis	1000	Myxothiazol A	Affects respiratory-chain	12
Anisomycin	Inhibition of protein biosynthesis	45	Neopeltolid	Affects respiratory-chain	100
Aphidicolin	Inhibition of DNA polymerization	1000	Nocodazol	Inhibits tubulin polymerization	12
Apicidin	HDAC inhibitor	100	Okadiac acid	Inhibits proteinphospatases	10
Apicularen	V-ATPase inhibitor	31	Oligomycin	F-ATPase inhibitor	70
Archazolid B	V-ATPase inhibitor	3	Oxamflatin	HDAC inhibitor	1200
Argyrin A	Proteasome inhibitor	1000	PD169316	p38-MAP kinase inhibitor	10000
Brefeldin A	Destroys golgi apparatus	100	PMA	activates protein-kinase C	3500
Camptothecin	Topoisomerase I inhibitor	450	Podophyllotoxin	Inhibits tubulin polymerization	2,5
Chelerythrin	Protein kinase C inhibitor	1000	Puromycin	Inhibits protein-biosynthesis	500
Chivosazol A	actin polymerisation inhibitor	1,3	Purvalanol A	Inhibits CD kinase	2000
Chondramid C	Stabilizes actin filaments	10	Rapamycin	PI3 kinase inhibitor	11
Colchicin	Destroys Microtubuli	10	Ratjadon C	blocks nuclear receptor	3,5
Cruentaren A	F-ATPase inhibitor	14	Rhizopodin A	Inhibits Actin polymerization	20
Cycloheximid	Inhibits protein biosynthesis	450	Saframycin Mx1	Inhibits DNA synthesis	40
Cyclosporin A	Effects calcium-regulation	5500	SB202190	p38-MAP kinase inhibitor	10.000
Cytochalasin D	Promotes actin depolymerization	1000	SB203580	p38-MAP kinase inhibitor	10.000
Dexamethason	Shows immunosuppressive effect	4500	Scriptaid	HDAC inhibitor	4000
Doxorubicin	Topoisomerase II inhibitor	340	Simvastatin	Inhibits cholesterol-biosynthesis	800
Emetin	Inhibits protein biosynthese	41	Soraphen A	Inhibits lipid synthesis	400
Epothilon B	stabilizes microtubuli	0,55	Staurosporin	Inhibits protein kinases	3
Etoposid	Topoisomerase inhibitor	2300	Taxol	Stabilizes microtubules	25
Gephyronic acid A	Inhibits protein synthesis	60	Trichostatin	HDAC inhibitor	310
Griseofulvin	Inhibits mitotic-spindle formation	10000	Tubulysin B	Inhibits polymerization microtubules	0,4
H89	Protein kinase A inhibitor	10000	Tunicamycin	Accumulates misfolded proteins	700
Indirubin-3'-monoxim	Inhibits CD kinase	8000	Velcade	Proteasome inhibitor	11
LY294002	PI3 kinase inhibitor	10000	Vinblastin	Inhibits polymerization microtubules	0,5
Methotrexat	Inhibits DNA synthesis	50	Wortmannin	Inhibits PI3-kinase	10000